Dipartimento di Scienze Biomediche, Sperimentali e Cliniche – Firenze

Dipartimento di Biotecnologie, Chimica e Farmacia – Siena

Biochemistry and Molecular Biology – Bibim 2.0

XXXV Ciclo

New perspective on type 2 diabetes and obesity treatment: study and development of new natural/synthetic inhibitors of tyrosine phosphatase 1B (PTP1B).

Tutor

Prof. Paolo Paoli

Coordinatore

Prof.ssa Lorenza Trabalzini

Dottorando

Massimo Genovese

Anno Accademico 2022-2023

Contents

Introduction

Diabetes mellitus

Characteristics and global impact

Diabetes is a chronic disease characterized by several disorders affecting glucose, lipid and protein metabolism. Its main feature regards the onset of high blood sugar levels over a long period of time (hyperglicemia) since body is no longer capable to produce enough amount of insulin and/or target cells develop resistance to it (insulin resistance - IR)[1].

Tipical signals of diabetes occurence are increased thirst and appetite, frequent urination and hyperglicemia condition which, if left untreated, could bring to the onset of several complications on acute and long term. Among them: diabetic ketoacidosis, cardiovascular complications and stroke, kidney failure, foot ulcers, damages to eyes and nerves[1,2].

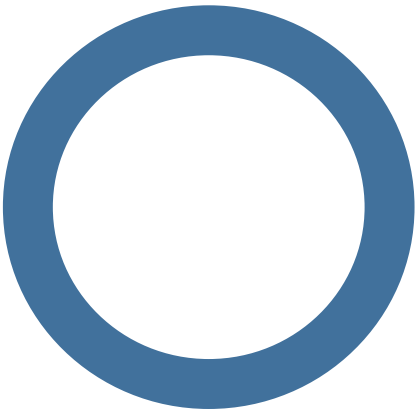

Fig.1. The blue circle is the global symbol for diabetes, introduced by the **International Diabetes Federation.**

As said before, this condition occurs when physiological role of insulin is compromised: pancreas could not produce enough amount of it or target cells are not correctly responding[3]. Insulin role is to regulate the metabolism of carbohydrates, fats, proteins and promotes the uptake of glucose from bloodstream in cells such as skeletal muscle and liver[4]. In this way, glucose uptaken from food is used for energy. An healthy subject shows bloodstream glucose levels between 60-99 mg/dl; diabetes is confirmed when it reaches levels beyond 126 mg/dl[5].

This could happen for various reasons, so diabetes could be divided in three main types:

1. **Type 1 diabetes**.

   It occurs since pancreas produces not enough amount of insulin. It happens because of the loss of beta cells by autoimmune reaction which causes are still unknown[4]. Also known as 'juvenile diabetes', it typically begins in childhood or adolescence[6]. It is believed that both genetic and environmental factors are involved in such effect and, once that beta cells are destroyed, insulin treatment is required for survival[4].

2. **Type 2 diabetes**

   On the other hand, type 2 diabetes (T2D) occurs since cells are not responding properly to insulin (IR)[4]. That brings to high glucose level and to the onset of several associated pathologies. It represents almost 90% of all diabetes cases and it mainly occurs due to obesity conditions, lack of exercise, high sugars and fats diet consumption[7].

3. **Gestational diabetes**.

   Its onset regards pregnant women that develop high blood sugar levels [7]. Generally their blood sugar level returns normal by time, but if they could have an higher risk to develop type 2 diabetes later in lifetime.

T2D is characterized by an inadequate level of insulin since body gets resistant to it. This condition affects mainly muscles, liver and adipose tissue[8]. Normally, glucose release from liver is inhibited by insulin, but, in this case, it is redirected in bloodstream enhancing its level even more[9]. Generally, it seems that the onset of T2D is a combination of IR and a defect on insulin production and the proportion differs among individuals.

In association with IR, this disease is also characterized by an enhanced lipolysis which brings to an increased fats flux in bloodstream, high glucagon levels, osmotic alteration in kidneys and alteration in central nervous sistem metabolism [9]. In the first phases of insulin resistance, beta cell expand in order to produce more insulin trying to compensate its inefficacy, but, later in the disease, FOXO1 is activated by fatty acids and results in an induction of apoptosis [10].

T2D is caused by several factors affected by a combination of lifestyle and genetic. It is known that eccess weight and obesity, low excercise, sedentary lifestyle are risk factors[11]. Insulin resistance seems to be connected with these conditions. High triglycerides levels bring to an increased volume of adipocytes, which are insulin resistant, so it is difficult to arrest lipolysis throug insulin interaction. So free fatty acids (FFA) and glicerol levels are enhanced, resulting in an overload in liver and muscle tissue[12]and several side effects (lipotoxicity).

High level of glucose is toxic for the organism, bringing to several irreversible damages[13]. Oxidative metabolism of glucose results in the production of reactive oxygen species (ROS) which need to be neutralized. Otherwise its accumulation could seriously damage cells, particularly in tissues with a lower level of catalase, superoxide dismutase and glutathione peroxidase responsible for ROS detoxification[13]. In such conditions, NFkB activity could be enhanced, increasing its chances of activation resulting in apoptosis of beta cells[12]. Moreover, PDX-1 (Pancreas Duodenum homeboX 1) also known as insulin promoter factor 1 and is important for pancreatic development, seems to be reduced[12].

Globally talking, T2D is considered a real pandemic and represents one of the main challenges for the 21th century human health. According to International Diabetes Federation (IDF) datas, in 2019 almost 463 million of people were affected by T2D all around the world. It is feared that this number could even rise to 578 million by 2030 up to 700 million by 2045[14]. And to make matters worse, over 4 million of people aged 20-79 years died due to diabetes in 2019 (representing one of the top ten causes of death)[14].

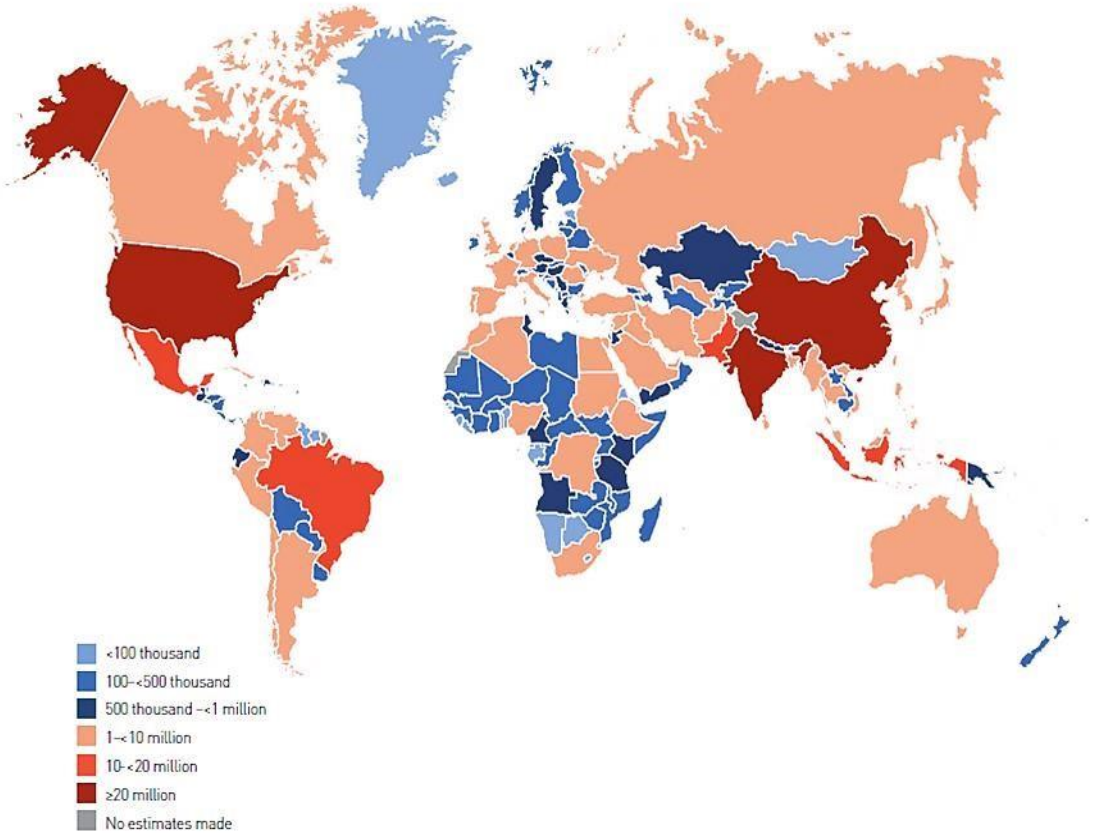

Fig. 2. The picture shows the estimation of the amount of people (between 20-79 years old) affected by diabetes in 2019[14].

Even if the risk of T2D development is related with aging, the number of children affected by it is globally rising every year. This is caused by the increasing of obesity cases connected with the reduction of physical activity, so diabetes represents an health problem which affects also children and adolescents[14].

Among diabetes associated pathologies it is described a rising risk of hypertension and hypercholesterolemia, but, fortunately, some of them could be avoided with primary and secundary prevention[15]. In many studies performed on several populations, it is confirmed that by modifying lifestyle bad habits, risk of diabetes development was reduced by 30-50 %. For example, by performing aerobic exercise of medium intensity for 20-30 minutes per day, the risk of T2D development was reduced by 60% resulting in a preventive strategy of great impact[16].

Modifying also food habits seems to be crucial, it is described that a fiber rich and low glucose diet could be beneficial against T2D, just as replacing saturated fatty acids with mono-polyunsaturared ones[5].

Actual therapies and drugs

As always, prevention is the best option: this approach is secure, convenient and long lasting. Otherwise, drug therapy is needed, taking into account its side effects. Some of these drugs act by enhancing insulin secretion, increasing insulin sensitivity, or by reducing glucose intake at intestinal level. Such as:

- **Biguanide class**: among which we find phenformin (withdrawn from markets in late 1970s due to high risk of lactic acidosis fatal in 50% of cases), buformin and metformin, which is the most used for T2D treatment[17]. Metformin lowers glucose level in bloodstream, induce more sensitivity to insulin and reduces the risk of hypoglycaemia. It is unclear how, but it is capable to reduce the uncontrolled release of glucose by liver, probably by acting on AMPK protein kinase (which is involved in gluconeogenesis genes expression). Moreover metformin lowers cardiovascular risks[18,19].

- **Sulfonylureas:** just as glyburide, glipizide, gliclazidee and glimepiride. They enhance insulin secretion, by interacting with specific receptor on the membrane of pancreatic beta cells and inducing a membrane depolarization. In this way the insulin-containing vescicles exocytosis. is triggered. The resulting hyperinsulinemia overcomes insulin resistance and glucose levels begin to lower. Among side effects are described hypoglycaemia and weight gain[20].

- **Thiazolidinediones** (TZD): are a class of insulin-sensitizing agent. In other words, they enhance endogenous insulin effect on peripheral tissues, like skeletal muscle and adipose tissue, liver acting on gene expression. They include troglitazone, rosiglitazone and pioglitazone. These drugs are high affinity ligands targeting the nuclear receptors PPAR-γ (Peroxisome Proliferator-Activated Receptor gamma). Without going into detail, their stimulation results in an enhanced GLUT4 (glucose transporter), glycogen synthase and pyruvate dehydrogenase transcription increasing in this way glucose metabolism. Fatty acids oxidation is also involved and increased, more smaller adipocytes are produced and exhibit insulin sensitivity. In this way FFA release and their storing in liver and muscle is reduced [21].

- **α-glucosidase inhibitors**: in this class we find acarbose, miglitol and voglibose. These compounds are competitive inhibitors of glucosidases, which are enzymes located in the brush border of the small intestine that break down starch and disaccharides to glucose. In this way the glucose uptake from food is limited, reducing post-prandial blood glucose excursions[22].

- **Incretin**: these hormones are released in the instestine following meals, such as GLP-1 (Glucagon-Like Peptide 1). They stimulate insulin secretion but they have a short half-life since are degraded by the dipeptidyl peptidase-IV (DPP-IV). The idea is to develop incretins analogues non-degradable and with inhibition action on DPP-IV. Other examples of strategy are the usage of agonist of GLP-1 and inhibitors of the sodium/glucose cotransporter 2

(SGLT2) involved in glucose reabsorption in the kidney. In this way, less glucose is reabsorbed and a big amount is discarded through urine. Glucose in bloodstream lowers in this way[23].

Several approaches of therapy are confirmed but, despite the beneficial effects, many of them seem to be transient, in medium-long term diabetic patients get a worsening of their health condition. On first place the reaction is to up-scale the dosage in order to take under control glycemic level but adverse effects of such approach inevitably occurs[24]. This mono-drug therapy seems to be uneffective on long time since it is not capable to replace the effect of insulin, which is, of course, a multi-factorial agent. In other words, these drugs could compensate a specific metabolic defect but they trigger unbalances in others. New approach are needed and new ideas are being tested, in the following chapter an interesting therapeutical target will be described which is the purpose of this work: the **Protein Tyrosine Phosphatase 1B** (**PTP1B**), which seembs to be connected with the development of insulin resistance [25].

PTP1B as therapeutical target for T2D treatment

One of the most used signalling pathways strategies is the alteration of phosphorylation status of proteins. Two protagonists take part in this oppositely: kinases and phosphatases. The first transfer a phosphate group from ATP (adenosine triphosphate) to target amino acid residues, the second work in opposite way by hydrolyzing such bond releasing the phosphate. Regarding tyrosine residues, such activities on them are performed by phosphotyrosine kinases (PTKs) and phosphotyrosine phosphatases (PTPases). An alteration on their activities may be linked with the onset of several disease, PTP1B is considered an interesting therapeutical target for the treatment of diabetes and obesity[26]. It has been demonstrated it role as negative regulator of insulin and leptin signalling (leptin resistance causes the hunger feeling even if the body as enough fat stores). In detail, PTP1B interacts with insulin receptor removing phosphate groups from its tyrosine residues, deactivating it. The consequence is the modulation/stoppage of insulin signalin transduction[26].

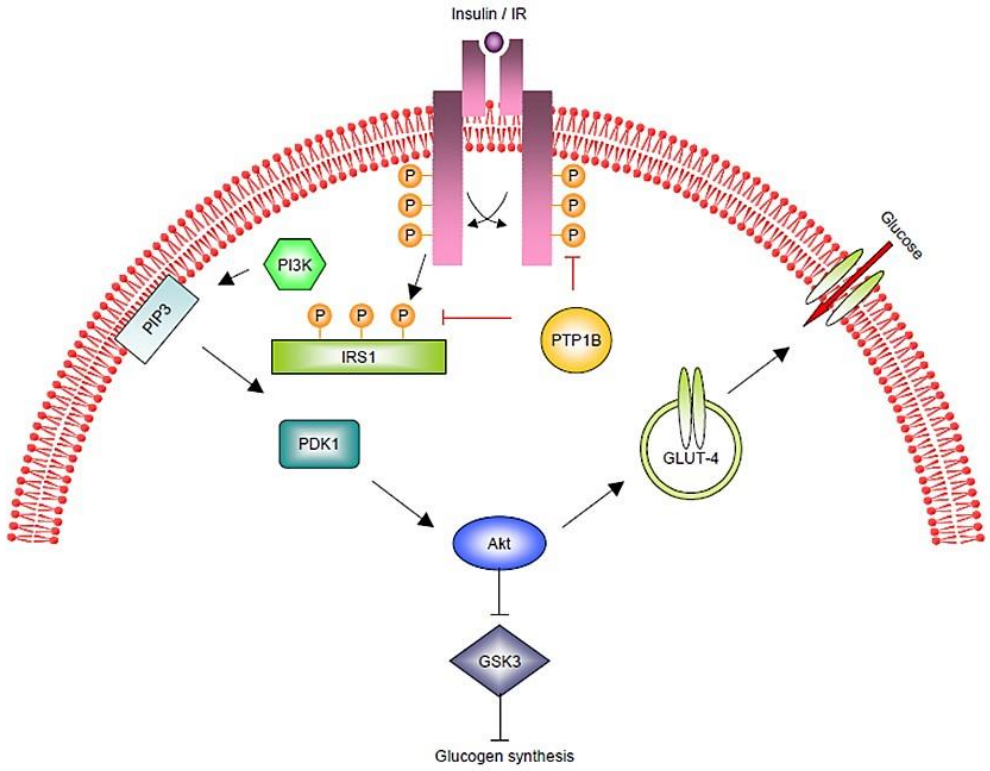

Fig. 3. Summarizing picture of the PTP1B role in insulin signalling pathway[26]. This enzyme regulates negatively the insulin receptor and other factors such as IRS1 and it seems to be one of the main responsibles of the type 2 diabetes occurrence.

Regarding leptin signalling, the PTP1B seems to target Jak-2 protein. Leptin is produced mainly by adipose tissue and interact with hypothalamic receptors Ob-R1. The consequence is the activation of Jak 2 and as result it is triggered the transcription of genes involved in the fatty acid homeostasis. If this balance is alterated, fats begin to accumulate in liver and muscle causing lipotoxicity. In

obesity cases, leptin-resistance is observed, just as insulin-resistance is associated with T2D. Inhibiting the PTP1B has a great therapeutical potential in both cases[27].

Several studies on PTP1B deficient mice, showed an increased sensitivity toward insulin and an enhanced activation of IR through phosphorylation in liver and muscle tissues. These mice resulted less inclined to take weight and showed less free triglycerides even when fed with a high fats diet. That could be explained by a larger energy expenditure which is related, probably, with leptin enhanced sensitivity[26].

PTP1B is a 50 kDa protein that includes 435 amino acids and an extended C-terminal segment; its catalytic site is formed by residues 30-278, oriented towards cytosol. The 35 hydrophobic residues of the C-terminal segment, ensures the enzyme at cytosolic interface of endoplasmic reticulum (ER)[28]. Previous studies confirmed the presence of an insulin-indipendent interaction between PTP1B and IR at ER level which take place during the receptor biosynthesis. During insulin stimulation, IR is internalized via endosome and interacts with PTP1B on ER[29].

PTP1B shares several structural features with other tyrosine phosphatases: the P-loop (Phosphate binding loop) and the WPD loop. The active site interacts with the target phosphate through the catalytic cysteine Cys 215, the interaction is stabilized by several hydrogen bonds between the phosphate and the P-loop. Other residues (Phe182, Tyr46, Lys120, Gln262, Val49, Arg47 e Asp181) are crucial for the substrate recognition through hydrophobic/electrostatic interactions and hydrogen bonds[28].

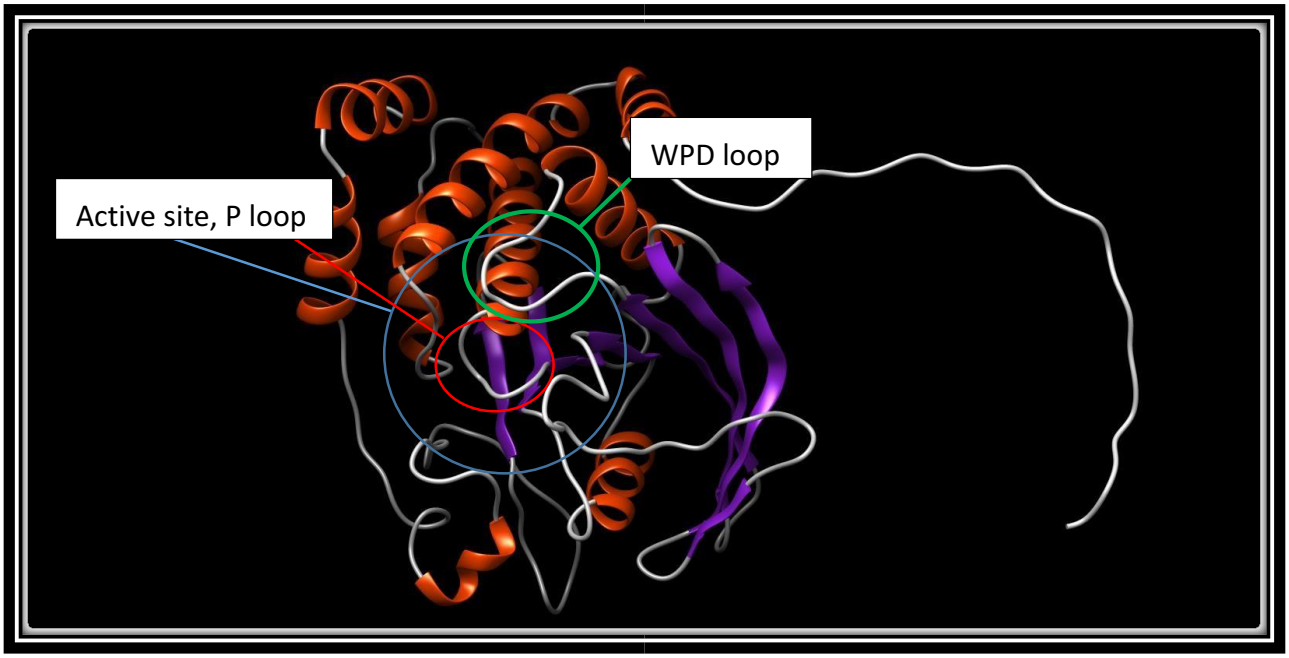

Fig. 4. PTP1B structure showed by using UCSF Chimera software. The structure was obtained from PDBank database (https://www.rcsb.org/). Both active site (P-loop) and WPD-loop are shown on protein surface.

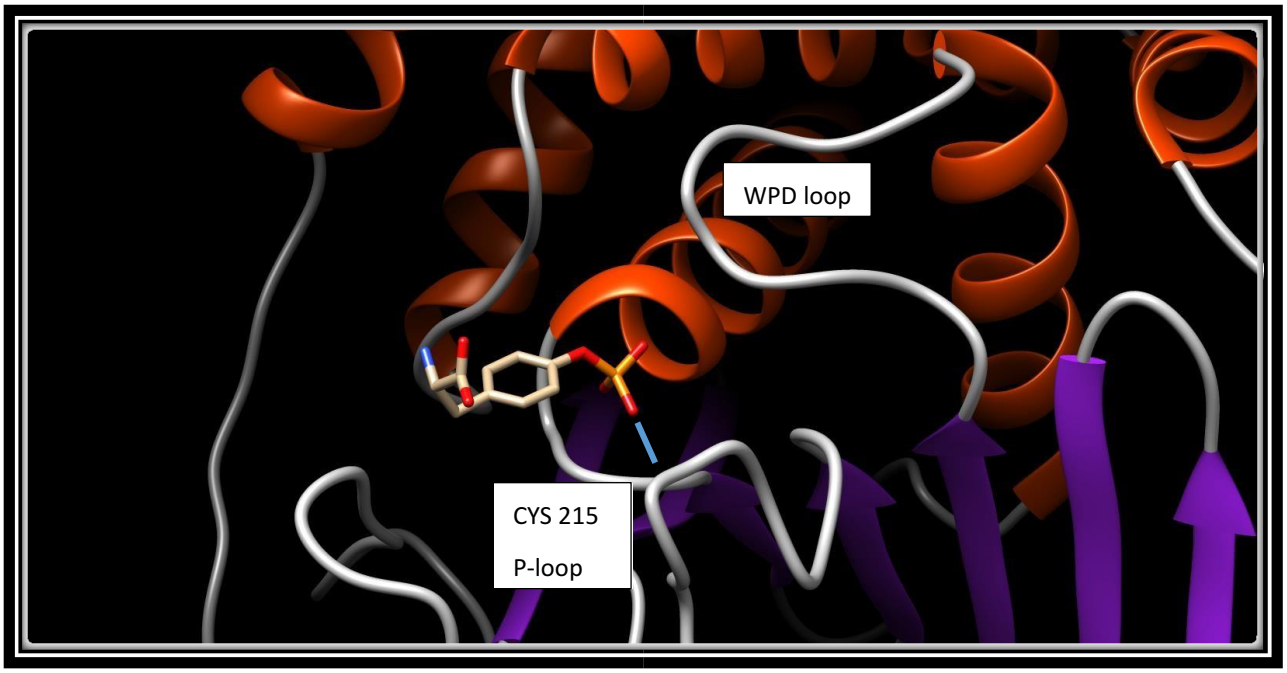

Fig. 5. In this figure, the tyrosine phosphate (target residue) is represented in the active site of PTP1B (interacting with CYS 215, the core of the reaction).

PTP1B catalysis happens in two steps. At first there is the formation of enzyme-substrate complex (phosphotyrosine containing substrate). The WPD loop changes is conformation from open to a closed one, with the formation of interactions between Phe180 and Asp181 and the phosphotyrosine. At this point Cys215 of the catalytic site, binds covalently the phosphate group by performing a nucleophilic attack on phosphorous atom, later the Asp 181 breaks its bond with phenyl group by acting as acid.

The second step sees the bond between phosphate group and enzyme broken by hydrolisis reaction.

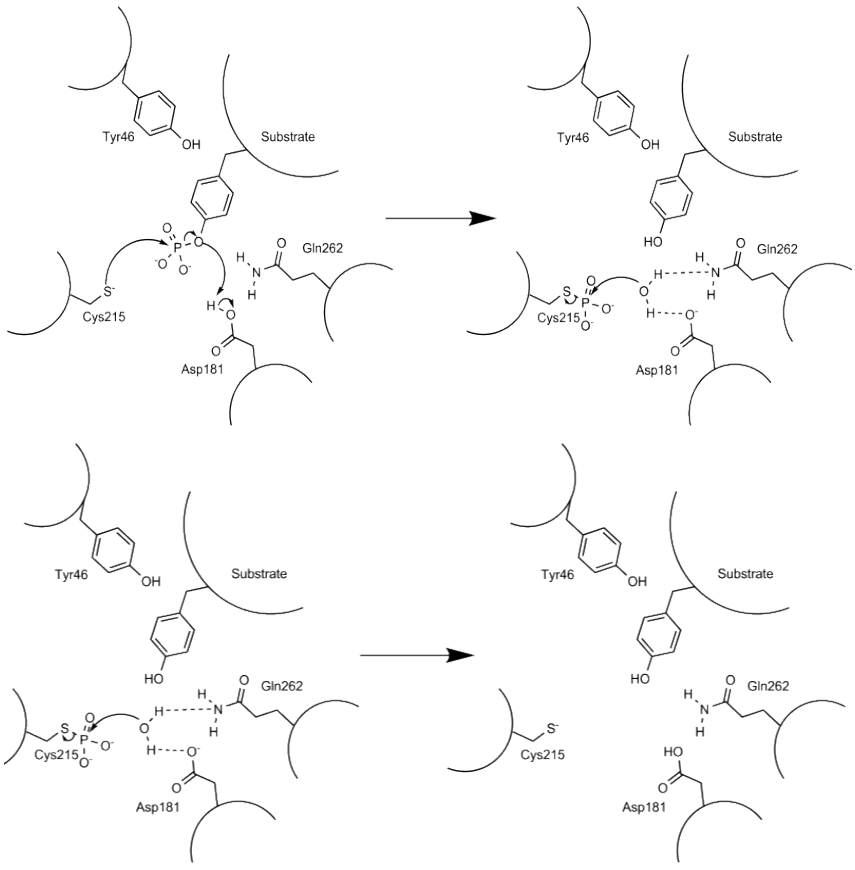

Fig. 6. Picture of PTP1B catalysis mechanism summarized in two steps[41].

The Asp181 recovers a proton from water and the activated water molecule performs a nucleophilic attack on phosphorous atom releasing inorganic phosphate. At this point, the WPD loop recovers its open conformation[40].

In last years many molecules, natural and synthetic, were identified to be able to inhibit specifically PTP1B, with the idea to develop new drugs for the treatment of T2D and obesity starting from these scaffolds[30]. Thousands of new natural inhibitors are discovered each year, covering a great variety of chemical classes. In this way numerous different scaffolds could inspire the synthesis of new compounds, going over the bioavailability issue. These new structures would be optimized following the needs of pharmacokinetics and dynamics, specificity, lowering side effects, and so on.

Among them we find:

- **Phenols**: this class is the most representative of natural PTP1B inhibitor compounds, showing several beneficial effects on human health such as anti-inflammatory, anti-oxidant, anti-viral and anti-bacterial ones[31]. This class is characterized by flavonoids, phenolic acids, bromophenols, benzofurans, tannins and lignans. Each of these groups offers strong PTP1B inhibitors, suggesting many different structures for drug development[32].

- **Steroids**: structural component of plasmatic membrane. Most of them were largely used in medicinal chemistry and showed inhibitory activity on PTP1B33. They can be found marine organism like algae and sponges, in plants and other sources.

- **Alkaloids**: organic compounds containing nitrogen, in plants they play a defense role against pathogens. They show anti-inflammatory, anti-cancer and anti-diabetic properties. Just as an example, some of them isolated from *Houttuynia cordata* showed inhibitory activity on PTP1B with range of IC_{50}* within 1.3-2.7 µM[34].

  *****: indicates how much of a particular inhibitory substance (e. g. drug) is needed to inhibit, *in vitro*, a given biological process or biological component by 50%[35].

- **Fatty acids**: Many elements of this class showed interesting inhibitory activity on PTP1B, among saturated and unsaturated ones (Showed in **Table 1**).

Table 1

Type	Name	IC_{50} (µM)	Alkyl chain lenght
Saturated	Palmitic acid	8.8	16
	Stearic acid	2.3	18
	Arachidic acid	1.6	20
Unsaturated	Palmitoleic acid	16.1	16
	Oleic acid	6.2	18
	Linolenic acid	9.7	18
	Linoleic acid	6.4	18
	Eicosenoic acid	1.4	20

These studies confirmed that the inhibition potency does not correlate with the degree of unsaturation, but it seems that depends on the number of carbons in alkyl chain: the longer the chain, the stronger the inhibition[32].

Other studies investigated their mechanism of action, and it seems that by inhibiting PTP1B, PI3K/PDK1/Akt pathway resulted improved and Akt kinase activity enhanced[36]. PI3K-Akt signaling pathway is a signal transduction pathway that promotes survival and growth in response to extracellular signals. Crucial proteins involved are PI3K (phosphatidylinositol 3kinase) and Akt (protein kinase B). Akt signalling correlates with an increase in glucose metabolism and enhances the translocation of glucose transporters GLUT1 and GLUT4 to the plasma membrane[37].

As said before, developing selective drugs to target PTP1B is quite changeling since tyrosine phosphatases active site is well conserved across the class. Many studies confirmed the importance of sites adjacent to catalytic one which could be specific for each phosphatase[38]. The sites are crucial for substrate recognition, and, by targeting them, the catalysis may be successfully compromised while not affecting other phosphatases.

The most homologous phosphatase to PTP1B is the T-cell protein tyrosine phosphatase (TCPTP) with 72% identity in the catalytic domain. It is a regulator of hematopoiesis and cytokine response[39] and its inhibition is related to bone marrow destruction. Since the structures are so similar, TCPTP could be used as reference for assessing the specifity of PTP1B inhibitors[40].

Among synthetic inhibitors we found analogues of nicotinic acid showing IC_{50} values at nanomolar range, and tetrazole analogues with IC_{50} of 5.2-21.8 nM[30]. By now several synthetic compounds are being developed and act as potent inhibitors with various mechanisms of action. Among the strategies, some of them target the allosteric sites, while others are developed to interact with catalytic site and the specific area around it.

Wiesmann et al. described a novel binding site on this enzyme thanks to co-crystallization procedures with three non competitive inhibitors (PDB ID: 1T48, 1T49, 1T4J)[42]. This allosteric site could suggest the development of specific inhibitors of PTP1B. It is believed that these inhibitors move the Trp291 of α7 helix and take its position, interacting in this way also with residues belonging to α3 and α6 helices. During the catalysis several hydrogen bonds between these helices are necessary to the closure of WPD loop. These inhibitors interfere with such dynamic destabilizing hydrogen bonds network and preventing the correct movement of WPD loop[43]. Several studies including molecular dynamics (MD), helix modelling, energy analysis were performed on allosteric sites and inhibitor and it turns out that α7 helix has a critical role in WPD loop dynamics[40].

Since this site has some different residues with TCPTP one, it could represent an exclusive allosteric site of PTP1B interesting for specific drug development[40]. The protein tyrosine phosphatases family is also represented by other enzymes called Low molecular weight PTPs (LMW-PTPs)[44]. These 18kDa proteins show a very limited sequence similarity to the PTP superfamily while displaying, of course, a conserved signature motif in the catalytic site. LMW-PTPs associate and dephosphorylate many growth factor receptors, such as platelet-derived growth factor receptor (PDGF-r), insulin receptor

and ephrin receptor, thus downregulating many of the tyrosine kinase receptor functions that lead to cell division. In particular, LMW-PTP acts on both growth-factor-induced mitosis, through dephosphorylation of activated PDGF-r, and on cytoskeleton rearrangement, through dephosphorylation of p190RhoGAP and the consequent regulation of the small GTPase Rho. LMW-PTP activity is modulated by tyrosine phosphorylation on two specific residues, each of them with specific characteristics. LMW-PTP activity on specific substrates depends also on its localization. Moreover, LMW-PTP is reversibly oxidized during growth factor signaling, leading to inhibition of its enzymatic activity. Recovery of phosphatase activity depends on the availability of reduced glutathione and involves the formation of an S–S bridge between the two catalytic site cysteines. Furthermore, studies on the redox state of LMW-PTP in contact-inhibited cells and in mature myoblasts suggest that LMW-PTP is a general and versatile modulator of growth inhibition[44]. Two of them correspond to the classical active isoforms 1 and 2, IF1 and IF2 and no differing physiological effects between them have so far been demonstrated[44]. In this study LMW-PTPs were also used to assess any specificity in inhibition potential of tested compounds over the PTPs.

Recently, Zhang has proposed a novel approach to develop competitive inhibitors of PTP1B by interacting with its catalytic site. Despite the fact that target site is well conserved through PTPs family, these promising molecules could target exclusively PTP1B[45].

Zhang and collaborators managed to develop these inhibitors (with Ki values of nanomolar range), by using nonhydrolyzable pTyr mimetics[45]. These inhibitors could act in bivalent way, the pTyr portion would afford substrate recognition and access to the active site, while the remaining part could interact to the peripheral pockets around it that are specific and non conserved through PTPs family. These molecules show high affinity and selectivity. Moreover, they described several nonhydrolyzable pTyr mimetics that were enough polar to penetrate cell membrane[45].

A special focus will be given to the natural world as an inspiring source of molecules that can be used for drug development.

Drug discovery

Get inspired by nature

Nature displays a huge number of compounds that cover a wide range of different structures. This chemiodiversity played a significative role in drug discovery and development for the treatment of diseases.

These natural compounds offer new scaffolds as basis of new modification: once identified a potential treatment application on a disease, they could be chemically synthetized and optimized to preserve the natural source[46].

Most of them found application for HIV, malaria, diabetes and cancer treatment but we are still far from the end of this battle. There is still the need for novel drug discovery and development and nature can offer solutions. For example, drugs with anticancer activity such as taxol (*Taxus brevifolia*) and vinblastine (*Catharanthus roseus*) were all discovered from natural products and showed effective results.

These compounds have been through selective evolution processes and found a role in ecosystem. As secundary metabolites they give a selective advantage to the organism and are not required for growth or reproduction.

Plants, for example, conquered the entire environment, despite their sedentariness and continous stresses working on them. The winning strategy was to develop chemical defence mechanisms against predators, competitors and other environmental stresses[47]. These compounds are responsible of aromas, color and of course toxicity and many records report the usage of them for medical purposes[46].

These natural products were used as source of drugs for many applications, such as anticancer and microbial[46]. With great success, almost a quarter of approved drugs are plant based: Paclitaxel and Morphine are two examples, respectively isolated from *Taxus brevifolia* and *Papaver somniferum*[48]*.* Traditional approach used plant extracts and they were given as mixture. Patiens perceived an improvement of their condition and some of these methods fortunately survived through centuries. Focusing on a disease, it is possible that these beneficial effects are the resulting of a synergistic action of the present bioactive molecules. This effect makes sense, considering that diseases like diabetes and cancer are characterized by several factors involved in. In this scenario, acting on these critical protagonists at once could be a valid approach. We think that important informations are hidden in these traditional approaches and by identifying and studying the responsible molecules could suggest a strategy of treatment. Several new drugs could be discovered and, by coordinating their effects on these key factors, could bring to an improvement of health condition[49].

In order to trace them from the mixtures, the fractionation and extraction are valid options. Enzyme-assisted extraction, molecular distillation methods, membrane separation, high performance liquid chromatography, mass spectometry, nuclear magnetic resonance and others, are sofisticated extraction methods and could bring us to the identification of the key components of a natural extract[46]. As described before, unbalanced diet is one of the main factors linked to T2D, so a healthy

nutrition is one of the best prevention strategies[22]. Food rich in bioactive molecules could help to improve glycemic control. One example of such food is tea extract.

Tea is one of the most popular drink around the world and it is largely believed that regular intake brings many beneficial effect for health like preventing diabetes onset and other chronical diseases[50]. In fact, several preclinical studies confirmed that tea components are able to improve insulin sensitivity, glucose uptake and glycogen synthesis[51]. We decided to perform specific analysis to identify its bioactive molecules and to assess any effect on PTP1B. Our hypothesis was confirmed as many of these molecules have strong inhibitory effect on PTP1B such as the Epigallocatechin-gallate (IC_{50} of nanomolar range), suggesting a new scaffold for antidiabetic drug development[50]. Details will be described in Results section.

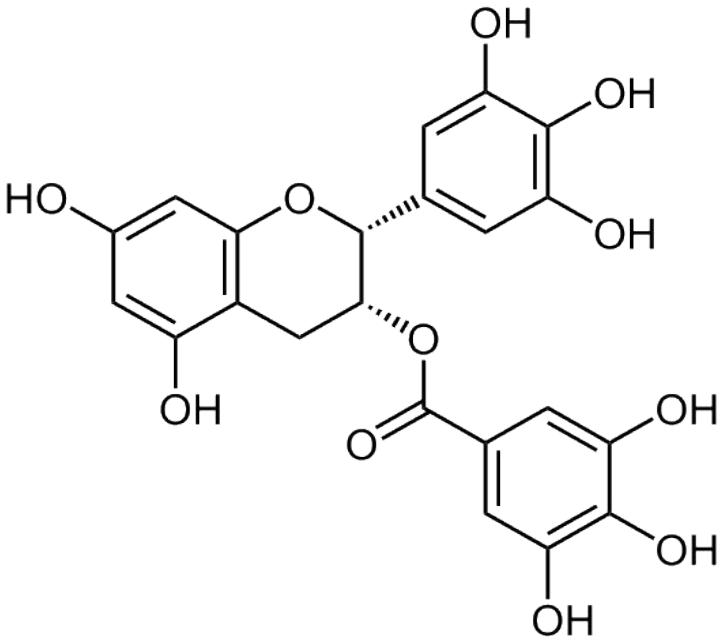

Fig. 7. Epigallocatechin gallate structure.

Fig. 8. Gossypetin structure.

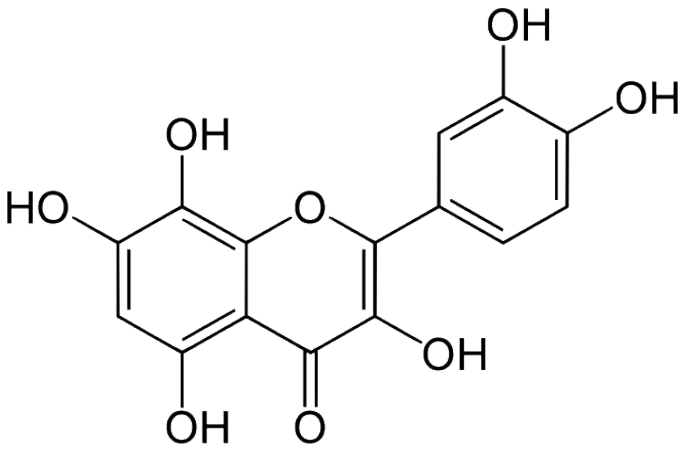

As mentioned in previous chapter, many PTP1B natural inhibitors belong to flavonoid class, they show different chemical structures characterized by many different substituents such as aliphatic chains, aromatic rings, hydroxyl groups[52]. Among these compounds, Gossypetin emerged as the most potent PTP1B inhibitor among flavonoids (Ki: 49.2 ± 9.8 nM). So we decided to compare its structure with less potent flavonoids in order to identify key substituents responsible of this strong effect. More details will be given later in this thesis.

Natural chemiodiversity is closely linked with ecosystem biodiversity: generally, the larger the number of organisms interacting each other, the higher the variety of chemical compounds evolved in the environment.

Marine environment is populated by many sessile invertebrates such as sponges, corals, ascidians and so on, which produce a huge variety of chemical compounds. These molecules found role as

feeding deterrent, keeping competitors under control or as predation tool[53]. Generally the producers of these compounds are symbiotic bacteria.

Sponges in particular were a source of inspiration for the development of pharmacological active compounds like peptides, alkaloids, steroids, terpenes, lactones, polyketides, glycoproteins, biopolymers and others of therapeutical interest[53]. For example, Halichondrin B was isolated from the sponge *Halichondria okadai* and it is active on B-16 melanoma cell line showing an IC_{50} of 0.09 nM. Further studies confirmed that this compound exerts it cytotoxic activity through tubulin interaction by destabilizing it. This effect bring to apoptosis since chromosomes cannot correctly segregate in mitosis. Halichondrin B went through preclinical studies but the amount was limited to the natural source. So several analogues were synthetized in order to find the minimum pharmacophore and some of them were succesfully active[54].

Sponges apart, also abscidian are prolific producers of bioactive natural products. It is a class of marine invertebrate filter feeders which produce several molecules with ecologic function (selfdefence for example). They are generally characterized by biologically active heteroatoms, nitrogen and oxygen[53]. As example, the lepadin family was identified from abscidians belonging to genera *Clavelina*, *Didemnum* and *Aplidium.*

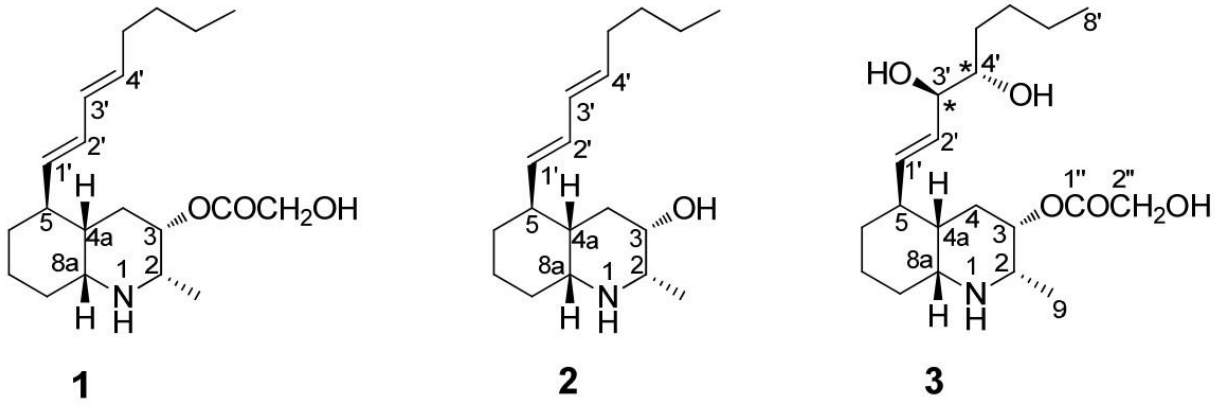

Fig. 9. Structures of Lepadin A (1), B (2) and L (3)[53].

Lepadin alkaloids showed several biological activities ranging from cytotoxic effects on cancer cell lines, inhibition of tyrosine kinase and butyrylcholine esterase activity, and antiparasitic properties. Thus, lepadins may represent a promising class of marine natural products for the development of novel therapeutic agents. Alongside these interesting and varied pharmacological activities, the limited amounts of natural metabolites which can be isolated by complex screening procedures with the risk to have altered biological responses, as well as the hard issue to solve the definitive configurational assignments, have encouraged several researchers to undertake synthetic protocols for obtaining lepadins.

However, the synthesis of lepadins requires a conspicuous number of highly stereoselective synthetic steps which represents a not easily accessible route for obtaining the native metabolites. Indeed, only recently, Tong et al. have reported a more attractive synthetic strategy for constructing the common cis-fused decahydroquinoline ring of several lepadins by a green chemistry approach[55].

For this reason, the isolation of new examples of lepadin alkaloids remains a key factor to enlarge the great chemodiversity associated to this chemical class, and to provide further new structural motifs that can represent a valuable resource both to grow up the knowledge on their bioactivities and to assess accordingly structure-activity relationships.

An exhaustive examination of the chemical constituents of the Mediterranean ascidian *Clavelina lepadiformis* was performed to expand the knowledge on the alkaloid composition of this marine organism with the addition of a new decahydroquinoline-based compound named lepadin L (3)[53]. The three isolated alkaloids, the known lepadins A and B (1 and 2), as well as the new lepadin L (3), were evaluated for their antiproliferative activity against a panel of cancer cell lines (A375, MDAMB-468, HT29, HCT116 cells, and C2C12 myoblasts).

It was demonstrated that lepadin A behaved as strong cytotoxic agent toward A375, HCT116 cells, and C2C12 myoblasts, whereas lepadins B and L showed weak or no activity against all tested cancer cell lines. Lepadin A strongly inhibits migration and self-renewal capability of A375 cells and interferes with S phase inducing G2/M phase cell cycle arrest in this cell line. Together, these results suggested that lepadin A behaves as an antitumoral agent able to block cells cycle, cell migration, cell renewal ability, and to induce cell death. These findings agree with previous results showing that lepadin A, and to lesser extent lepadin B, was cytotoxic against several tumoral cell lines[53].

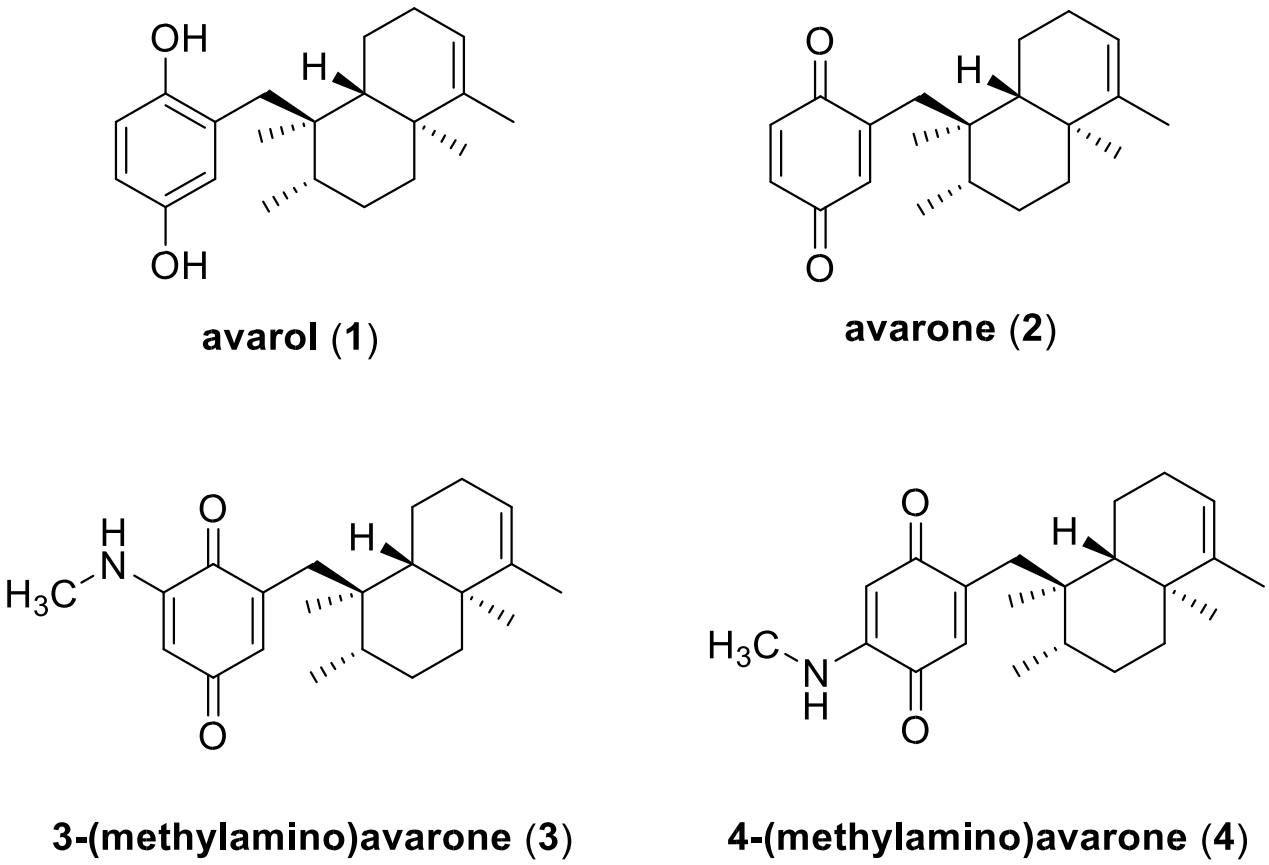

Fig. 10. Picture of Avarol (1), Avarone (2) and its methylamine derivative (3-4) structures[56].

Other marine compounds of interest are Avarol and Avarone, among first examples of natural hydroquinone and corresponding quinine that were isolated from the mediterranean sponge

Dysidea avara in 1976 by Minale et al.[56]. These compounds showed several pharmacological properties including cytotoxic, antimicrobial, antiinflammatory, antioxidant, antiplatet, antipsoriatic and anti-HIV activities. These interesting properties inspired us to test them on PTP1B and check if they exert any effect useful for treating diabetes. The outcome is of great interest and results will be later shown and discussed.

The choice of the most appropriate hypoglycemic drug for a patient depends on several factors, such as the health general condition, the presence of comorbidities, tolerance, and the responsiveness to it. Generally, most diabetic patients in early phase respond positively to singledrug based therapy, showing control over blood sugar levels and an improvement of their general conditions. However, many clinical studies showed that benefits obtained with this approach are transient, and in the medium to long term, patients experience a gradual rise in blood sugar and a worsening of general health conditions. In some cases, the up-scaling of drug dosage can be enough, with the hope that, at the same time, no adverse effects occur.

The failure of mono-drug therapy is mainly due to the inability of such drugs to replace physiological functions of insulin. As mentioned before, even if these drugs are able to compensate a specific metabolic defect, they unexpectedly induce severe unbalance in other metabolic pathways. The combination of two or more anti-hyperglycemic drugs acting on different biological targets is valid alternative. From a theoretical point of view, the purpose of this strategy is to generate a synergistic effect by acting on different factors. However, despite the undoubted advantages, many clinical trials revealed that multi-drug therapies are difficult to manage for the majority of patients for different reasons. It is required a fine dosage adjustment, and their assumption has to follow their different pharmacokinetics.

Sometimes this is very difficult to achieve and the consequent uncontrolled fluctuations in blood sugar can be deleterious, forcing patients to change treatment to avoid further complications. A practical solution to this problem may arise from taking combinations of oral hypoglycemic drugs in fixed and pre-established doses depending on the desired effects. This strategy reduces the complexity of therapeutic regimen and improves patient adherence to treatment. Overall, the clinical studies carried out so far confirmed that combinatorial therapies imply, in the short to medium term, significant benefits compared to mono-therapy. However, in the long term, the efficacy of this therapeutic approach remains to be confirmed. In conclusion, all evidence suggests that multitargets therapies seem to guarantee a better quality of life for people affected by T2D[57].

Multiple designed ligands (MDLs) for T2D treatment

Many single-target drugs resulted to affect several factors *in vivo*, which brings to side effects onset of therapy. This feature increases with the administration of several drugs at once since it is very difficult to follow different pharmaco-kinetics and dynamics that could lack in specificity and interact each other. On the other hand, while treating a multifactorial disease just like T2D diabetes, it seems to be essential to target different entities at once involved into this pathology.

It is becoming popular the idea to develop a single molecule which could target different factors. In this way it could be possible to lower side effects without losing the advantages of combinational therapy. Moreover, a single molecule results easier to follow since the pharmaco-kinetics and dynamics regard a single compound[57].

In T2D scenario, a multiple designed ligand (MDL) could improve glucose uptake by targeting the muscle tissue while reducing the total glucose intake from diet by working on gut. The most effective strategies to find promising dual target scaffolds are large-scale screening and knowledge-based approaches. Several *in-silico* methods could be used to identify the pharmacophores of interest for assembling new MDLs. That is beneficial since easy to perform and considers databases made of hundred of thousands of different molecules. The pharmacophores could be linked together to produce new potential MDLs ready to be tested and improved if necessary[57].

Coskun and co-workers projected and synthesized dual glucosedependent insulinotropic polypeptide receptor (GIP-R) and glucagon-like peptide-1 receptor (GLP-1) agonists and demonstrated that treatment with such molecule stimulated insulin release, leading to a significant reduction of both fasting and postprandial glycaemia[58]. In recent years, convincing evidence suggested that GLP-1 acts as anorexigenic peptide binding to GLP-1R in the hypothalamic region, inducing satiety[57]. Interestingly, it has been demonstrated that, in the brain, GLP-1 acts synergistically with PYY (peptide YY), a peptide that is co-secreted with GLP-1 from enteroendocrine L cells of the intestine and binds NPY2R (Neuropeptide Y receptor Y2 receptor). This finding stimulated many researchers to evaluate the activity of new GLP-1R/NPY2R agonists as antidiabetic agents. It has been demonstrated that GLP-1R/NPY2R dual agonists *in vivo* exert anorectic effects along with the ability to reduce blood glucose levels, thereby confirming that they could act as promising anti-obesity and antihyperglycemic agents[59].

Among all biological targets, peroxisome proliferation-activated receptors (PPARs) are considered some of the most effective ones for treatment of T2D. Various type of PPARs are differently expressed in human tissues; namely, PPAR-α, δ, and γ, have been identified and characterized to date. The PPAR-α is highly expressed in liver, kidney, heart muscle, and vascular endothelial cells, where its activation promotes fatty acid oxidation, thereby avoiding accumulation of intracellular lipids depots. Treatment with PPAR-α agonists increases cardiac performances in diabetic patients, reducing the risk of stroke[60].

PPAR-δ is ubiquitously expressed, and its activation leads to different effects. In muscle cells, PPARδ activation stimulates fatty acids oxidation, while reducing glucose utilization. In adipose cells, PPAR-δ activation increases the expression of genes involved in fatty acids β-oxidation and energy dissipation via uncoupling of fatty acids oxidation and ATP production[61]. Interestingly, it has been demonstrated that the balance of fatty acids oxidation and synthesis can affect inflammatory and

immunosuppressive T cells and macrophages. In macrophages, PPAR-δ activation impairs polarization toward M2-like phenotype with reduced inflammatory potential. According to this hypothesis, antidiabetic functions of PPAR-δ have been associated with reduced inflammatory signalling[62]. PPARγ is largely expressed in adipose tissue, and its activation promotes proliferation and differentiation of preadipocytes into adipocytes. Moreover, PPARγ agonists stimulate deposition of fatty acids into adipocytes, lowering fatty acids blood levels, preventing hyperlipidemia, and increasing peripheral insulin sensitivity. Saroglitazar, a PPARα/γ dual agonist, has been recently approved in India for treatment of diabetic dyslipidemia based on the promising results obtained in clinical trials[63].

Diabetic patients treated with Saroglitazar showed no adverse events, an improved lipidemic profile, an increased insulin sensitivity and β-cell function[64]. Recently, a novel dual peroxisome proliferator-activated receptor alpha/delta (PPAR-α/δ) agonist was synthesized and tested on animal models. Besides protecting the liver from inflammation, and fibrosis, the administration of dual agonists decreased hepatic lipids accumulation, protecting animals from the development of liver steatosis[65]. Finally, many efforts have been made to generate pan PPAR agonists combining the pharmacophore motif of known PPAR-agonists. Such molecules reduce lipids accumulation in the liver and improve liver damage, inflammation, fibrosis, and insulin resistance[66,67].

Although many new pan PPAR agonists have demonstrated their efficacy as antidiabetic drugs in the preclinical phase, subsequent clinical studies have shown their limitations and revealed their intrinsic toxicity. For these reasons, studies on these molecules have not progressed further[57].

Very recently, Qi Pan and coworkers evaluated the antidiabetic activity of GLP-1- Fc-FGF21 on diabetic and obese mice models. This new dual targeting agonist, able to target both the GLP-1 and FGF21 (Fibroblast growth factor 2) pathway, showed a potent antihyperglycemic activity and caused a marked weight loss, suppressing the appetite and reducing caloric intake. Together, these results suggested that GLP-1/FGF21 dual agonists possess all characteristics to become promising new drugs to fight diabetes and obesity[68].

We are convinced that MDLs targeting both PTP1B and α-glucosidases could be used to control glucose level in T2D.

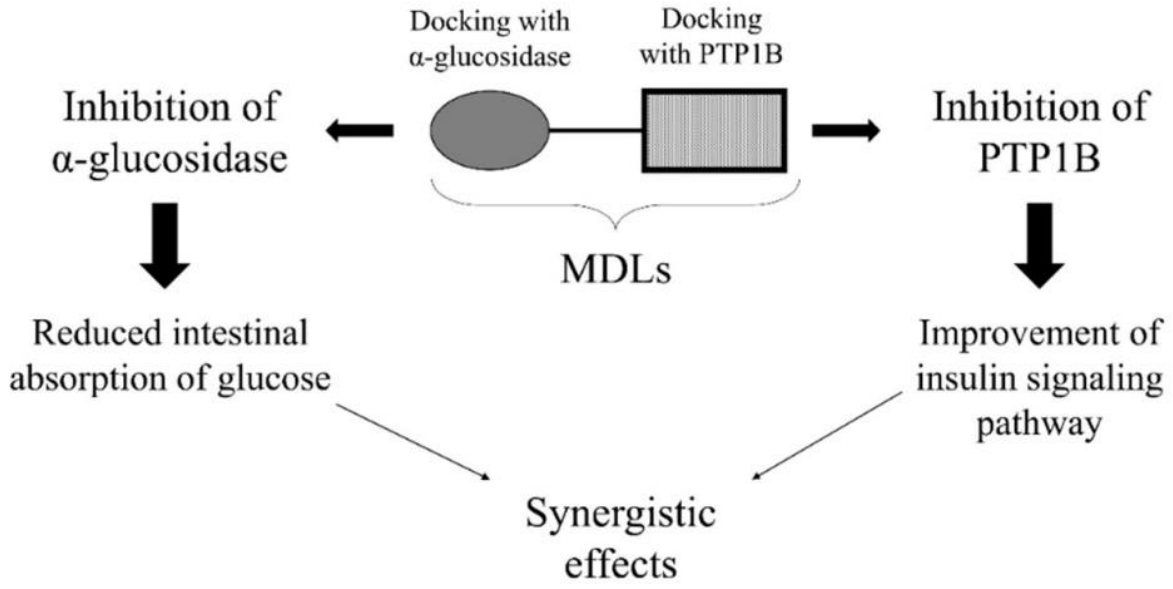

Fig. 11. Mechanism of action of a dual PTP1B/α-glucosidase inhibitor. Such molecules possess a structure able to inhibit both targets involved in the same disease, inducing a synergistic effect[57].

Monosaccharides, such as glucose, fructose, and galactose, are the only sugars absorbed by gut. Oligosaccharides derived from starch digestion are processed by pancreatic α-amylase and intestinal α-glucosidase to produce free glucose that is then uploaded from intestinal cells. Therefore, the rate of blood glucose mainly depends on the gut glucose concentration that, in turn, is influenced by the activity of glucosidases present in the gut. This finding inspired many researchers to challenge glucosidase inhibitors as pharmaceutical tools for the treatment of T2D based on the hypothesis that such molecules could delay the release of glucose from complex carbohydrates, slowing down the rise in blood sugar levels observed after a meal. In the last decades, different kinds of glucosidases inhibitors have been produced and approved as antihyperglycemic drugs[57].

Today, such molecules are used as first-line therapy for T2D patients or administrated in combination with other oral anti-diabetic drugs when metformin/biguanides mono-drug based therapies failed the achievement of the glycemic goal[69]. The evidence that glucosidases inhibitors act synergistically with different oral antihyperglycemic drugs suggested that α-glucosidase/PTP1B dual inhibitors could be successfully projected and used as drugs for treatment of T2D.

Some studies conducted in the last three years demonstrated the potential effectiveness of dual αglucosidase and PTP1B inhibitors. In 2017, Mei-Yan Wang et al. demonstrated that (azole-2-yl) sulfonylalkanamides can target both α-glucosidase and PTP1B, paving the way for the development of new MDL antidiabetic drugs. The most potent compound among them showed IC_{50} values for αglucosidase and PTP1B of 10.96 and 13.45 μM, respectively, and a good selectivity for PTP1B[70].

Recently, Xhenti Ferhati et al., demonstrated that by linking an iminosugar moiety with a phosphotyrosine mimetic, it is possible to create a new generation of antidiabetic drugs affecting both PTP1B and α-glucosidases and showing IC_{50} values for α-glucosidase and PTP1B in the 4–200 μM range. Moreover, tests carried out on HepG2 cells demonstrated that some of these compounds show a good insulin-mimetic activity, enhancing phosphorylation levels of Akt in the absence of insulin stimulation. We can hypothesize that, in absence of insulin, the PTP1B inhibition results in an enhancement of insulin receptor phosphorylation level, promoting the activation of insulin signaling pathway[71].

Finally, in 2020, Malose J. Mphahlele et al. investigated the properties of a series of orthohydroxyacetyl-substituted 2-arylbenzofuran derivatives, showing that some of these have IC_{50} values in the submicromolar and in the micromolar range for α-glucosidase and PTP1B, respectively[72].

We analyzed literature data looking for natural molecules showing both α-glucosidase and PTP1B inhibitory activity that should be used as scaffold molecules for the synthesis of new dual-target antidiabetic drugs. Data collection from the literature was performed by querying the PUBMED database, using specific keywords, such as "PTP1B and alpha-glucosidase inhibitors" (which yielded 79 results), "alpha-glucosidase and PTP1B" (48 results), "Dual targeting PTP1B and glucosidase" (6 results), and "PTP1B and multitarget inhibitors" (6 results). Every single study was downloaded and analyzed in depth to extract the data of interest. The collected compounds were classified into twelve different groups based on their chemical structure. Surprisingly, we found that, in the last twenty years, more than 200 compounds showing dual α-glucosidase/PTP1B inhibitory activity have been discovered and characterized[57].

Aldose reductase (AR) has become another potential for T2D treatment and its complications. It is a cytosolic enzyme involved in the polyol pathway, in which glucose is converted to sorbitol that is, in turn, transformed in fructose through the NAD+-dependent action of sorbitol dehydrogenase.

In hyperglycaemic conditions, due to saturation of the glycolytic enzyme hexokinase, an increased flux of glucose is redirected towards the polyol pathway, leading to several metabolic alterations. In particular, the accumulation of the osmolyte sorbitol increases cellular osmolarity, inducing a deleterious cell swelling. At the same time, the advanced glycation end product formation, linked to increased fructose levels, promotes ROS generation and NF-kB expression, leading to oxidative stress. In addition, the NADPH depletion linked to AR activity impairs the glutathione-reductasedependent recovery of reduced glutathione. On the other hand, the increase in NADH/NAD+ ratio might lead to NADH oxidase upregulation, thus further promoting oxidative stress. Under these conditions, lipid peroxidation occurs, with the consequent formation of cytotoxic aldehydes, including 4-hydroxy-trans-2-nonenal and its derivative conjugated with glutathione (GS-HNE). AR reduces GS-HNE in the corresponding alcohol (3-glutathionyl-1,4-dihydroxynonane), which promotes the expression of NF-kB. In conclusion, the enhanced activity of AR promotes not only the onset of oxidative stress linked to insulin resistance, but also the long-term complications linked to T2D[73]. Based on the above, the potential of facing the complex and multifactorial T2D disease by combining two selective inhibitors into one molecule with dual PTP1B and AR modulator activity is evident.

A dual inhibitor of the PTP1B and AR enzymes could be useful to treat both the condition of insulin resistance and chronic complications associated with T2D[74]. Several natural marine compounds have been reported as inhibitors of both PTP1B and AR enzymes; they include terpenes, polyketides, steroids, phenols, and alkaloids, mainly isolated from marine invertebrates[75,76]. Recently, a new PTP1B inhibitor has been isolated from the Mediterranean ascidian *Sidnyum elegans*, the phosphoeleganin (PE)[77,78].

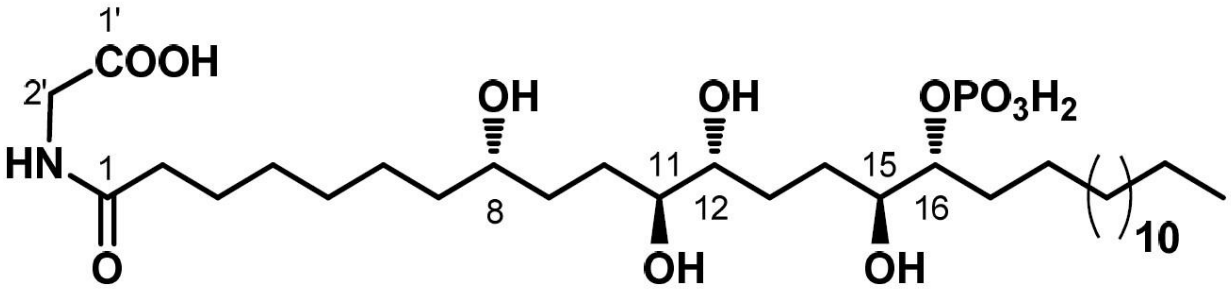

Fig. 12. Structure of the marine-derived polyketide phosphoeleganin (PE)[71]

In order to explore the potential of PE to be developed as a multitarget drug to treat insulin resistance and chronic complications associated with T2D, we have carried out an in-depth study on its inhibitory mechanism, including analysis of the insulin signalling pathway; in parallel, we have evaluated the AR inhibitory activity of PE. The results reported here show that PE inhibits both enzymes, acting, respectively, as a mixed-type inhibitor of AR and a pure non-competitive inhibitor of PTP1B. In addition, *in silico* docking analyses were performed to describe how PE could interact with both enzymes. Finally, tests carried out using HepG2 cells confirmed that PE possesses an insulin-sensitising activity. Details will be showed later in this work.

A drug design strategy frequently used to obtain DMLs starts from the knowledge of the distinct pharmacophores of agents active on each of the individual targets and consists in the integration of these pharmacophores into a single structure to obtain hybrid molecules. Hybridization should be carried out in such a way that the pharmacophoric elements inserted in a resulting DML maintain the ability to interact with specific sites of the different selected targets, thus producing simultaneously the desired effects. In order to obtain molecules endowed with appropriate druglike properties, it is often preferred to partially overlap the different pharmacophores, by using or merging them. However, by applying the different possible approaches for the design of DMLs, it is quite likely to achieve lead compounds endowed with high potency towards only one of the desired targets, with less effect on the others; therefore, it is often necessary to carry out a balancing process, using structural modifications of the lead compound, aimed to modulate and balance the activity towards the selected targets until to reach an optimal ratio[79–82].

Recently we have reported an initial investigation on 4-thiazolidinone derivatives active as dual inhibitors of AR and PTP1B, in the context of our search for new candidates for the treatment of type 2 diabetes mellitus and its complications[83].

Therefore, starting from a knowledge-based approach, recently we merged (5-arylidene-4oxothiazolidin-3-yl) acetic acid derivatives, which are endowed with excellent AR inhibitory activity and 4-[(5-arylidene-4-oxothiazolidin-3-yl) methyl] benzoic acids, which we identified as potent PTP1B inhibitors, to obtain a series of new 4-thiazolidinone derivatives (shown in figure below) that were evaluated as dual inhibitors of both human AR and PTP1B enzymes[83].

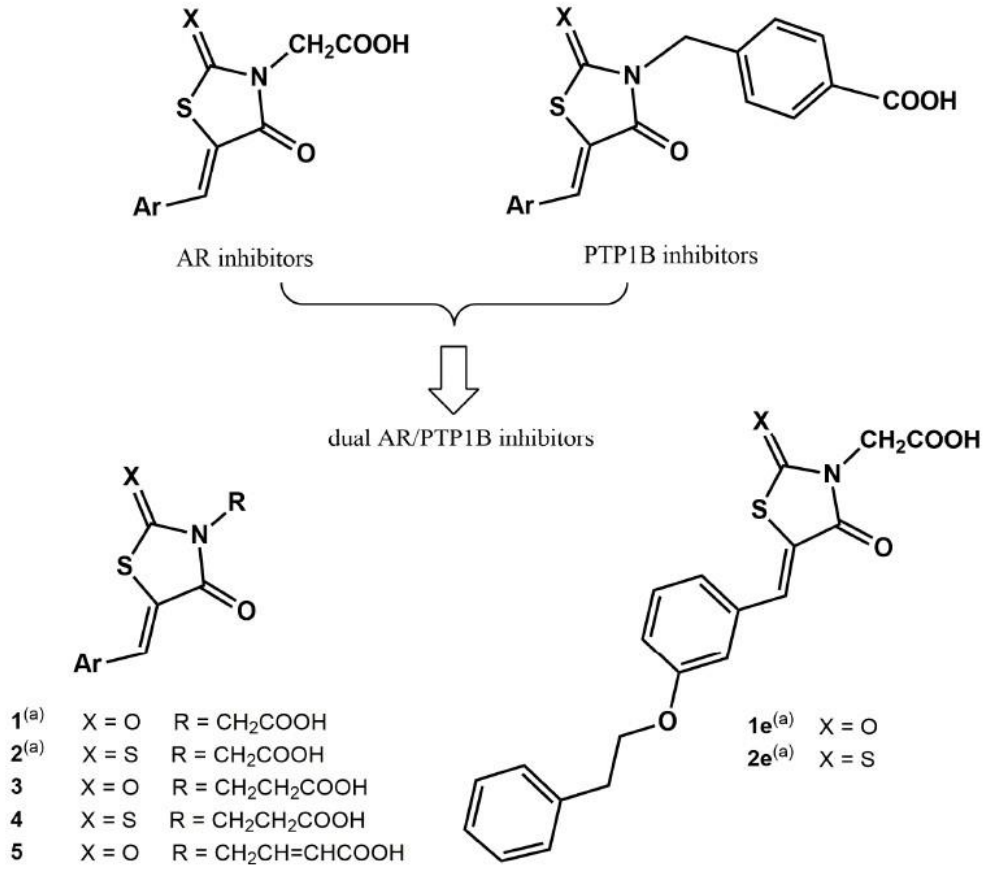

Fig. 13. Structures of 4-thiazolidinone derivatives active on AR and PTP1B[83].

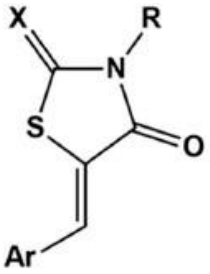

	X	R	Ar	AR IC_{50} (μM)	PTP1B IC_{50} (μM)
3a	O	$(CH_2)_2COOH$	3-OC_6H_5-C_6H_4	11.9 ± 0.9	79% at 50 μM
3b	O	$(CH_2)_2COOH$	4-OC_6H_5-C_6H_4	43.8 ± 7.1	56% at 50 μM
3c	O	$(CH_2)_2COOH$	3-$OCH_2C_6H_5$-C_6H_4	14.3 ± 1.0	76% at 50 μM
3d	O	$(CH_2)_2COOH$	4-$OCH_2C_6H_5$-C_6H_4	35.7 ± 3.0	77% at 50 μM
3e	O	$(CH_2)_2COOH$	3-$OCH_2CH_2C_6H_5$-C_6H_4	27.9 ± 3.1	64% at 50 μM
3f	O	$(CH_2)_2COOH$	4-$OCH_2CH_2C_6H_5$-C_6H_4	50.2 ± 4.6	46% at 50 μM
4a	S	$(CH_2)_2COOH$	3-OC_6H_5-C_6H_4	2.2 ± 0.1	34.1 ± 0.5
4b	S	$(CH_2)_2COOH$	4-OC_6H_5-C_6H_4	7.6 ± 0.6	29.5 ± 0.4
4c	S	$(CH_2)_2COOH$	3-$OCH_2C_6H_5$-C_6H_4	3.8 ± 0.1	42.8 ± 0.7
4d	S	$(CH_2)_2COOH$	4-$OCH_2C_6H_5$-C_6H_4	8.4 ± 0.7	34.9 ± 0.7
4e	S	$(CH_2)_2COOH$	3-$OCH_2CH_2C_6H_5$-C_6H_4	2.3 ± 0.1	55.5 ± 0.8
4f	S	$(CH_2)_2COOH$	4-$OCH_2CH_2C_6H_5$-C_6H_4	5.3 ± 0.4	12.7 ± 0.3
5a	O	CH_2CH=$CHCOOH$	3-OC_6H_5-C_6H_4	3.9 ± 0.2	42.1 ± 0.3
5b	O	CH_2CH=$CHCOOH$	4-OC_6H_5-C_6H_4	84% at 10 μM	39.7 ± 0.1
5c	O	CH_2CH=$CHCOOH$	4-C_6H_5-C_6H_4	88% at 5 μM	34.8 ± 0.5
5d	O	CH_2CH=$CHCOOH$	1-naphthyl	3.7 ± 0.2	40.3 ± 0.5
5e	O	CH_2CH=$CHCOOH$	2-naphthyl	86% at 10 μM	37.1 ± 0.4
	Epalrestat			0.102 ± 0.005	
	Vanadate				0.4 ± 0.01

Table 2. IC_{50} (μM) or % enzyme residual activity at the indicated concentration. Values are expressed as the mean ± S.E.M[74].

The appreciable *in vitro* activity of compounds 4a, 4e and 4f as well as 5a and 5d as dual AR/PTP1B inhibitors provided further insights into the possibility to develop 4-thiazolidinone derivatives as new potential multitarget antidiabetic candidates. Taking into account that the partial inhibition of selected targets, in particular enzymes, may be therapeutically more effective than the total control of a single target, these dual inhibitors, along with previous analogues 1e and 2e, appear to be promising as lead compounds, whose inhibitory activity towards both target enzymes might be further improved. In particular, compound 4f exhibited the most interesting profile, with balanced AR/PTP1B inhibitory effectiveness at low micromolar concentrations, along with promising insulin sensitizing activity in cultured cells. The IC_{50} values of 4f against both human PTP1B and human AR resulted in being in the low micromolar range, whereas those of the corresponding acetic acid analogue of series 2 differ of two orders of magnitude. Therefore, although the elongation of the carboxylic chain on N-3 of the thiazolidinone scaffold produced a decrease in AR inhibitory effectiveness, this structural feature was responsible for a gain in potency against PTP1B, thus providing a more balanced inhibition profile towards the two target enzymes.

The SARs that emerged fromour enzyme inhibition data, also considering our previous findings, highlighted that the AR inhibitory potency of the investigated 4-thiazolidinones is mainly influenced by the nature of the substituents in positions 2 and 3 of the heterocyclic scaffold and only in a lesser extent by the nature of the 5-arylidene moiety. On the other hand, this latter structural portion appeared to be critical to achieving good PTP1B inhibition, considering that a more extended 5arylidene portion, in particular a (2-phenylethoxy) benzylidene moiety, showed to be more beneficial. In addition, a thiocarbonyl group in position 2 of the thiazolidinone scaffold generally proved to be advantageous to achieve gain in potency towards both target enzymes.

The elongation of the carboxylic chain on N-3 in several cases improved inhibitory effectiveness towards PTP1B; propanoic acid derivatives 4a, 4e and 4f as well as 2-butenoic acid derivatives 5° and 5d exhibited good capability to inhibit both human PTP1B and AR. The data reported here allowed us to extend the SARs of this class of DMLs, which were rationalized by *in silico* docking experiments into both target enzymes. Therefore, these findings were useful for the design of new 4-thiazolidinone derivatives endowed with improved pharmacological profiles. As part of this study, such new molecules were tested and their multi-target potential evaluated.

Aim of the work

This PhD program mainly focused on the investigation of natural and synthetic compounds for the inhibition of PTP1B for antidiabetes drug development. We performed *in vitro*, *in vivo*, and *in silico* studies that were focused on the evaluation of the enzyme kinetic behaviour, inhibitor effects on insulin signalling pathway and glucose uptake rate.

Results are divided in five parts focused on specific molecules: catechins identified in tea extracts; the flavonoid Gossypetin from *Hibiscus sabdariffa*; compound Avarone from the marine sponge *Dysidea avara*; the phosphoeleganin (PE) from the Mediterranean ascidian *Sidnyum elegans* and the synthetic compounds (5-arylidene-4-oxo-2-thioxothiazolidin-3-yl) alkanoic acids. 4 sections out of 5 describe results from successfully published works.

Our results show that the compounds herein described could potentially be employed for the development of effective T2D drugs.

Materials and methods

Materials

All the reagents were obtained from Merck Life Science S.r.l. (Germany), unless otherwise specifed. Human insulin (Humulin R) was from Eli Lilly and Co. The following antibodies were used: pIR β subunit Y1162/1163 (sc25103-R) and β-actin clone C-4 (sc-47778) were from Santa Cruz Biotechnology (Dallas, Texas, USA); IR β subunit clone CT-3 (MABS65) was from Merck-Millipore (Burlington, MA, USA); phospho-protein kinase B (pAkt) (9271S) and Akt (9272S) antibodies were from Cell Signalling Technology (Danvers, Massachusetts, USA). Secondary antibodies were from Santa Cruz Biotechnology. Detection was performed using Clarity western ECL substrates (Bio-Rad Laboratories, Inc.). The 2-(N-(7-Nitrobenz-2-oxa-1,3-diazol-4-yl) Amino) -2-Deoxyglucose, (2-NBDG) was from Thermo Fisher Scientific (Thermo Fisher Scientific 168 Third Avenue Waltham, MA USA 02451).

Tested new (5-arylidene-4-oxo-2-thioxothiazolidin-3-yl) alkanoic acids compounds were synthetized by our colleagues from University of Messina, names and affiliations will be later shown.

Isolation of sesquiterpenes from the sponge *D.avara*

The hydroquinone avarol and its oxidized form, the quinone avarone, were obtained in pure form by extraction of a sample of the Aegean sponge *D. avara* available at the Department of Pharmacy of University of Naples Federico II. Indeed, it was taken a sample of the sponge (collected in Narlidere, Bay of Izmir, Turkey, 38°24'45N 27°8'18E) from the existing collection of natural sources, and it was extracted according to previuosly reported procedure[84]. Indeed, specimens of *D. avara* were thawed, homogenized, and firstly extracted with methanol (3 × 500 mL) at room temperature and, subsequently, with chloroform (3 × 500 mL) providing different extracts that were combined and concentrated in vacuo. The obtained suspension was dissolved in water, partitioned first with ethyl acetate and, then, with n-BuOH. The latter extract (800 mg after evaporation of the solvent as dark brown oil) was chromatographed on a RP-18 silica gel flash column as reported[84]. The most interesting fraction, labeled as A (23.2 mg), was eluted with MeOH/H2O 8:2 (v/v) showing the presence of diagnostic NMR signals related to hydroquinone/quinone derivatives. Accordingly, fraction A was subjected to HPLC purification on a RP-18 column (Luna, 5 µm C-18, 250 × 4.6 mm, flow rate= 1.00 mL/min), using MeOH/H2O 95:5 (v/v) as mobile phase. This analysis afforded avarol (1, 6.2 mg, tR= 5.1 min), and avarone (2, 7.7 mg, tR= 9.0 min) in pure form. As for the ethyl acetate soluble material (550 mg), it was chromatographed by open column on silica gel with the elution started from 100% n-hexane and gradually increased to 100% EtOAc. Then, it was followed by a step gradient of CH2Cl2: MeOH in different concentrations, and incresed up to 100% MeOH. The fraction eluted with CH2Cl2: MeOH 8:2 (v/v), labeled as fraction B (13.6 mg), was chromatographed on RP18 column (Luna, 5 µm C-18, 250 × 4.6 mm, flow rate= 1.00 mL/min), with a mixture MeOH/H2O 9:1 (v/v), affording compounds 3 (2.2 mg, tR= 14.4 min) and 4 (2.8 mg, tR= 16.6 min) in pure state. The

identity of the isolated compounds has been confirmed by comparison of their spectroscopic properties (1H and HRESI-MS) with those reported in literature[84–86]. Moreover, their purity (≥ 99.7 %) was confirmed by HPLC analyses.

Collection, Extraction and Isolation of PE from Specimens of *S.elegans*

Specimens of *S. elegans* were collected at Pozzuoli (Naples, Italy, April 2019). They were frozen immediately after collection and kept frozen until extraction. Fresh thawed animals (21.3 g of dry weight after extraction) were extracted according to a previously reported procedure[77]. The most polar organic layer (n-BuOH material) was chromatographed by MPLC over a C-18 column following a gradient elution H2O → MeOH → CHCl3. The fraction eluted with MeOH/H2O 7:3 (v/v) was further purified by HPLC on reversed phase (column: Synergi RP-MAX 4 µm, eluent: MeOH/H2O 8:2 + 0.1% of TFA) and afforded compound PE (tR = 20.5 min, 15.8 mg) in pure form. Phosphoeleganin (PE): colourless oil; all data agree with those reported in the literature[77,78].

Enzymes expression and purification

The coding sequences of human LMW-PTP isoforms (IF1 and IF2), and truncated form of human PTP1B (1-302 aa) were cloned in bacterial expression vector pNic28 in frame with a poly-His (6xHis) sequence. This plasmid was used to transform the E. Coli BL21 bacteria strain. Then, BL21 bacteria were grown until reach 0.8 OD and then incubated with IPTG (50 µg/L) for 2 hours at 37°C. After this time, bacteria were pelletted by centrifugation and stored at -20°C. The recombinant proteins were purified from bacterial lysate by affinity chromatography using a column packed with a Ni-NTA Agarose resin (Termo Fischer Scientific). Once eluted from column, the fusion proteins was dialyzed to remove the excess of imidazole, and concentrated until 2 mL using centrifuge concentrators (Millipore). Finally, the enzyme solution was loaded on Superdex G-75 column and eluted in 50 mM Tris-HCl buffer, containing 150 mM NaCl and 0.5 mM mercaptohetanol. The solutions containing the proteins were aliquoted in 500 µL fractions and stored at -80 °C.

Cell cultures

HepG2 liver cell line and C2C12 myoblasts were purchased from the American Type Culture Collection (ATCC, Manassas, VA, USA). HepG2 and C2C12 were routinely cultured in Dulbecco's Modifed Eagle's Medium (DMEM)-high glucose (4500 mg/L) supplemented with 10% Fetal Bovine Serum (FBS, Euroclone), 2 mM glutamine, 100 U/mL penicillin, and 100 µg/mL streptomycin. Cells were incubated at 37 °C in humidifed atmosphere with 5% CO2. To induce myoblast diferentiation, 80% confuent myoblasts were incubated in diferentiation medium (DMEM containing 2% horse serum) for 5 days.

Preparation of tea extracts

Cold tea extracts were prepared as follows. 2 g of dry tea leaves was added to 50 mL of deionized water and incubated at 25 °C for 1 h under agitation. Samples were then centrifuged, and supernatants fltered using a 0.22 µm flter to remove any debris. Obtained samples were stored at 4 °C. The protocol used to prepare hot tea extracts refers to the method described by Perva-Uzunalic and co-workers[87]. Specifcally, to prepare hot tea extracts, 2 g of tea was diluted in 50 mL of boiling water. Before adding the tea, the heat source, that was used to boil water, was removed. The tea samples were incubated in hot water for 5 min and then transferred into a box containing water and ice to favor the rapid cooling of the extract. Once the samples reached the temperature of 25 °C, they were centrifuged, and supernatants fltered using a 0.22 µm flter to remove any debris. The samples were stored at 4 °C.

Enzymatic assays and determination of IC_{50} values

Enzymatic assays were carried out as previously described [88]. The IC_{50} value of compounds against PTP1B, IF1 and IF2 was determined measuring the hydrolysis rate of the enzymes in the presence of 2.5 mM p-Nitrophenyl Phosphate (p-NPP) and increasing inhibitor concentrations (generally 14– 16 diferent concentrations). Each test was carried out in triplicate. Experimental data were normalized respect to control samples and then fitted using a non-linear fitting software, as previously described[74]. A dilution test was carried out to evaluate whether inhibitors act reversibly or not[74].

Determination of the mechanism of action inhibitors on PTP1B

The inhibitory mechanism was determined studying the dependence between the main kinetics parameters (KM and Vmax) and the inhibitor concentrations as previously described[83]. Data obtained were fitted using Michaelis–Menten equation and a non-linear fitting software. Then, data were analyzed using the double reciprocal plot (Lineweaver–Burk method). Secondary plots were used to calculate the Ki values.

HPLC analysis and sample fractioning

HPLC analyses were performed using a Thermo Scientifc UltiMate 3000 UHPLC system equipped with a Variable Wavelength Detector and a Kinetex C18 column 5 µm, 100 Å, 250×4.6 mm (Phenomenex). In our study, we performed two diferent protocols for preparative or analytical run, using the following solvent system: 10 mM trifuoroacetic acid (TFA) in acetonitrile (solvent A); 10 mM TFA in water (solvent B). In both analyses, the gradients used were: 2–15% of A for 15 min, 15–30% of A for 10 min, 30–45% of A for 6 min, 45–100% of A for 4 min. The analytical run was carried

out at a fow rate of 0.8 mL/min, using 10 µL injection volume. For all runs, detection was based on the absorbance at 214, 280 and 330 nm. Sample fractionation was performed using a 100 µL injection volume loaded onto a Jupiter® C4, 5 µm, 300 Å, column 250×10 mm (Phenomenex) at 2.0 mL/min. Fractions were collected according to the retention time: fraction 1 8–12 min; fraction 2 12–16 min; fraction 3 16–20 min; fraction 4 20–24 min and fraction 5 24–28 min.

Gas chromatography-mass spectrometry (GC-MS) analysis

For SCAN mode, HPLC tea fractions were dried under vacuum and then dissolved in 60 µL of 2% methoxyamine hydrochloride in pyridine (Thermo Fisher Scientific, Waltham, MA, USA), and incubated at 30 °C for 2 h. After dissolution and reaction, 90 µL N-Trimethylsilyl-N-methyl trifuoroacetamide (MSTFA)+1% trimethylchlorosilane (TMCS) were added and samples were further incubated at 37 °C for 60 min. Gas chromatographic runs were performed with helium as carrier gas at 0.6 mL/min. The split inlet temperature was set to 250 °C and the injection volume of 1 µL. A split ratio of 1:10 was used. The GC oven temperature ramp was from 60 to 325 °C at 10 °C/min. The data acquisition rate was 10 Hz. For the Quadrupole, an Electron Ionization (EI) source (70 eV) was used, and fullscan spectra (mass range from 50 to 600) were recorded in the positive ion mode. The ion source and transfer line temperatures were set, respectively, to 250 and 290 °C. The MassHunter data-processing tool (Agilent, Santa Clara, CA, USA) was used to obtain a global metabolic profling. Fiehn Metabolomics RTL library (Agilent G1676AA) was used to identify metabolites.

Determination of total polyphenol content

The total polyphenol content of tea extracts was determined using Folin–Ciocalteu reagent, as previously described[88].

Evaluation of synergistic activity of Gossypetin

The nature of synergy in the combined effect of Gossypetin with Vanadate, inorganic phosphate, Morin and betulinic acid, was investigated according to the procedure indicated by Chou T.C.[89]

Molecular docking

Docking simulations were carried out with AutoDock Vina and AutoDock Tools (version 1.5.6rc3)[90] using the 1PTY and 2HNP structures of PTP1B downloaded from the Protein Data Bank. The structures were restored from missing residues using MODELLER 10.2[91]. Ions, co-crystallized ligands, water molecules and co-factors were removed from structure. Polar hydrogen and charges were added to protein and missing atoms restored, then it was saved in PDBQT format. The grid map of

the interaction energies for various atoms of the ligand with the macromolecule was calculated using AutoGrid software. Ligand structure was prepared and energy minimization performed using DS viewer pro 6.0 (Accelrys, San Diego), the structure was saved in PDB format. Graphical representations of docked structures were performed using UCSF Chimera[92].

Regarding the analysis of the new (5-arylidene-4-oxo-2-thioxothiazolidin-3-yl) alkanoic acids, X-ray crystal structure selection and preparation of the AR-idose complex was PDB: 3V36[93] and PTP1B (PDB: 1Q6T[94]) were performed as described in previous studies[74,83]. Docking studies with GOLD (version 2020)[95] were performed into the catalytic site of PTP1B and AR, into the AR-idose complex and into the previously described allosteric binding pocket of PTP1B[74,83]. 25 Docking poses were generated with standard settings using the scoring function CHEMPLP. The obtained binding modes were subsequentially clustered based on LigandScouts[96,97] pharmacophore RDF-Code (radial distribution function) similarity. The docking poses were minimized in LigandScout with the MM94 Force Field[98]. 3D Pharmacophores were developed using LigandScout and 3D depictions of proteinligand complexes depictions were rendered in MOE (version 2020)[99].

Visualization of ligand-protein interactions

The potential intermolecular interactions between the ligand and the protein were calculated automatically by LigPlot+ software (version 2.2), that generated 2D schematic representations of protein–ligand complexes displaying hydrogen bonds and hydrophobic interactions within the binding pocket[100] or using Biovia Discovery Studio Visualizer[101].

Analysis of the insulin-signalling pathway

To evaluate the effect of tea extracts on the insulin-signaling pathway, HepG2 and C2C12 cells were grown in 35-mm culture dishes. Chronic stimulation was achieved incubating cells for 90 min in the presence of starvation medium (DMEM supplemented with 2 mM glutamine, 100 U/mL penicillin, and 100 µg/mL streptomycin) containing 5 µL/mL of tea extract. After this time, the medium was removed, cells were washed with PBS, and further incubated with fresh starvation medium for 24 h. The treatment was repeated four times before stimulation with 10 nM insulin (Humalog, lispro insulin) for 30 min. The impact of EGCG on C2C12 diferentiated cells was evaluated by stimulating muscle cells for 30 min with EGCG concentrations in the range 0.1–10 µM or with cold Indian green tea extract before the analysis. Both treated and control HepG2 and C2C12 cells were lysed in Laemmli bufer 1X, containing 2% SDS, 10% glycerol, 5% 2-mercaptoethanol, 0.002% bromophenol blue, 0.0625 M Tris–HCl pH 6.8, according to Lori et al.[88]. After that, SDS-PAGE was performed on whole cell extracts and then proteins were transferred on PVDF membranes. Membranes were incubated overnight at 4 °C with anti-IRβ, anti-pIRβ, anti-Akt and anti-pAkt primary antibodies diluted 1:1000 in PBS-Tween 0.1% containing 5% of bovine serum albumin (BSA). β-Actin was used as loading control for total protein lysates. After washing several times with PBS-Tween 0.1%, membranes were incubated for 1 h at room temperature with horseradish peroxidase-conjugated secondary antibodies, diluted 1:5000 in PBS-Tween 0.1% containing 1% BSA. Images of the proteins

were obtained by chemiluminescence using Clarity Western ECL substrate (BioRad) and Amersham Imager 600 luminometer (Amersham, Buckinghamshire, UK). Bands were quantifed using the Amersham quantification software.

The ability of Gossypetin to potentiate the insulin signalling pathway was evaluated on both liver HepG2 and muscle C2C12 cell lines. They were stimulated for 30 min with 10 nM insulin, Gossypetin, or Insulin-Gossypetin combination. Further tests were carried out to evaluate also the effects of chronic treatment with Gossypetin: liver cells were treated for 4 days with 1 µM Gossypetin and then stimulated or not with Insulin. Western blot analysis was used to evaluate the phosphorylation levels of IR, Akt, PTP1B and LMW-PTP.

The same approach was used to evaluate any effect of Avarone, Phosphoeleganin and new (5arylidene-4-oxo-2-thioxothiazolidin-3-yl) alkanoic acids compounds on insulin signalling pathway.

Glucose uptake

Glucose uptake assay was performed using C2C12 murine muscle cell line. Plates containing myotubes were starved for 20 h, and then treated for 30 min with 10 nM insulin or with increasing EGCG concentrations. Stimulated cells were then incubated in the presence of 0.5 mCi/mL of 2deoxy- D-1,2-[3H]-glucose (Perkin Elmer) for 15 min, washed with cold PBS and lysed using 0.2 M NaOH solution. The amount of radiolabeled glucose incorporated by cells was determined using αβscintillation-counter. Data were normalized on protein concentration and reported as percent respect to the control experiment.

In other studies 2-NBDG was also used for glucose uptake test through flow cytometer (FACSCanto II, BD Biosciences, San Jose, CA, US) as previously described[102]. Briefly, 80% confluence C2C12 muscle cells were starved for 24 h and then stimulated with 10 nM insulin, or tested compound for 15-30 min and then incubated in the presence of 40 µM of 2-NBDG (Invitrogen) for 3 h. Then, cells were washed with PBS, tripsinized, pelleted by centrifugation and analysed using a flow cytometr. All tests were carried out in triplicate. For each sample 1 × 104 events were acquired. Data obtained were then analysed with FlowJo software. Cells autofluorescence values were determined before sample analysis and subtracted to each sample.

Seahorse XFe96 Metabolic assay

C2C12 cells (3×104 cells/well) were plated in XFe96 cell culture plates. After 24 h incubation at 37°C, cell growth medium was substituted with an XF base medium supplemented with 2 mM glutamine, 1 mM sodium pyruvate, and 25 mM glucose. The plate was then tranferred in a non-CO2 incubator for 1 h at 37°C to pre-equilibrate the cells before analysis. An XF Mito Stress Test was performed to assay the cells' ability to exploit mitochondrial oxidative metabolism, according to the manufacturer's instructions[103]. The oxygen consumption rate (OCR) was evaluated after the injection of a sequence of compounds that interfere with the electron transport chain: oligomycin

(1 µM), carbonyl cyanide-4 (trifluoromethoxy) phenylhydrazone (FCCP) (1 µM), and Rotenone/Antimycin A (0.5 µM). All data were normalized on protein content of each well.

Statistical analysis of data

Data are reported as means ± S.E.M. from at least three independent experiments. Data obtained were statistically analyzed using Unpaired Student's T test. p values ≤ 0.05 were considered statistically significant (* p value < 0.05, ** p value < 0.01).

Results

Differential impact of cold and hot tea extracts on tyrosine phosphatases regulating insulin receptor activity: a focus on PTP1B and LMW-PTP

Results and brief discussion

Tea extract preparation

Tea extracts were prepared using either cold or hot water. Seven different types of tea were used to obtain cold extracts: Indian earl grey and Indian English breakfast teas, Sri Lanka black tea, Indian, Chinese and Iranian green teas, and Chinese white tea. Hot extracts were prepared using Indian earl grey, and Indian and Iranian green teas. All extracts were filtered and stored at 4 °C in sterile tubes.

Preliminary screening and determination of IC_{50} values of tea extracts

Preliminary enzymatic screening assays underlined that cold extracts obtained from all the seven different types of tea behave as potent inhibitors of both PTP1B and LMW-PTP (Fig. 14). To confirm this, we determined the IC_{50} values of each cold tea extract on both enzymes (Table 3). Data obtained show that the inhibitory potency of tea extracts is dependent on the type of tea analyzed. In particular, Indian earl grey, and Indian and Iranian green teas are the most efficient in inhibiting the activity of both phosphatases. Thus, we selected these three types of tea and prepared hot extracts to further investigate their inhibitory potential. Kinetic analyses on Indian earl grey, Indian green and Iranian green tea extracts revealed that hot extracts are more effective than the corresponding cold ones in inhibiting both PTP1B and LMW-PTP activities (Table 3). Remarkably, Indian green tea appears to be the most potent, with its cold extract displaying IC_{50} values of 0.04 µL/mL and 0.03 µL/mL on PTP1B and LMW-PTP, respectively, and its hot extract showing IC_{50} values of 0.007 µL/mL and 0.03 µL/mL on PTP1B and LMW-PTP, respectively (Table 3).

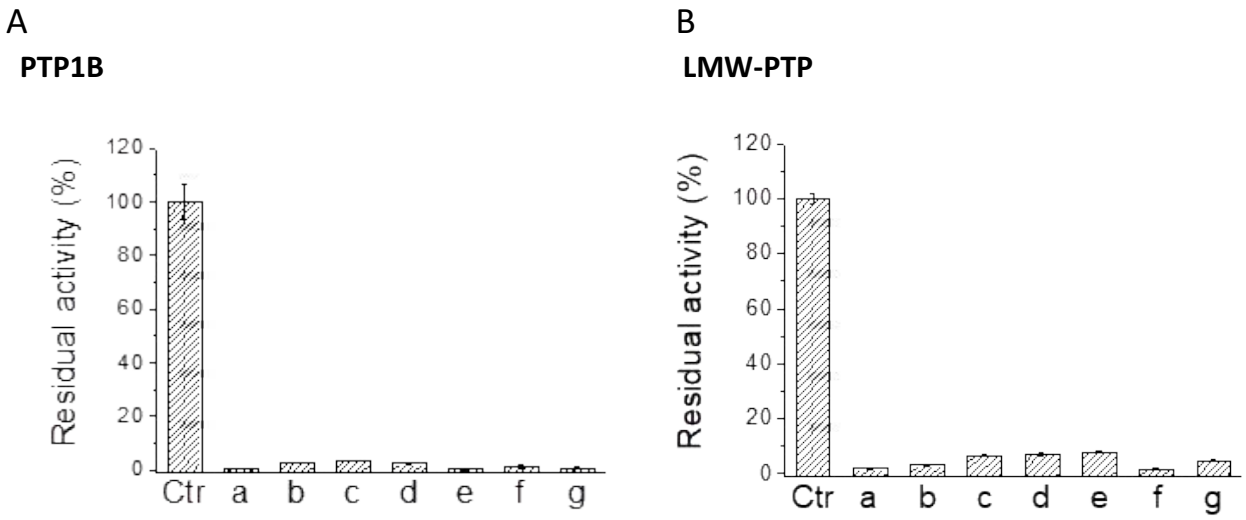

Fig. 14 Effect of cold tea extracts on the enzymatic activity of PTP1B (**A**) and LMW-PTP (**B**). To evaluate the inhibitory effects of cold tea extracts on PTP1B (**A**) and LMW-PTP (**B**) catalytic activity, tests were carried out diluting 5 µL of tea extracts in 1 mL of assay buffer. Each sample was marked with an alphabet letter: **Ctr** control, **a** Indian earl grey tea, **b** Indian green tea, **c** Chinese green tea, **d** Iranian green tea, **e** Chinese white tea, **f** Sri Lanka black tea, **g** Indian English breakfast tea. All tests were carried out in triplicate. All data obtained were normalized respect to control tests. Results reported in the figure represent the mean value ± S.E.M (n = 3).

Table 3: IC_{50} values calculated on PTP1B and LMW-PTP using both cold and hot tea extracts

Tea Extract	IC_{50} (µL/mL)			
	Cold extracts		Hot extracts	
	PTP1B	LMW-PTP	PTP1B	LMW-PTP
Indian Earl grey	0.030 ± 0.002	0.450 ± 0.030	0.030 ± 0.002	0.044 ± 0.003
Indian green	0.040 ± 0.001	0.030 ± 0.002	0.007 ± 0.001	0.030 ± 0.004
Chinese green	0.040 ± 0.002	0.900 ± 0.150	----	----
Iranian green	0.040 ± 0.001	0.070 ± 0.010	0.020 ± 0.001	0.016 ± 0.002
Chinese white	0.050 ± 0.001	0.180 ± 0.020	----	----
Sri Lankan black	0.050 ± 0.001	0.080 ± 0.005	----	----
English Breakfast	0.090 ± 0.002	0.100 ± 0.005	----	----

Kinetic mechanism of Indian green tea extract

We performed further analyses using Indian green tea to evaluate differences in the mechanism of action between cold and hot tea extracts. We found that the cold extract is a reversible inhibitor of both enzymes, while the hot extract acts as a non-reversible inhibitor (data not shown). Furthermore, kinetic analyses revealed that the cold tea extract acts as noncompetitive inhibitor of PTP1B, and as an uncompetitive inhibitor of LMW-PTP (Fig. 15). Experimental data related to PTP1B in the secondary plot described a hyperbolic curve, indicating that more than one molecule binds to the enzyme surface (Fig. 15B). Conversely, in the case of LMW-PTP, experimental points reported in the secondary plot described a straight line, suggesting that the inhibition results from the binding of a single molecule (in this case the K_i value is 0.13 ± 0.1 µL/mL) (Fig. 15D).

HPLC analysis of tea extracts

Qualitative analysis of both hot and cold tea extracts was carried out using an HPLC system. As expected, chromatograms obtained display several peaks with different elution times, thereby confirming that each sample contains different natural molecules. It is worth mentioning that the chromatograms generated by the hot and cold extracts are not perfectly superimposable, suggesting that the extracts are different both quantitatively and qualitatively. To confirm this hypothesis, the total polyphenol content of both cold and hot extracts was evaluated using the Folin–Ciocalteu reagent (Table 4). Data confirmed that the polyphenol content of hot extracts is higher than that of cold extracts. Finally, GC–MS analyses of both cold and hot extracts confirmed that these samples are qualitatively different (data not shown[50]).

Identification of bioactive HPLC fractions

The components of the Indian green tea extract were separated using the HPLC apparatus and then each fraction was analyzed separately. We found that the most active fractions were eluted at high organic solvent concentrations, even though the inhibitory activity of each fraction changes according to the enzyme assayed and the extraction temperature (Fig. 16).

GC–MS analysis of the active fractions

The most active fractions of hot (fractions 3 and 5) and cold (fractions 3, 4 and 5) extracts from Indian green tea were analyzed using a GC–MS apparatus. Each fraction contains several molecules, including different types of catechins. Interestingly, some of the identified molecules have already been described as PTP1B inhibitors (Table 5)[32,36].

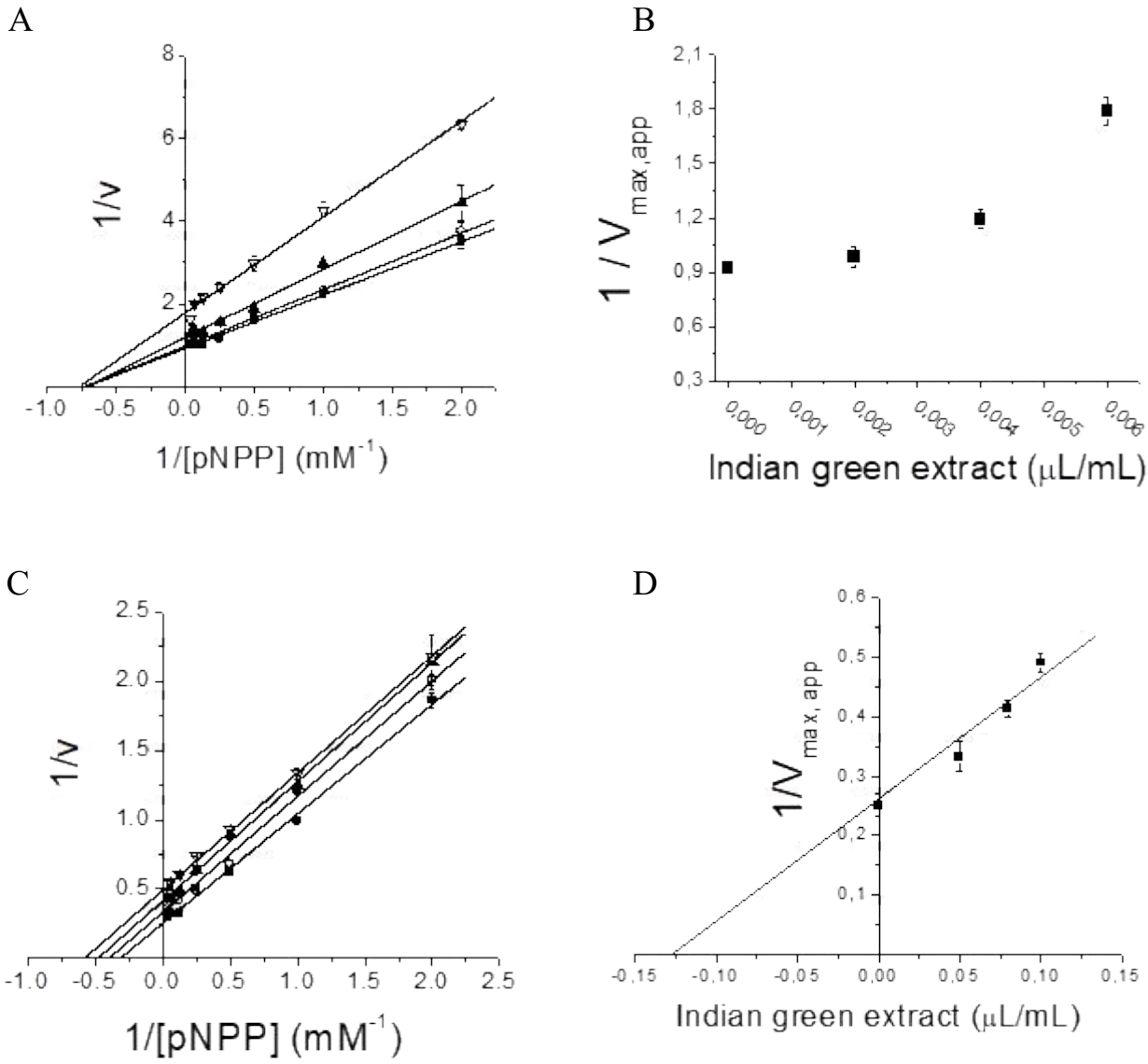

Fig. 15. Kinetic analysis of cold Indian green tea extract on PTP1B and LMW-PTP. To evaluate the mechanism of action of cold Indian green tea extract, we analyzed the dependence of K_M and V_{max} on the extract concentration. K_M and V_{max} were calculated measuring the catalytic rate of the enzyme in the presence of increasing p-NPP concentrations and plotting data using Michaelis–Menten equation. (**A**-**B**) For PTP1B: (A) double reciprocal plot. The final amounts of extract used were: (■), control; (○), 0.002 μL/mL; (▲), 0.004 μL/mL; (▽), 0.006 μL/mL; **B** secondary plot. (**C**–**D**) For LMW-PTP: **C** double reciprocal plot. The final amounts of extract used were: (filled square), control; (circle), 0.05 μL/mL; (filled triangle), 0.08 μL/mL; (inverted triangle), 0.1 μL/mL; **D** secondary plot. All tests were carried out in triplicate. Results reported in the figure represent the mean value ± S.E.M (n: 3).

Tea	Hot	Cold
	Total polyphenol content§ (µg/µL)	
Indian Earl grey	2.4 ± 0.2*	1.4 ± 0.1
Iranian green	1.9 ± 0.1*	1.7 ± 0.2
Indian green	3.7 ± 0.2*	3.0 ± 0.21

Table 4. Determination of total polyphenol content in tea extracts. *p < 0.05 hot versus cold extracts.

§ The results were expressed as µg catechin equivalents (CEQ) reported as gallic acid

Dissecting the inhibitory potency of catechins *in vitro*

We calculated the IC_{50} values of epigallocatechin gallate (EGCG), epicatechin gallate (ECG), epigallocatechin (EGC), epicatechin (EC) and gallic acid on both PTP1B and LMW-PTP. Interestingly, we found that EGCG and ECG are more effective towards PTP1B compared to LMW-PTP, while EGC, EC and gallic acid are inactive against both phosphatases. Finally, kinetic analyses revealed that both EGCG and ECG act as reversible inhibitors of PTP1B and EGCG behaves as a potent mixed-type noncompetitive inhibitor of PTP1B, with a K_i of 26 nM (Fig. 17).

Molecular docking

The interaction mode of EGCG and PTP1B was evaluated using AutoDock 4.2 and 1PTY crystal structure of PTP1B. Five ligand–protein conformations were then selected according to the docking energy. Specifically, the pose 1 belongs to the cluster with the most favorable binding energy. In this pose, the ligand forms four hydrogen bonds with several residues of the PTP1B active site (Ser216, Gly220, Arg221, Lys116 and Tyr46), and engages hydrophobic interactions with amino acids belonging to WPD loop (Asp181, Phe182) and the Q-loop (Gln262) (Fig. 18B). Similarly, in the pose 2, the EGCG establishes three hydrogen bonds with Gln262 and maintains hydrophobic interactions with Phe182 and hydrogen bonds with Ala264, belonging to WPD loop and the α-6 helix, respectively (Fig. 18C). In the pose 3, the ligand establishes both hydrogen bonds and hydrophobic interactions with residues in the α-6 helix (Asp265, Phe269), in the WPD loop (Thr178, Pro180, Phe182, Gly183, Val184, Pro185), and in the α-3 helix (Glu186) (Fig. 18D). Furthermore, in the pose 4, the ligand interacts with the amino acids belonging to helices α-6 (Glu276, Lys279, Ile275, Leu272), α-7 (Leu294) and α-3 (Ser187, Pro188, Ala189) (Fig. 18E). Finally, in the pose 5, the EGCG forms hydrogen bonds with Ile275 in the α-6 helix, and Asp284 in the loop connecting α-6 and α-7 helices. Moreover, it establishes hydrophobic interactions with residues in the α-6 helix (Lys279, Ala278), in the α-7 helix (Val287) and in the loop connecting these two helices (Gly283, Met282) (Fig. 18F).

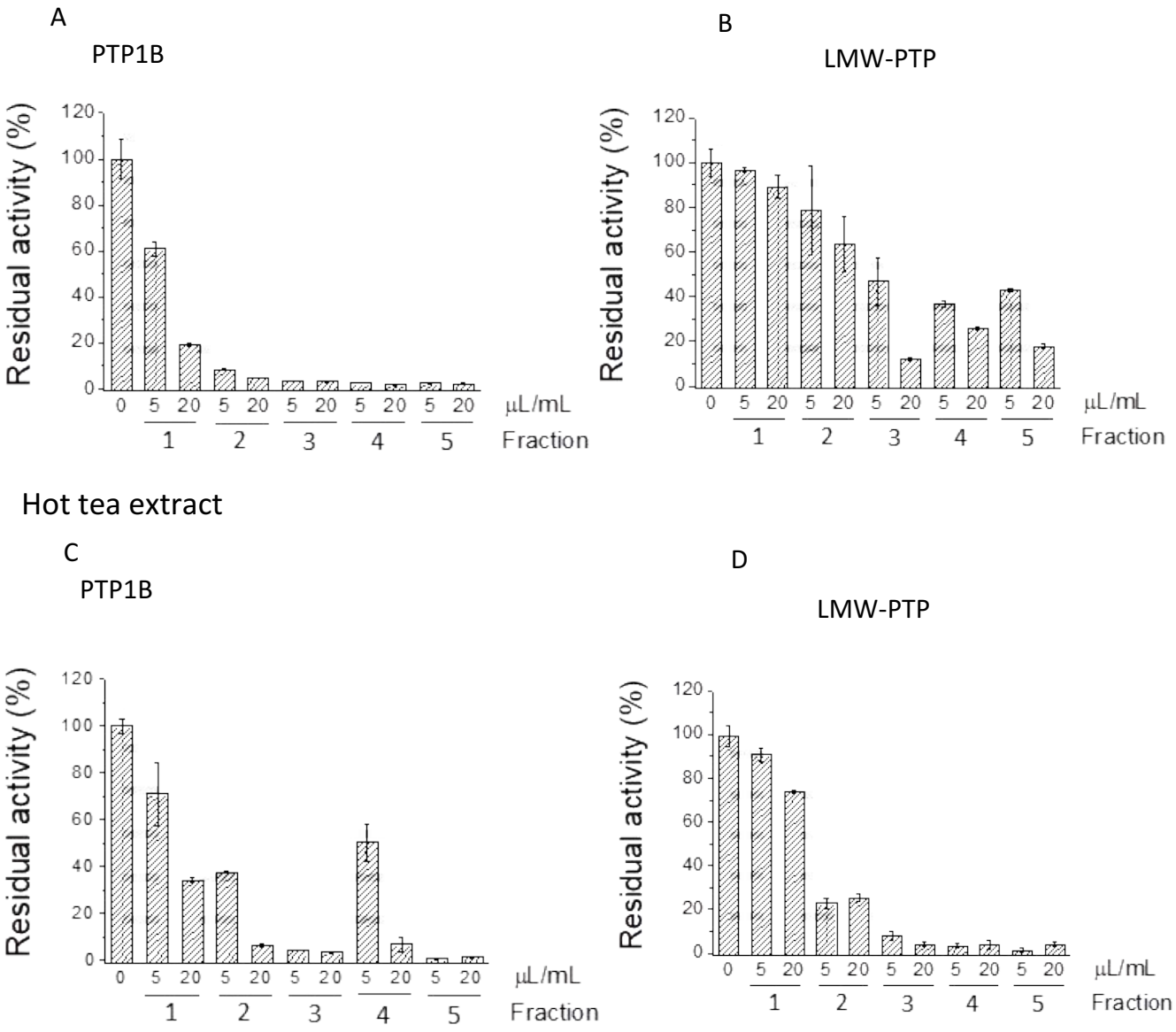

Fig. 16. Effect of cold and hot Indian green tea extract fractions, collected by HPLC, on the enzymatic activity of PTP1B and LMW-PTP. By equipping HPLC apparatus with a semi-preparative column and increasing the content of hydrophobic solvent, **A**–**B** 100 µL injection volume of cold Indian green tea extract was analyzed and five fractions were collected (for respectively, 5 and 20 µl/ml of each fraction in 1 ml of assay buffer. **C**–**D** 100 µL injection volume of hot Indian green tea extract was analyzed using HPLC apparatus equipped with semi-preparative column and five fractions were collected (for more details, see "Materials and methods"). Their inhibitory activity on **C** PTP1B and **D** LMW-PTP was tested by diluting, respectively, 5 and 20 µl/ ml of each fraction in 1 ml of assay buffer. All tests were carried out in triplicate. All data obtained were normalized respect to control tests. Results reported in the figure represent the mean value ± S.E.M (n = 3). * indicates a statistically significant difference according to Unpaired Student's T test data analysis (*p < 0.05, **p < 0.01)

Table 5: Known PTP1B inhibitors found in cold and hot green Indian tea extract.

	Cold indian green tea			Hot indian green tea		
Metabolites	**Fraction 3**	**Fraction 4**	**Fraction 5**	**Fraction 3**	**Fraction 5**	**References**
Epicatechin	-	✓	-	-	-	51
Palmitic Acid	✓	✓	✓	✓	✓	32,36,104
Behenic acid	-	-	✓	-	-	32,36
Catechin	✓	✓	✓	✓	✓	51
Epicatechin gallate	-	-	✓	-	✓	51
Chlorogenic acid	✓	-	-	✓	-	105,106
Stearic acid	✓	✓	✓	✓	✓	32
Linoleic acid	✓	✓	✓	✓	✓	32
Oleic acid	-	-	-	✓	-	36
Epigallocatechin gallate	✓	✓	-	-	-	51
Epigallocatechin	✓	✓	✓	✓	✓	51
Acetophenone	✓	✓	✓	-	-	107
Myristic acid	-	✓	✓	-	-	32
Salicylic acid	-	✓	-	-	-	108,109
Gallic acid	✓	✓	✓	✓	✓	110

Modulation of the insulin-signaling pathway activity by tea extracts and catechins

With the aim of evaluating the effects of EGCG on the insulin-signaling pathway in myoblasts, further tests were performed on C2C12 cells. We found that 30 min treatment with EGCG increased IR phosphorylation at all used concentrations (Fig. 19A, B), reaching phosphorylation levels close to those obtained using 10 nM insulin. Furthermore, glucose uptake in C2C12 cells is increased only after treatment with 10 µM EGCG. Further tests were carried out to assess the effects of chronic treatment of liver cells with cold Indian green tea extract, which gave the best *in vitro* inhibition result. We found that in non-insulin stimulated cells the chronic treatment resulted in a significant increase of IR levels (Fig. 19c, D), and a decrease of both pIRβ and pIRβ/IRβ ratio (Fig. 19c, E, F). However, by evaluating the relative increase of pIRβ/IRβ ratio after insulin stimulation, we found that the strongest increase was observed in extract-treated cells, suggesting that IR becomes more responsive to insulin stimulation after tea extract administration. Moreover, in C2C12 cells, treatment with either cold Indian green tea extract alone or in combination with 10 nM insulin strongly increases Akt phosphorylation levels. Finally, we also analyzed the effect of hot Indian green tea extract on HepG2 cells. Surprisingly, no significant differences in the pIRβ/IRβ ratio were observed between untreated and tea extract-treated cells stimulated with insulin, suggesting that treatment with hot tea extract does not significantly improve insulin sensitivity in liver cells.

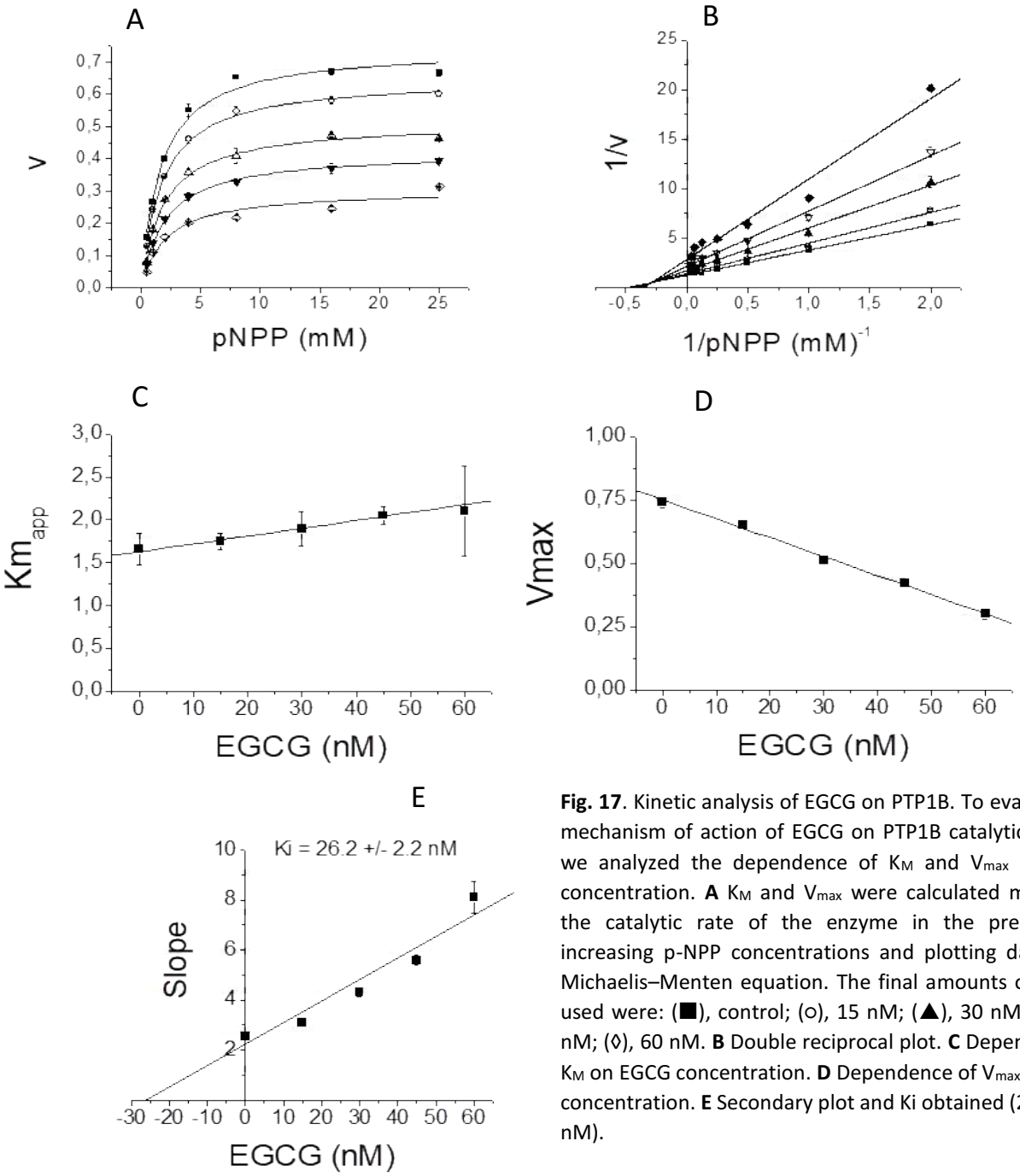

Fig. 17. Kinetic analysis of EGCG on PTP1B. To evaluate the mechanism of action of EGCG on PTP1B catalytic activity, we analyzed the dependence of K_M and V_{max} on EGCG concentration. **A** K_M and V_{max} were calculated measuring the catalytic rate of the enzyme in the presence of increasing p-NPP concentrations and plotting data using Michaelis–Menten equation. The final amounts of extract used were: (■), control; (○), 15 nM; (▲), 30 nM; (▼), 45 nM; (◊), 60 nM. **B** Double reciprocal plot. **C** Dependence of K_M on EGCG concentration. **D** Dependence of V_{max} on EGCG concentration. **E** Secondary plot and Ki obtained (26.2 ± 2.2 nM).

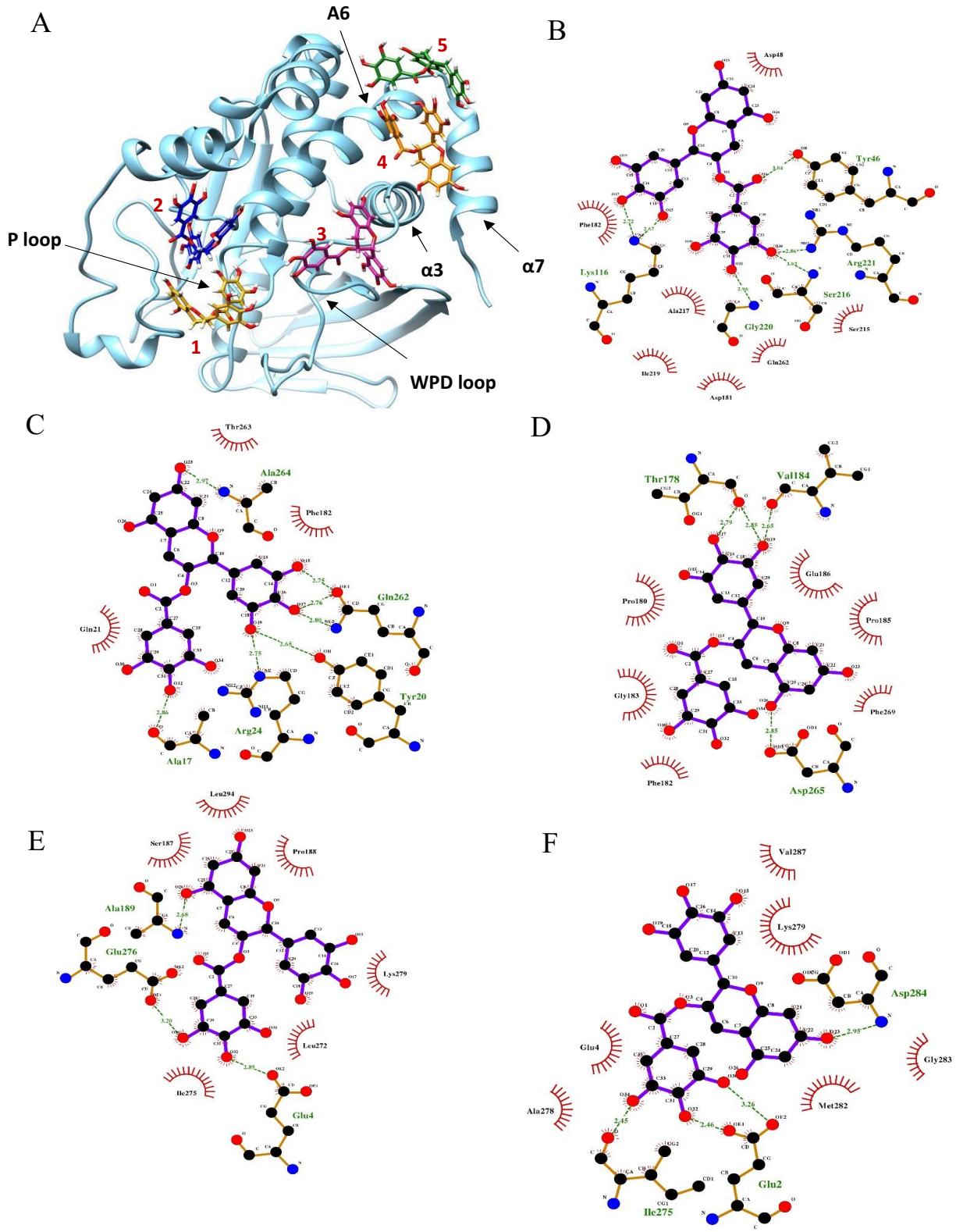

Fig.18. Docking analyses of EGCG on PTP1B structure. Docking simulations of EGCG on PTP1B structure (PDB code: 1PTY) were carried out using AutoDock and Ligplot+ software as described in detail in "Materials and methods". **A** Several interaction sites of the ligand were found on PTP1B structure and indicated with numbers from 1 to 5. **B**–**E** 2D schematic representations of the intermolecular interactions between the enzyme and the ligand EGCG. Ligand bonds are reported as purple lines; EGCG interactions with PTP1B are reported as red lines for hydrophobic interactions, and as green lines for H-bonds. Specifically, **B** interactions between PTP1B and EGCG in position '1', related to the active site of the enzyme; **C** interactions between the enzyme and EGCG in position '2', close to the PTP1B active site; **D** interactions between PTP1B and EGCG in position '3' close to the WPD loop, which contains essential residues for the catalysis; **E**, **F** interactions between the phosphatase and EGCG in position '4' and '5', close to PTP1B allosteric sites.

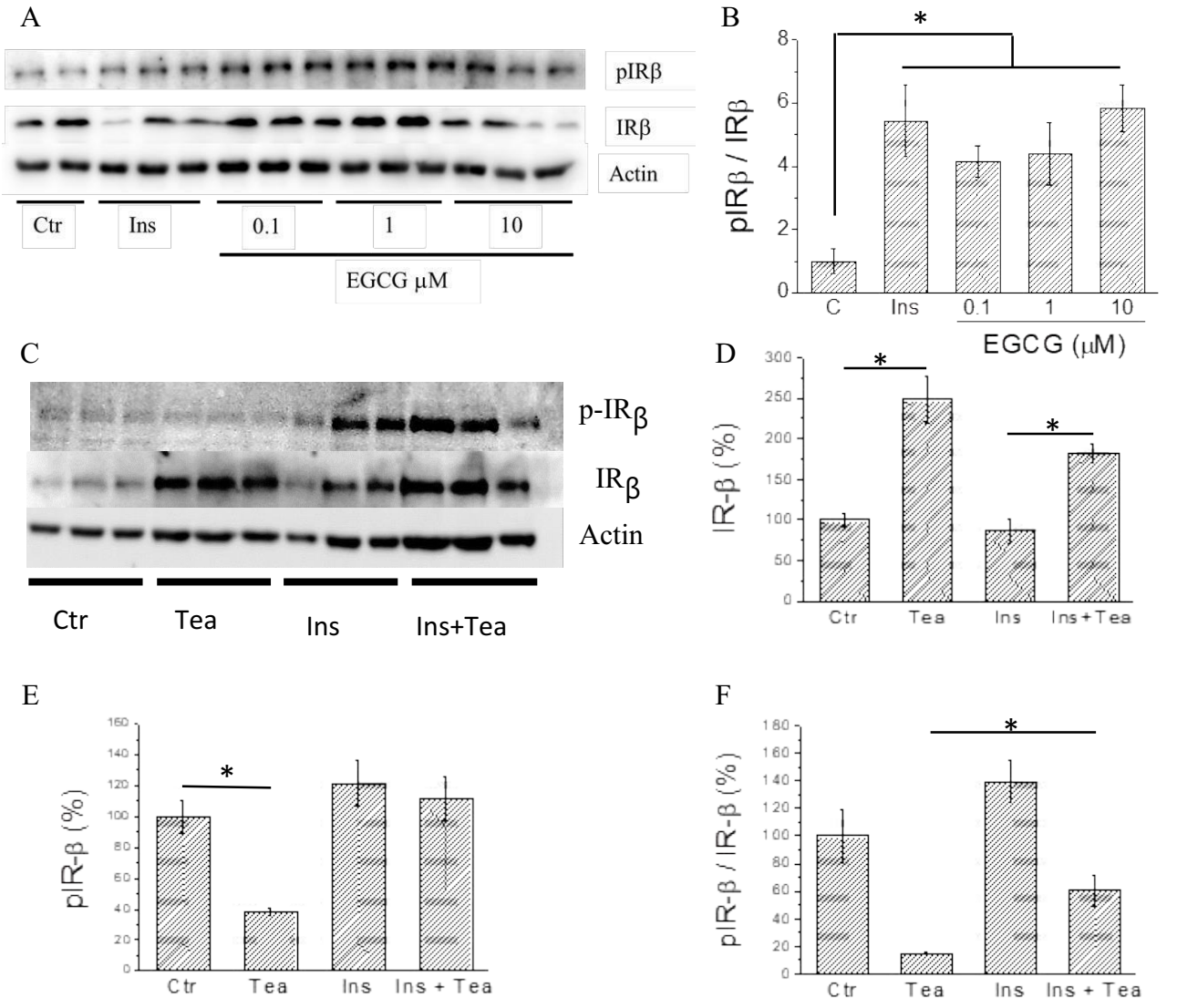

Fig.19. Western blot analyses of C2C12 and HepG2 cells treated with EGCG and cold Indian green tea extract, respectively. (**A**) Western blot analysis of C2C12 cells treated for 30 min with 10 nM insulin or increasing amounts of EGCG (0.1, 1, 10 μM). Images show the expression levels of pIRβ and IRβ. Anti-β actin antibody was used to ensure equal loading. (**B**) Densitometric analysis of pIRβ/IRβ ratio. The EGCG treatment induces an increase in IR phosphorylation levels. No significant differences between samples treated with insulin alone or with increasing EGCG doses were detected. (**C**) Representative images of western blot analysis of HepG2 cells treated chronically for 4 days with cold Indian green tea extract and stimulated with insulin 10 nM for 30 min before cell lysis. Liver cells treated with cold extract resulted in a significant increase of IR expression levels (**D**), and a decrease of both pIRβ (**E**) and pIRβ/IRβ ratio (**F**). Results are mean values ± S.E.M (n: 3). *Statistically significant difference according to Unpaired Student's T test data analysis (*$p < 0.05$).

In this work we confirmed that both hot and cold tea extracts inhibited PTP1B and LMW-PTP activities, suggesting the presence of bioactive molecules that could exert antidiabetic effects through tea consumption.

Our tests confirmed different mechanisms of inhibition and that could depend on the type of extraction method used. Higher temperature could enhance the amount of biomolecules extracted and could modify them[111]. Ma and co-workers reported similar results, underlining that pre-

incubation of PTP1B with hot tea extract improves its inhibitory effects. This finding indicated that tea extracts act as slow binding or non-reversible PTP1B inhibitors[51]. Our data confirmed that Indian green tea hot extract is a non-reversible inhibitor of both enzymes, thereby reinforcing the hypothesis that high temperature of extraction could modify the biological properties of the solution. Therefore, to eliminate such confounding factors, we focused our attention on the activity of the cold extract one. Kinetic assays confirmed that this extract acts as a potent and reversible inhibitor of both PTP1B and LMW-PTP and that catechins present are crucial protagonists of such activity. Interestingly, we noted that only EGCG and ECG were active on both enzymes, while EGC, EC and gallic acid were not. Reasonably, we think that these differences can be attributed to the greater structural flexibility of EGCG and ECG respect to other catechins lacking the galloyl group[112].

In this context, our results disagree with Kuban–Jankowska and collaborator's data, showing that catechins possess a limited inhibitory activity against PTP1B[113]. We propose that structural flexibility of EGCG and ECG is responsible of PTP1B and LMW-PTP inhibition, which are characterized by strong structural differences. Moreover, it is noteworthy that both EGCG and ECG showed higher affinity for PTP1B over LMW-PTP, suggesting that these catechins possess a marked specificity for the first enzyme. Accordingly, Ma and co-workers reported that both black and green tea extracts display a marked selectivity for PTP1B over TC-PTP[51]. Altogether, these data reinforce the evidence that EGCG and ECG display a significant selectivity for PTP1B over other PTPs.

We wondered if the selectivity of EGCG for PTP1B has anything to do with its allosteric sites. Accordingly, we demonstrated that EGCG acts as a mixed-type non-competitive inhibitor of PTP1B, indicating that this molecule is able to bind to multiple sites on the enzyme surface. Furthermore, docking studies confirmed that EGCG interacts with amino acids located in the active site, the WPD loop[42], as well as with amino acids located between α3, α6 and α7 helices, where the ligand occupies pockets close to those already described for other allosteric PTP1B inhibitors[42]. Although further analyses will be necessary to identify the binding site(s) of EGCG on PTP1B structure, we believe that these molecules represent interesting lead compounds for the development of novel potent and selective inhibitors of PTP1B. Our data showed that *in vitro* EGCG acts as a potent inhibitor. However, the physiological relevance of our results remains to be clarified. For instance, it is not clear whether *in vivo* EGCG can reach reasonable concentrations to exert these effects.

Studies performed on human volunteers reported that, after taking a cup of tea, blood concentration of free catechins rapidly increases reaching a Cmax of 25–55 nM, and then slowly decreases over several hours[114]. This evidence suggests that after the dietary intake of a cup of tea, blood contains a consistent reservoir of EGCG that may favor its accumulation in liver cells, allowing liver cells to accumulate quantities of EGCG sufficient to inhibit this enzyme. Accordingly, several preclinical studies confirmed that the administration of EGCG causes an increase in insulin sensitivity in liver cells[115,116].

Validation of the ability of EGCG to cross cell membrane and affect insulin signaling pathway comes from tests carried out using both HepG2 and C2C12 cells. HepG2 is a human hepatoma cell line that has been largely used for investigating insulin-signaling pathway. Although Molinaro and collaborators recently suggested that hepatoma cell lines do not accurately model primary hepatocytes in terms of insulin action, they demonstrated that in HepG2 cells the response of IR to hormone stimulation substantially recapitulates IR activity in primary hepatocytes[117]. In agreement

with this finding, we used HepG2 cells to evaluate the impact of tea extracts and tea catechins only on IR phosphorylation status.

Conversely, we selected C2C12 murine muscle cell line as experimental model to evaluate the impact of tea extracts on IR and Akt phosphorylation levels and on glucose uptake. This cell line is recognized as a suitable model to study the molecular mechanisms of insulin resistance and the potential of natural and drug/synthetic compounds in maintaining glucose homeostasis[118]. We observed that the acute treatment of myotubes with 0.1 μM EGCG results in increased phosphorylation of IR, confirming that EGCG can easily cross cell membrane and inhibit PTP1B. However, we also pointed out that only treatment with EGCG concentrations higher than 10 μM leads to a significant increase of glucose uptake in C2C12 cells, suggesting that the insulin-mimetic activity of EGCG is strictly dose-dependent. Remarkably, these data agree with results from a previous study showing that the treatment of primary hepatocytes with EGCG concentrations lower than 1 μM failed to activate insulin receptor substrate 1 (IRS1) or Akt, two downstream effectors of IR[119]. Therefore, our data confirmed that the acute effects of EGCG are strictly dose-dependent, and for this reason, it is difficult to reproduce them in a physiological context in which the amount of absorbed EGCG can be influenced by several factors. Interestingly, further tests showed that acute treatment of C2C12 cells with cold Indian green tea extract enhances Akt phosphorylation either when administered alone or in combination with insulin, confirming that in muscle cells the tea extract is able to potentiate insulin sensitivity.

Previous studies underlined that chronic treatment of diabetic rodents with EGCG reduces glucosestimulated insulin secretion[120], suggesting that the chronic treatment with tea catechins could be more effective than acute one. Surprisingly, we observed that liver cells chronically treated with small amount (0.5%) of tea extract display higher IR levels and a strongly decreased ratio of phosphorylated IR over total IR (pIRβ/IRβ), compared to control samples, indicating that treated cells are enriched of the non-phosphorylated form of IR. However, by analyzing the relative increase of pIRβ/IRβ ratio after stimulation with insulin, we observed that tea-treated cells are more sensitive to insulin than untreated ones.

To date, we are far from identifying the specific tea components responsible for this effect on cell lines, and from assessing whether the enhancement of IR levels is due to the increased rate of IR synthesis/recycling or to a slower rate of degradation. Nevertheless, a similar increase was not observed in muscle cells acutely treated with EGCG, thereby indicating that the upregulation of IR levels requires a long-time treatment. In our opinion, this observation could have important clinical implications. Indeed, changes in both the number and the affinity of liver IR have been already described following chronic insulin stimulation[121], treatment of liver cells with saturated fatty acids[122] or in mice models fed with high fat-diet[123], or that assumed alcohol[124]. In all these cases, the downregulation of IR is accompanied by the onset of liver insulin resistance. Noteworthy, our data suggest that IR downregulation is a transitory condition that could be reverted by the regular intake of tea.

Intriguingly, none of these effects were detected in liver cells treated with the same dose of hot tea extracts, despite their higher total polyphenol content. These contradictory results could be due to chemical modifications or aggregation of tea components resulting from higher temperature of extraction, that leads to the extraction of molecules with decreased effects on the insulin-signaling

pathway[125]. This hypothesis is in part confirmed by superimposing the HPLC fingerprints of hot and cold tea extracts, revealing that the composition of the two extracts is rather different both quantitatively and qualitatively. Therefore, the extraction temperature is overall a key variable influencing the beneficial effects of tea extracts on glucose homeostasis. To date, further studies are ongoing to identify tea components able to influence IR levels in liver cells, hoping that in future such compounds could be used as lead molecules to develop a new generation of drugs able to counteract the onset of liver insulin-resistance.

In this study, the bioactivity of tea extracts was characterized, focusing on their ability to modulate the activity of the main tyrosine phosphatases that regulate IR phosphorylation. Kinetic analyses revealed that all extracts act as potent inhibitors of both PTP1B and LMW-PTP, with a mechanism of action strongly dependent on the extraction temperature. Further investigations led to the identification of EGCG and ECG as critical tea components responsible for the inhibition of both the phosphatases. Specifically, from a mechanistic point of view, we demonstrated that EGCG acts as a mixed-type inhibitor, showing a K_i value of 26 nM. In addition, assays performed on muscle cells demonstrated that acute treatment with EGCG increases IR phosphorylation, suggesting that EGCG acts as an insulin-sensitizing agent. Besides, we showed that chronic treatment of liver cells with tea extracts produces the increase of IR levels and insulin sensitivity. In conclusion, data reported in this study provide useful information to understand the biological effects of tea and support the hypothesis that this beverage has a potential antidiabetic activity.

Identification of Gossypetin as new potent PTP1B inhibitor: kinetic analyses, docking *in silico*, and cell-based assays.

Results and brief discussion

Determination of the IC_{50} values

To start our study, we created a library of 19 flavonoids characterized by different number and position of OH groups. For each compound, the IC_{50} value on PTP1B was determined and reported in Table 1. Among all the flavonoids analyzed, 7-hydroxyflavone (1) and 5,7-dihydroxyflavone (2, Chrysin) showed IC_{50} values for PTP1B greater than 1 mM, suggesting a relatively weak inhibition potential. However, the 3,5,7-trihydroxyflavone (3, Galangin), the 4',5,7-trihydroxyflavone (4, Apigenin) and the 5,6,7-trihydroxyflavone (5, Baicalein) showed an enhanced inhibitory activity (the calculated IC_{50} values were 38.5, 34.5 and 4.3 µM, respectively). These data suggested that the introduction of a new hydroxyl group to 5,7-dihydroxyflavone moiety, strongly contributed to stabilize the flavonoid-PTP1B complex, probably through the formation of new hydrogen bonds.

However, it was evident that the OH group in position C6 (Baicalein) resulted more effective in stabilizing the flavonoid-PTP1B complex than OH groups in C3 (Galangin) or C4' (Apigenin). Moreover, the introduction of an additional OH group on "B" ring of Galangin generated the 3,4',5,7tetrahydroxyflavone (6, Kaempferol) that showed an IC_{50} value 2.4 fold lower than that of Galangin. Futhermore, the introduction of one OH group on C3' of Apigenin lead to 3',4',5,7Tetrahydroxyflavone (8, Luteolin), which resulted 10.9 folds more potent than Apigenin.

Finally, the introduction of one OH group on C4' of Baicalein lead to 4',5,6,7-tetrahydroxy-flavanone (7, Scutellarein), that resulted an inhibition 4.9 fold more potent than Baicalein (Figure 1). These observations suggested that the flavonoids bearing an OH group on C6 resulted stronger PTP1B inhibitors than those showing an addition OH group on "B" and "C" rings.

It is interesting to note that the shift of one OH group from C5 to C3 of Luteolin generated the 3,3',4',7-Tetrahydroxyflavone (9, Fisetin) with an IC_{50} value 5.6 folds lower than Luteolin. This finding suggested that the OH group in C5 has a detrimental effect in stabilizing the inhibitory activity of Luteolin. Moreover, the introduction of OH group on C3 of Luteolin slight improved the inhibitory activity of C5,7,3',4'flavonoids, as demonstrated by the fact that the 3,3',4',5,7pentahydroxyflavone (11, Quercetin) showed an IC_{50} values of 0.98 µM. It is singular that the 3,2',4',5,7-pentahydroxyflavone (10, Morin), showed an IC_{50} value very close to Quercetin one.

Number	Compound	IC_{50} (μM)	Classification
1	7-Hydroxyflavone	> 1000	Flavone
2	Chrysin	> 1000	Flavone
3	Galangin	38.5 ± 2.9	Flavonol
4	Apigenin	34,5 ± 1.4	Flavone
5	Baicalein	4,3 ± 0.6	Flavone
6	Kaempferol	14,1 ± 0.4	Flavonol
7	Scutellarein	0.88 ± 0.1	Flavone
8	Luteolin	3,16 ± 0.1	Flavone
9	Fisetin	0,56 ± 0.07	Flavonol
10	Morin	1,1 ± 0.03	Flavonol
11	Quercetin	0,98 ± 0.04	Flavonol
12	Taxifolin	317 ± 178	Flavanone
13	Naringenin	600 ± 40	Flavanone
14	Eriodictyol	33.4 ± 1.8	Flavanone
15	(+)-Catechin	76.9 ± 4.9	Flavan-3-ol
16	Myricetin	0,41 ± 0.01	Flavonol
17	Gossypetin	0.09 ± 0.1	Flavonol
18	Genistein	1100 ± 90	Isoflavone
19	Daidzein	105 ± 15.4	Isoflavone

Table 6: calculated IC_{50} values of natural flavanoids for PTP1B.

This suggested that the shift of OH group from C3' to C2' does not lead to further stabilization of the flavonoid-PTP1B complex (Figure 20).

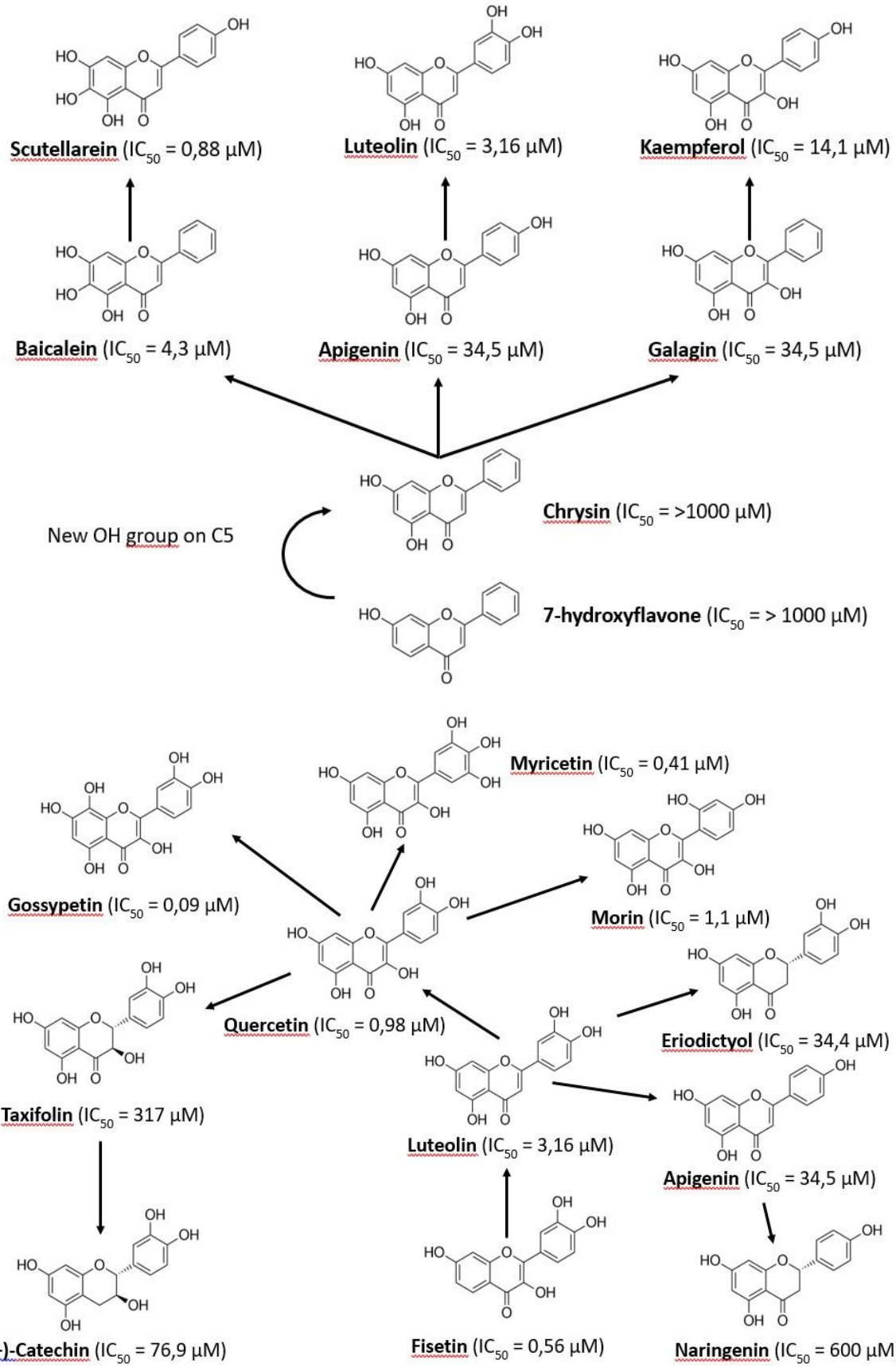

Fig. 20. Structures of tested flavonoids with IC_{50} values.

Another interesting observation is that the loss of double bond between C2-C3 dramatically affected the flavonoid-PTP1B complex stability. According with this hypothesis, we found that dihydroquercetin (12, Taxifolin), was a weaker inhibitor of PTP1B (its IC_{50} values was 325 folds lower than that of Quercetin). Furthermore, we found that 4',5,7-trihydroxyflavanone (13, Naringenin) showed an IC_{50} value of 17.4 folds of Apigenin, while the 3',4',5,7-tetrahydroxyflavanone (14, Eriodictyol), resulted 10.9 times less effective than Luteolin in inhibiting PTP1B (Figure 1). Suprisingly, Taxifolin, which carries an additional OH group to Eriodyctiol, showed an IC_{50} value 9.5 times higher than this, while the (2S, 3R) -2- (3,4-dihydroxyphenyl) croman-3,5,7- triol (15, (+) -catechin), which lacks the carbonyl group on C4, was 4 times more efficient in inhibiting PTP1B than Taxifolin. This result suggests that following the loss of the double bond on the "C" ring the carbonyl group and the OH group on C3 hinder each other, preventing taxifolin from forming a stable complex with PTP1B.

Furthermore, both 3,5,7,3',4',5'-Hexahydroxyflavone (16, Myricetin) than 3,3',4',5,7,8Hexahydroxyflavone (17, Gossypetin) resulted more potent than Quercetin. Interestingly, Gossypetin, which bears three-hydroxyl group on “A” ring, showed an IC_{50} value of 90 nM, exactly 4.2 folds lower than Myricetin that possess three OH groups on “B” ring, and resulted 2.4 folds more effective than Quercetin. This finding suggested that position of OH groups, other than their total number, is essential to stabilize the favonoid-PTP1B complex. In our knowledge, Gossypetin is the most potent flavonoid inhibitor described so far (Figure 20).

The 5,7,4'-Trihydroxyisoflavone (18) Genistein resulted a weaker inhibitor than Apigenin (IC_{50} of Genistein and Apigenin were 1100 and 34.5 µM, respectively), confirming that the shift of phenol ring from C2 to C3 impaired the ability to interact with PTP1B. On the other hand, 7,4'Dihydroxyisoflavone (19) Daidzein behaved as a better inhibitor than Genistein, showing an IC_{50} value of 105 µM. This discovery confirmed that the loss of the OH group on C5 altered the interaction of flavonoids with PTP1B and its loss allowed Daidzein to bind PTP1B more stably.

Data obtained give some important information about chemical determinants that contribute to stabilize the strength of flavonoid-PTP1B complex. First, we can state that the number of OH groups, the presence of carbonyl group and of double bond (C2-C3) on “C” ring is essential to improve the inhibitory activity of flavonoids toward PTP1B. We observed that the correlation between the variable observed and the IC_{50} values steadily increase considering the total number of OH groups alone, the number of OH groups and the presence of the carbonyl group, or the number of OH groups plus the presence of the carbonyl group and the presence of double bound on “C” ring. It is interestingly to observe that the sum of these parameters explain about 90% of variability observed.

Moreover, OH groups on C5, 7, did not contribute or have a detrimental effect in stabilizing the flavonoid-PTP1B complex. Finally, the OH groups in C6, C8 and C4 'contribute to the generation of flavonoids with a high inhibitory power.

Protein	IC_{50} (μM)	Ratio ($IC_{50PTP1B}/IC_{50PTPs}$)
PTP1B	0.09 ± 0.10	1
TC-PTP	0.70 ± 0.1	0.13
IF1	0.43 ± 0.02	0.21
IF2	0.68 ± 0.02	0.13

Table 7: IC_{50} values of Gossypetin for PTP1B, TC-PTP, and the LMW-PTP isoforms, IF1 and IF2. The column on the right shows the ration between the IC_{50} for PTP1B and that calculated for the other PTPs.

Evaluation of mechanism of action of Gossypetin

Kinetic analyzes were performed to define the mechanism of action of Gossypetin. First, a dilution assay was performed to evaluate whether Gossypetin behaved as reversible or not-reversible inhibitor of PTP1B (Fig. 21A). We observed that after 1 h incubation of PTP1B in the presence of 1 μM Gossypetin, the enzyme recovered almost completely its activity when diluted in the assay buffer, suggesting the reversibility of inhibition. Then, we studied the dependence of both K_m and V_{max} from the Gossypetin concentration. We observed that the K_m of PTP1B increase while the V_{max} decrease as the dose of Gossypetin increased. Moreover, the analysis of Lineweaver-Burk plot showed that experimental data described straight lines intersecting one each other in a point on the left quadrant (Fig. 2B), confirming that Gossypetin behaved as a mixed type inhibitor of PTP1B.

To evaluate the specificity of Gossypetin action, we determined the IC_{50} value of Gossypetin for TCPTP and both isoforms of LMW-PTP, IF1 and IF2. We found that the IC_{50} values of Gossypetin for both LMW-PTP isoforms were IC_{50}: 0.7 ± 0.02 μM and 0.43 ± 0.02 μM for IF1 and IF2, respectively, moreover we calculated an IC_{50} value of 0.7 ± 0.1 μM for TC-PTP. Together, these results suggested that Gossypetin showed a marked specificity for PTP1B over both LMW-PTP isoforms, and TCPTP.

Synergic activity of Gossypetin

Kinetic analyses suggested that Gossypetin possess a specific binding site different from the active site of the enzyme. To evaluate whether the binding site of Gossypetin correspond to previously described allosteric sites[126,127], we studied its synergistic ability with different kind of molecules, including inorganic phosphate, vanadate, Morin and Betulinic acid using the method proposed by Chou-Talalay[128]. Both inorganic phosphate (Pi) and vanadate (V), are competitive inhibitors of PTP1B through active site interaction. Therefore, we expected that these behave as mutually exclusive inhibitors[129].

In agreement with this hypothesis, we observed that both inhibitors follow a first order kinetics and that the combination graph (Pi + V) describes a straight line parallel to those obtained by analyzing each inhibitor, individually (Figure 22A). These results agree with the observation made by Chou and Talalay[130] concerning two mutually exclusive inhibitors.

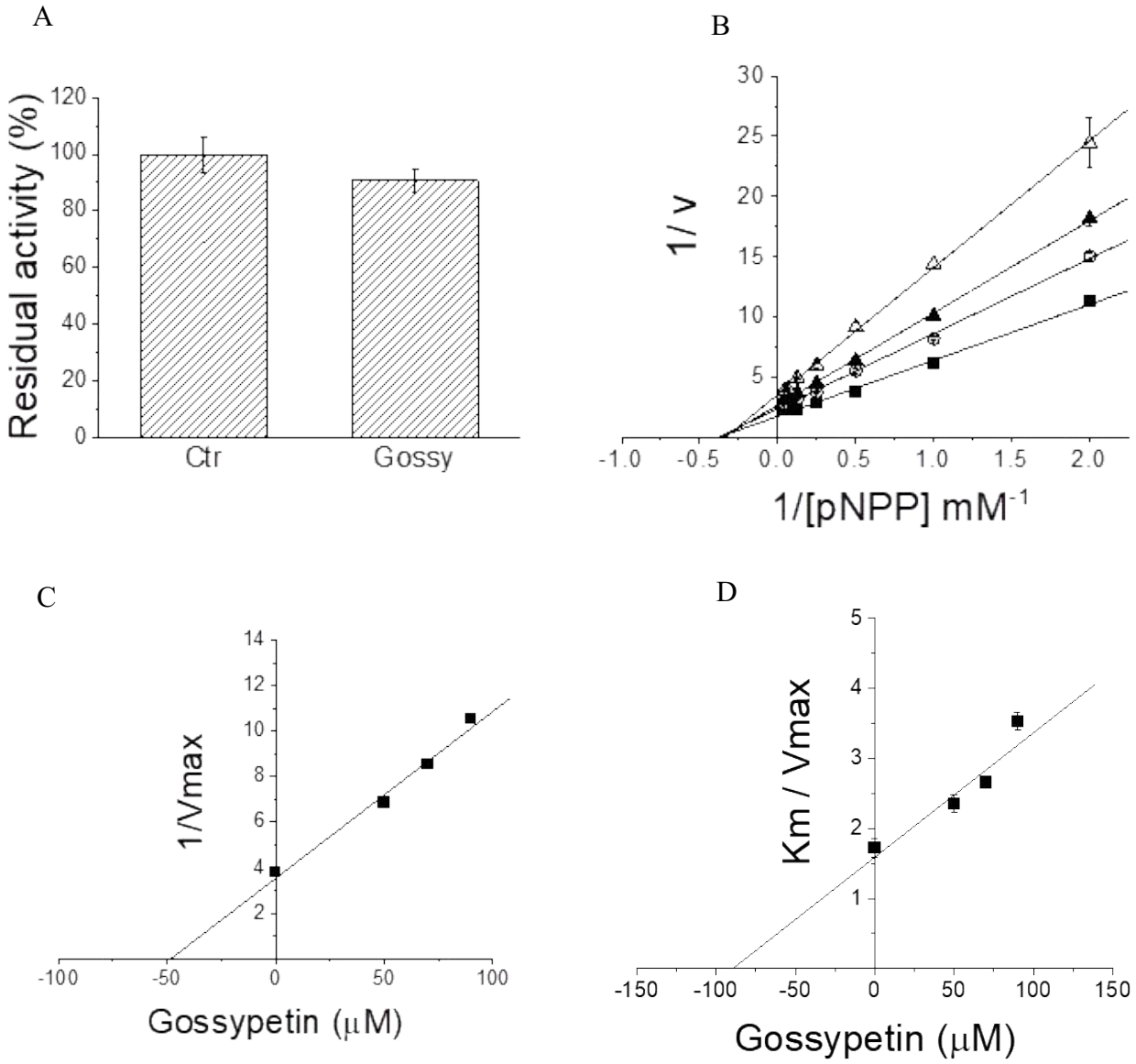

Fig. 21. Characterization of the mechanism of action of Gossypetin. (**A**), dilution assay. A sample containing the PTP1B was incubated in the presence of a saturating concentration of Gossypetin (1 μM) for 1 h at 37°C. After this time, an aliquot of enzyme was withdrawn and diluted 800 folds in the assay buffer to evaluate the residual enzymatic activity of the enzyme. The test was carried out in triplicate. The control assay was carried out diluting the sample in the same volume of DMSO, the solvent used to dissolve Gossypetin. All data were normalized respect to control test and reported in the figure as meand ± SD. All tests were carried out in triplicate. (**B**), Lineweaver-Burk plot. The concentrations of Gossypetin used were: ■, 0 nM; ○, 50 nM, ▲, 70 nM, △, 90 nM. Data reported in the figure represent the mean value ± SD (n=3). (**C**, **D**), secondary plots. The Ki and Ki' value were determined using the equation described in the material and method section. The calculated affinity values were K_i: 49.2 ± 9.8 nM and K_i': 89.6 ± 9.3 nM.

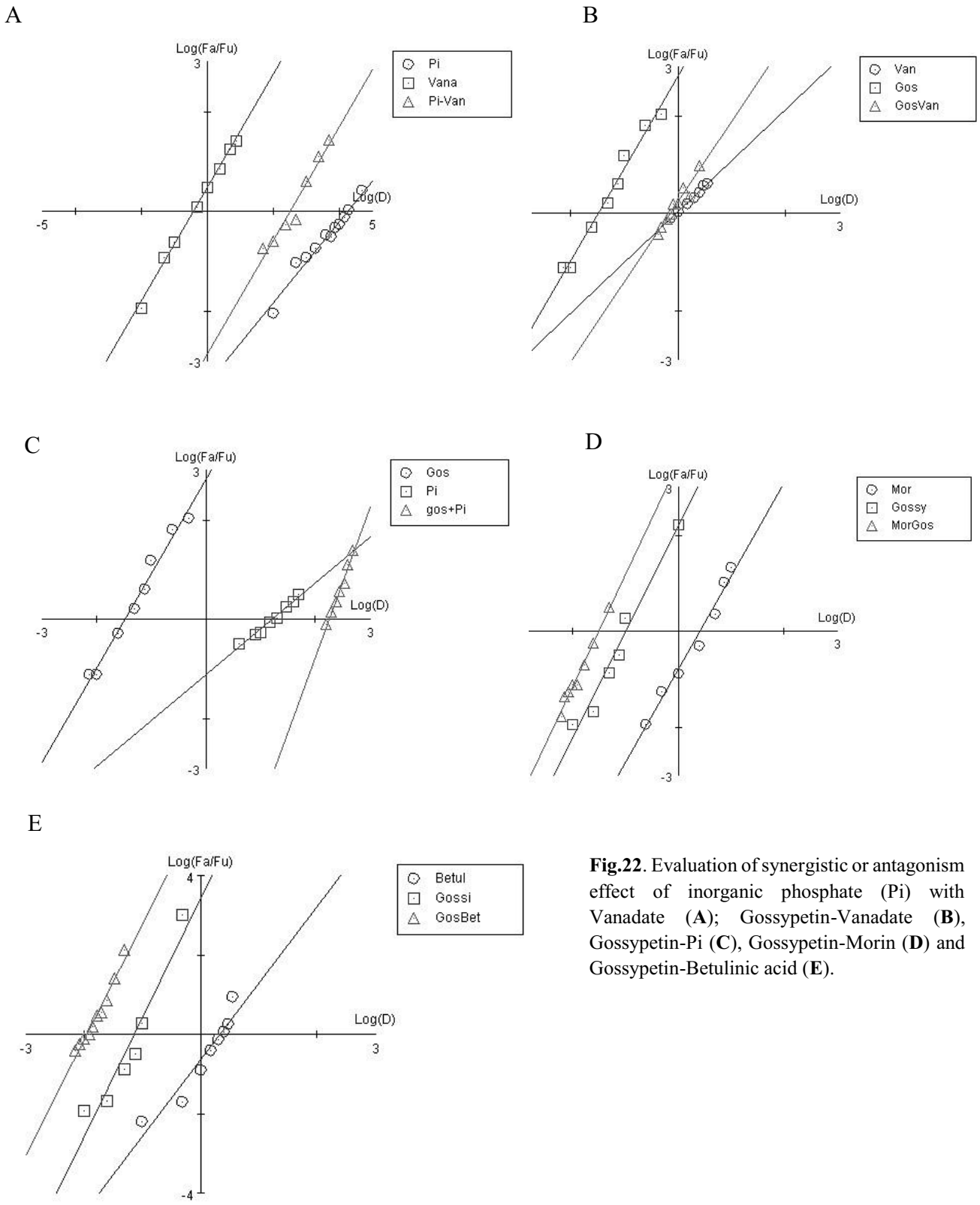

Fig.22. Evaluation of synergistic or antagonism effect of inorganic phosphate (Pi) with Vanadate (**A**); Gossypetin-Vanadate (**B**), Gossypetin-Pi (**C**), Gossypetin-Morin (**D**) and Gossypetin-Betulinic acid (**E**).

When the Gossypetin was challenged in combination with vanadate, we observed that the compination resulted less effective than Gossypetin alone, suggesting that V acted in an antagonistic manner respect to Gossypetin (Figure 22B). Similar results were obtained when we analyzed the behavior of Gossypetin versus Pi (Figure 22C). In this case, the straight line fitting the Gossypetin-Pi combination data resulted rigthward respect to Pi data, thereby confirming the presence of a strong antagonism between such molecules. Different results were obtained when we challenged the Gossypetin versus Morin, or Betulinc acid, two non-competitive inhibitors of PTP1B. In both cases, we observed that data referred to combination were leftward shifted respect to data points obtained using Gossypetin alone, suggesting that it was able to synergize with both Morin and Betulinic acid (Figure 22D, E). Together, these results indicated that Gossypetin binds PTP1B in a site independent from that of Morin and Betulinic acid. Furthermore, the strong antagonism observed between Gossypetin, Pi and V, could be justified by assuming that the Gossypetine binding site is located near the PTP1B P-loop.

Docking simulation

To analyze the interaction mode of Gossypetin with PTP1B, an *in silico* analysis was carried out. The first docking unbiased analysis to identify all possible binding site of Gossypetin on PTP1B surface. We identify 12 different binding sites of Gossypetin, with ΔG valued between -7.3 and -5.4 kcal/mole, and two of these are located near the WPD-loop of PTP1B. Interestingly, in one on these positions the Gossypetin engaged one hydrogen bond between Asp 181 and the OH group on C8 of Gossypetin, further two hydrogen bonds between OH in C4' and NH and CO groups of main chain of Trp179 and Thr177 residues (Figure 23). Hydrophobic interactions with Arg112, Glu115, Lys116, Thr178 and Pro180 contribute to stabilize interaction of Gossypetin with PTP1B into WPD-loop region. This finding reinforce the hypothesis that C4' and C8 OH groups have a key role in stabilizing the Gossypetin-PTP1B interaction in the region of WPD-loop, hindering its movement and inhibiting the catalytic activity of PTP1B. The identification of such site, not only contribute to explain the antagonism with Pi and V, but also can explain the synergistic effect observed with Morin and betulinic acid. In fact, such molecules possess not overlapping and independent binding sites, and for this reason can bind to PTP1B in the same moment, generating a synergistic inhibitory effect.

Effects of Gossypetin on insulin signalling pathway

To evaluate the ability of Gossypetin to improve insulin signaling pathway, we performed some tests using murine C2C12 and HepG2 liver cells. The acute treatment of differentiated C2C12 cells with Gossypetin did not result neither in enhancement of Akt phosphorylation (Figure 24) nor in an increased glucose uptake (data not shown). Similar tests were carried out also with HepG2 liver cells (Figure 25). We observed that insulin-stimulated liver cells show a weak increase in the phosphorylation state of the receptor. It is unusual to observe that after treatment with Gossypetin, the level of phosphorylation of the receptor decreases significantly, both in non-stimulated cells and in those treated with insulin. However, a significant increase in the level of Akt phosphorylation was

observed only in cells treated with the insulin-Gossypetin combination. This result suggested that Gossypetin acted as an insulin-sensitizing agent in liver cells.

A

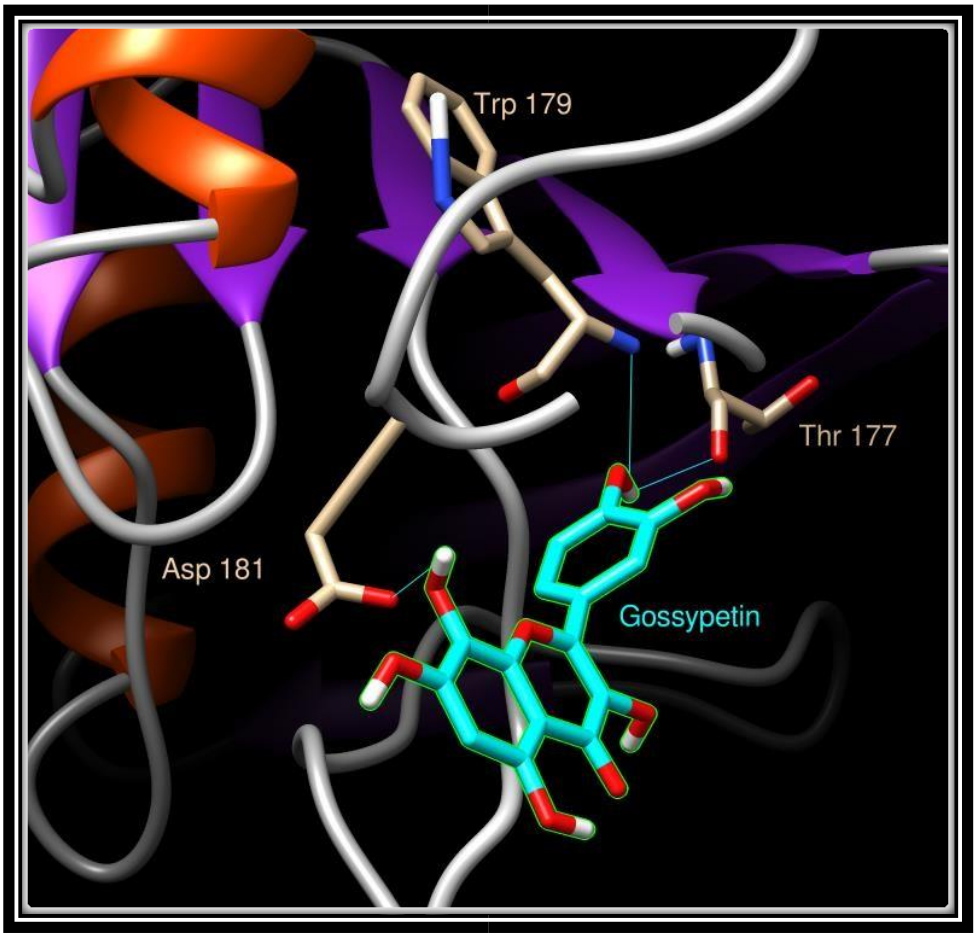

B

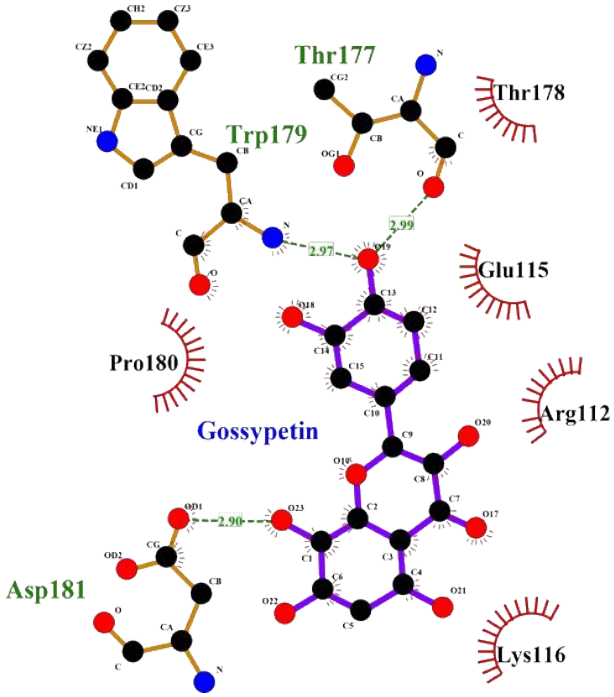

Fig. 23. Docking analysis of Gossypetin on PTP1B structure. **A**, representation of the most favourable docked position next to WPD - loop, blue lines represent hydrogen bonds between ligand and evidenced enzymes residues. **B**, 2D schematic representations of the intermolecular interactions between the enzyme and the ligand. Ligand is reported with purple lines; the red lines indicate hydrophobic interactions between enzyme and ligand while green dotted lines stand for H- bonds.

To evaluate the long-term effects of Gossypetin, liver cells were treated with Gossypetin for four days and then analysed by western blot (Figure 26). Similarly, to the first test, we observed that a non-significant increase in insulin receptor phosphorylation levels is observed in untreated cells. Also in this case, treatment with Gossypetine causes a decrease in the levels of phosphorylation of the insulin receptor; however, in this case, the differences in insulin receptor and Akt kinase phosphorylation between unstimulated and stimulated cells were significantly different. Moreover, we observed that treatment with Gossypetin did not affected the expression levels of PTP1B, but decreased the expression of LMW-PTP, a tyrosine phosphatase that contribute to regulate the activation of insulin receptor[131]. Together, these results suggested that the enhanced response to insulin in liver cells treated with Gossypetin could be the result of PTP1B inhibition and of LMW-PTP downregulation.

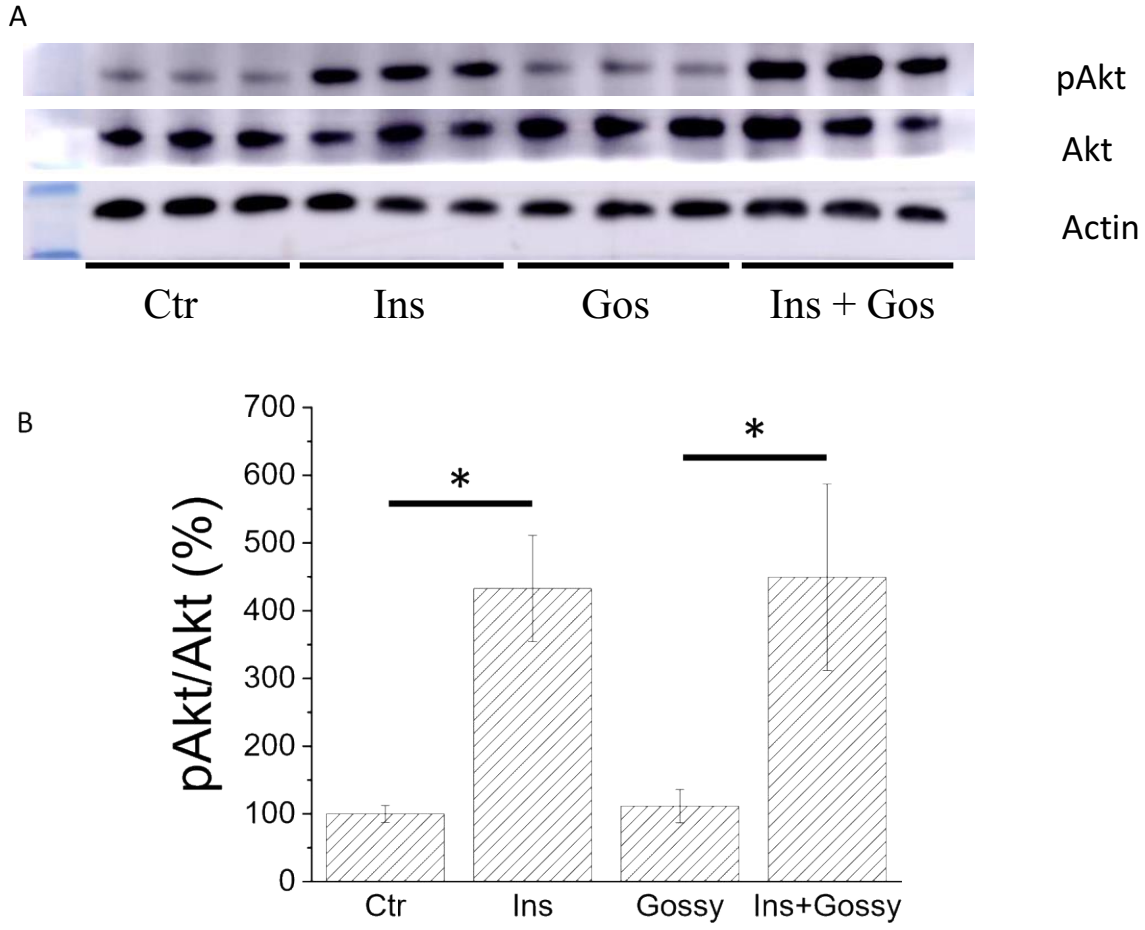

Fig. 24. Effects of Gossypetin on insulin signalling pathway. Differentiated C2C12 cells were starved for 24 h and then stimulated with 10 nM insulin, 5 µM Gossypetin or insulin-gossypetin combination for 15 min at 37°C. After, medium was removed, the cells washed with PBS and lysed using 1X Laemmli sumple buffer solution. The proteins of cell extracts were separated by SDS-PAGE, transferred to a PVDF membrane. Akt and pAkt levels were detected using specific antibodies capable to recognize non-phosphorylated and phosphorylated form of Akt. (**A**), image of the western blot. (**B**), quantification of the western blot. All tests were carried out in triplicate. Value obtained were normalized whit respect to that of the control experiment. Data reported in the figure (**B**) represent the mean values ± SD (n: 3).

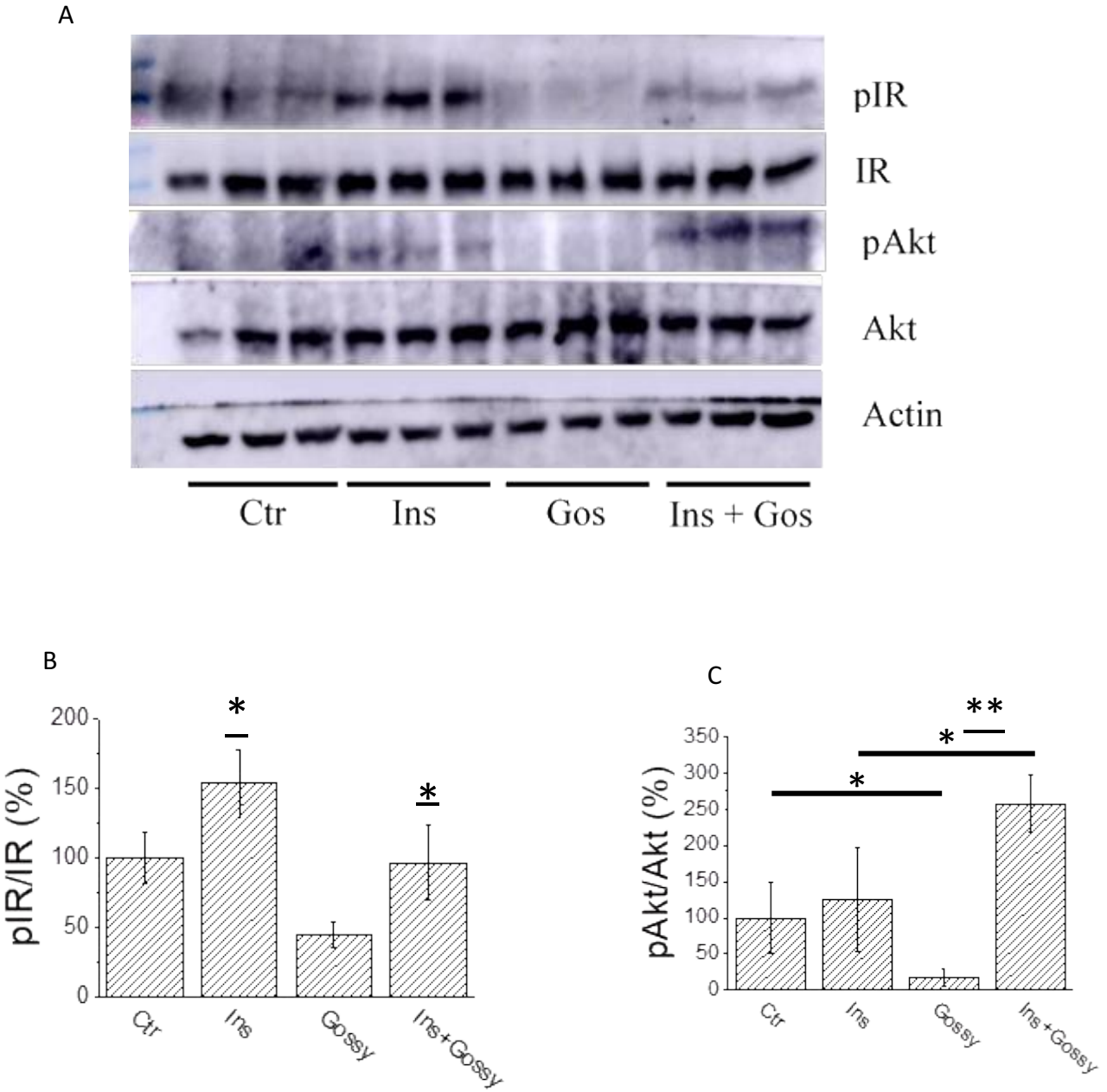

Fig. 25. Effects of acute gossypetin treatment on the insulin signaling pathway. Starved HepG2 cells were stimulated with 10 nM insulin, 5 µM Gossypetin of insulin-Gossypetin combination for 30 min at 37°C and then lysed. Phosphorylation levels of insulin receptor and kinase Akt was evaluated using antibodies capable to recognize both phosphorylated and non phosphorylated form of proteins. (**A**), image of western blot. Quantification of IR (**B**) and Akt (**C**) phosphorylation levels. All tests were carried out in triplicate. Values were normalized respect to control tests. Data showed in the figure (**B**) represent the mean values ± SD (n: 3). * $p < 0.05$; ** $p < 0.01$.

A

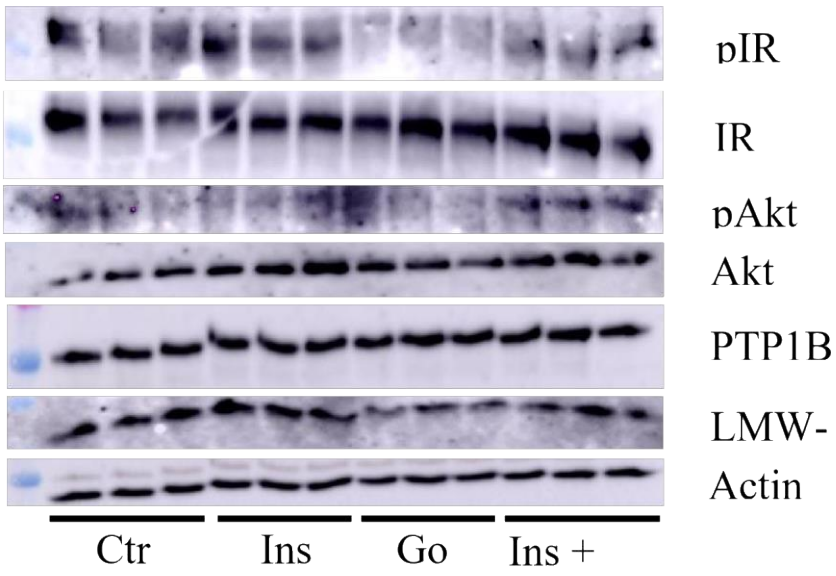
pIR
IR
pAkt
Akt
PTP1B
LMW-
Actin
Ctr
Ins
Go
Ins +

B

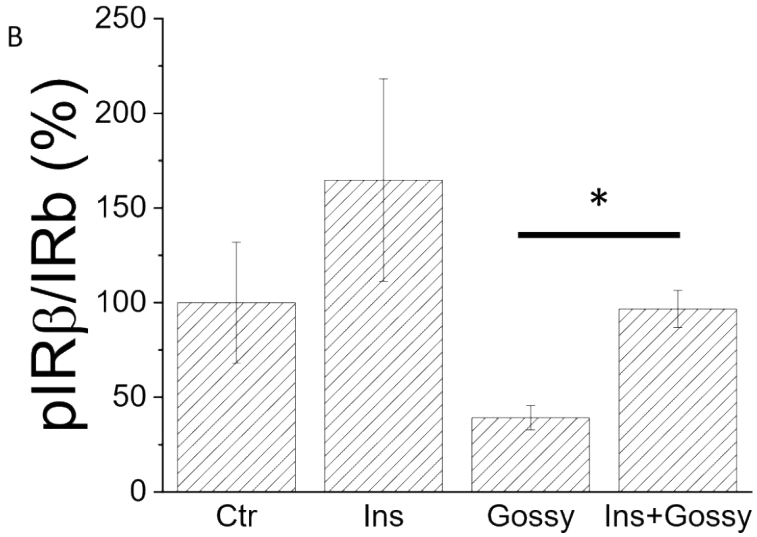
pIRβ/IRb (%)
250
200
150
100
50
0
*
Ctr
Ins
Gossy
Ins+Gossy

C

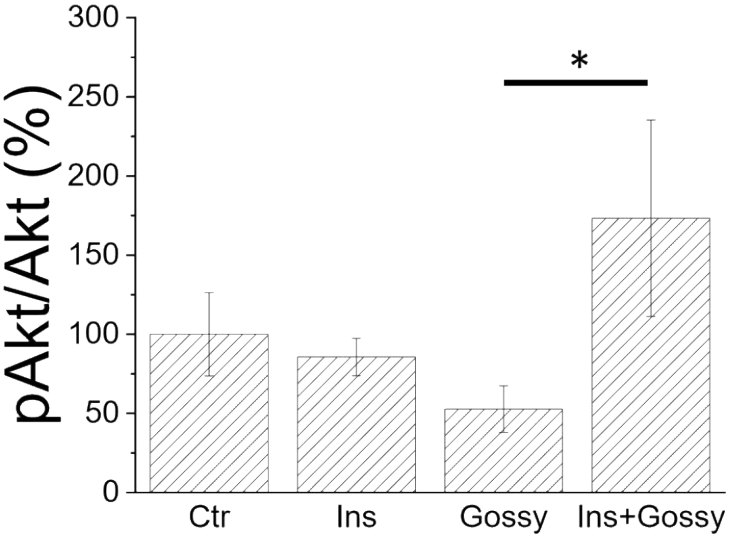
pAkt/Akt (%)
300
250
200
150
100
50
0
*
Ctr
Ins
Gossy
Ins+Gossy

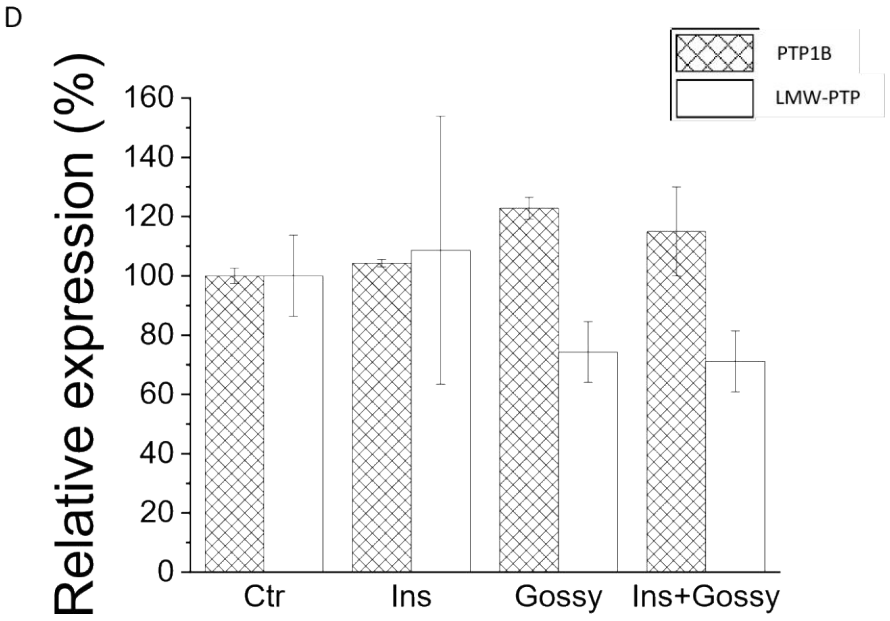

Fig. 26. Effects of chronic gossypetin treatment on the insulin signaling pathway. Starved HepG2 cells were treated with 1 µM Gossypetin for five days and then stimulated with 10 nM insulin. Each day, cell growth medium was replaced with a fresh medium containing Gossypetin. Phosphorylation levels of insulin receptor and kinase Akt was evaluated using antibodies capable to recognize both phosphorylated and non phosphorylated form of proteins. (**A**), image of western blot. Quantification of phosphorylated form of IR (**B**) and Akt (**C**), or expression levels of PTP1B and LMW-PTP (**D**). All tests were carried out in triplicate. Values were normalized respect to control tests. Data showed in the figure (**B**) represent the mean values ± SD (n: 3). * $p < 0.05$; ** $p < 0.01$.

The aim of this work was to evaluate the inhibitory effect of several flavonoids on PTP1B and, by comparison, to trace crucial structure features responsible for this effect. Our data show IC_{50} values in nanomolar range and, among all flavonoids, Gossypetin resulted to be the strongest showing an IC_{50} of 90 ± 0.1 nM.

It seems clear that the amount of OH groups and their position are crucial protagonists of the interaction between ligand and this enzyme. First, we can state that the number of OH groups, the presence of carbonyl group and of double bond (C2-C3) on "C" ring are essential to improve inhibition. As mentioned in introduction section, targeting PTPs is quite challenging. Zhang explained that targeting the active site of PTPs could bring the development of aspecific inhibitors that could even show membrane permeability issues[45]. Gossypetin could overcome this problem since flavonoid could easily get inside cells and we are confident that it is not targeting the active site. But what about the mechanism of action?

Our results show that it behaves as a mixed type inhibitor of PTP1B with affinity values of K_i: 49.2 ± 9.8 nM and K_i': 89.6 ± 9.3 nM suggesting the interaction with an allosteric site of the enzyme and supporting the idea that it could be specific for it over other PTPs. We confirmed it by testing Gossypetin over IF1 – IF2 and TC-PTP and the results confirmed the hypothesis of its specificity of action since IC_{50} values were several folds higher than the one found for PTP1B.

In order to improve our understanding of Gossypetin mechanism of action, we performed sinergistic assays with different molecules. The idea is to evaluate if Gossypetin binding site corresponds with others already described[126,127]. Even if Gossypetin doesn't bind the active site, the combination with Pi and Vanadate (which are confirmed to interact with it[129]) resulted to show strong antagonism and new experiments are needed to assess why.

Meanwhile, combination with Morin and Betulinic acid showed synergistic activity, suggesting the contemporary binding on different sites. Weissmann et al. described an allosteric site which is crucial for the correct closure of active site through WPD loop motion[42], betulinic acid was chosen for synergy assay since was demonstrated that interacts with this site[126]. It seems to prevent the correct movement of WPD loop, ''locking'' it in open conformation which is unfavourable for catalysis.

The synergistic effect of Betulinic acid with Gossypetin suggests that while the former interacts with Weissman's allosteric binding site, the latter could improve the inhibition by directly interacting with WPD loop, locking it in an open conformation. In this way the loop cannot move correctly for catalysis purposes. The synergistic effect of Morin with Gossypetin could suggest a simultaneously interaction on WPD loop. This hypothesis could explain the strong antagonism observed between Gossypetin, Pi and V, supporting the idea that its binding site is located near the PTP1B WPD-loop, forcing it in open conformation while Pi and V induce a closed one simulating the presence of substrate.

Thanks to docking simulations, we theorized an hypothesis of how Gossypetin interacts with the PTP1B. Among all positions obtained, the best one resulted across the WPD loop and supports our kinetic results and our theory. 2D representation of docked structure, suggest the involvement of several crucial PTP1B residues like Asp 181 (critical for catalysis[41]) which forms an hydrogen bond with the molecule while not being no longer available for catalysis purposes.

The docking simulation gives an idea of why the OH residues are important for interaction between flavonoids and PTP1B. Gossypetin high potency of inhibition could be related to their number and position, showing several hydrogen bonds formation across the WPD loop, suggesting the presence of a new allosteric binding site which is, of course, specific for PTP1B. The Gossypetin structure could suggest an interesting scaffold for drug development that shows small dimension, good cell membrane permeability and high specific interaction with this enzyme.

The insulin signalling pathway study is still preliminary. The acute treatment of differentiated C2C12 cells with Gossypetin showed no enhancement of Akt activation or in glucose uptake which are effects usually related to a strong inhibition of PTP1B[132]. Even if Gossypetin is a strong inhibitor, it is not clear why it does not bring to any effect on insulin signalling pathway on muscle cells suggesting to act on a different level. Flavonoids are described to be effective in inducing an activation of such pathway but probably a chronic stimulation of several days is needed to observe an effect on muscle tissue[133]. The acute treatment used on this study seemed to be ineffective, even if several other PTP1B inhibitors, showed effectiveness in 15 - 30 minutes of stimulation[74,134]. Probably Gossypetin needs more time to interact with muscle tissue.

Similar tests were carried out also with HepG2 liver cells and we observed an increase in the level of Akt phosphorylation induced by the insulin-Gossypetin combination in brief stimulation. We

decided to also evaluate the long-term effects of Gossypetin after four days of stimulation. The differences in insulin receptor and Akt kinase phosphorylation between unstimulated and stimulated cells were significantly different and, surprisingly, we found a decreased expression of LMW-PTP levels. Taken together all these effects suggested that Gossypetin in liver cells acted as an insulin-sensitizing agent by enhancing the effect on insulin. A decreased level of LMW-PTP could be beneficial since it regulates negatively insulin receptor like PTP1B does[135]. In same time insulin signalling pathway could be stimulated by the reduced level of IF1 combined with the strong inhibition of PTP1B by Gossypetin presence. It remains to be clarified the reason why liver cells seemed to be affected by the presence of Gossypetin even in acute stimulation while muscle cells did not. Probably the hepatocytes, considering their role and function, are more susceptible by the presence of flavonoids which were confirmed to be beneficial for the treatment of pathologies like non alcoholic fatty liver disease[136]. A chronic stimulation test on C2C12 is needed to enlight the differential effect (if confirmed) of Gossypetin on different tissues.

By now, we can say that this flavonoid has a great potential as scaffold for drug development for T2D treatment and it could probably suggest a new allosteric site on PTP1B not yet described.

Results and brief discussion

Evaluation of inhibitory effects against PTP1B and AR of compounds 1−4, and kinetic analyses of avarone (2)

Four structurally related quinones (1−4, see introduction for structures) were analysed to evaluate their ability to inhibit both PTP1B and aldose reductase. For each compound the IC_{50} values were determined on both PTP1B and AR (Table 8). As far AR is concerned, avarone (2) resulted the most potent among the tested compounds. Since IC_{50} value for 2 resulted of the same order of magnitude of AR concentration in the assay (67 nM on the basis of a molecular weight of 34 KDa), this compound was considered as a "tight binding" inhibitor.

Compound	**IC_{50} (μM)**	
	PTP1B	**AR**
avarol (**1**)	42.2 ± 18	0.58 (0.31-1.08)
avarone (**2**)	5.6 ± 1.0	0.08 (0.06-0.11)
3-methylaminoavarone (**3**)	15.2 ± 2.1	80 (55-117)
4-methylaminoavarone (**4**)	21.6 ± 1.0	60 (48-75)

Table 8. Calculated IC_{50} values for PTP1B and AR. Data were expressed as IC_{50} ± SD for PTP1B and IC_{50} with their 95% confidence intervals for AR.

Among the compounds analyzed, avarone (2) is also confirmed as the most powerful inhibitor of PTP1B, showing an IC_{50} value of 5.6 μM. Taking into account the high molar ratio (IC_{50}/PTP1B concentration), avarone cannot consider a tight binding inhibitor. The kinetic characterization carried using recombinant AR enzyme allowed the evaluation of K_i and K_i' values of 410 ± 94 and 55 ± 8 nM, respectively (Figure 27). Thus, avarone resulted as a non-competitive mixed type inhibitor, with a preferential binding to the ES complex with respect to the free enzyme.

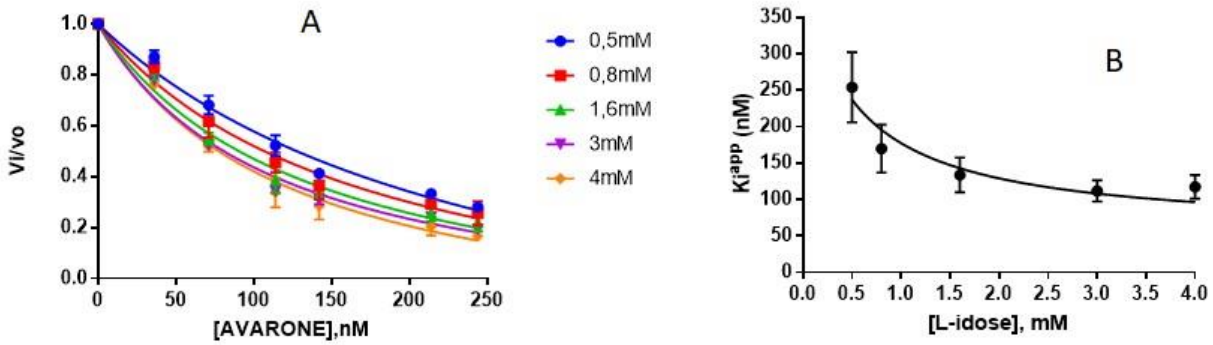

Fig. 27. Kinetic characterization of avarone as AR inhibitor. **A**, activity of the purified enzyme (8 mU) was measured at the indicated concentrations of avarone in the presence of the indicated L-idose concentrations.
B, experimental data reported in Panel A were fitted to Morrison Equation (see Methods, Equation A). The obtained apparent inhibition con-stants, K_i^app, were plotted against substrate concentration and fitted by nonlinear regression analysis to the equation B (see Methods) relative to a general case of tight binding non-competitive inhibition.

Further kinetic analyzes were performed to define the mechanism of PTP1B inhibition by avarone. By dilution assay, we confirmed that avarone behaved as a reversible inhibitor of PTP1B. Moreover, to dissect the mechanism of inhibition of avarone, we analysed the dependence of K_m and V_{max} from the concentration of the inhibitor. We observed that by increasing its concentration, the value of K_m also increased, but the V_{max} substantially did not change; furthermore, double reciprocal plot showed that experimental points described right lines intersecting one each other in a point on abscissa axis, suggesting that avarone behaved as a competitive inhibitor of PTP1B (Figure 28). However, it is evident that Km values increased non-linearly with increasing avarone concentration, raising the suspicion that the inhibition is determined by the binding of more than one avarone molecule within the site of the enzyme. Based on this evidence we describe the mechanism of inhibition of avarone for PTP1B as a "cooperative pure competitive inhibition by two non-exclusive inhibitor molecules". Such inhibition model foresees that the first inhibitor molecule (I_a) binds to the active site of the free enzyme and not to the ES complex. The second inhibitor molecule (I_b) can only bind to EI_a, generating the ternary complex (EI_aI_b). Taking into account the rapid equilibrium conditions prevail, it was possible derive the equation 1 that has used to calculate both K_i1 (15.1 ± 1.4 µM) and K_i2 (1.0 ± 0.1 µM) values. Moreover, we tested avarone on TC-PTP and showed lesser affinity compaired to PTP1B one, suggesting a specific interaction mechanism not shared with other PTPs (Figure 29).

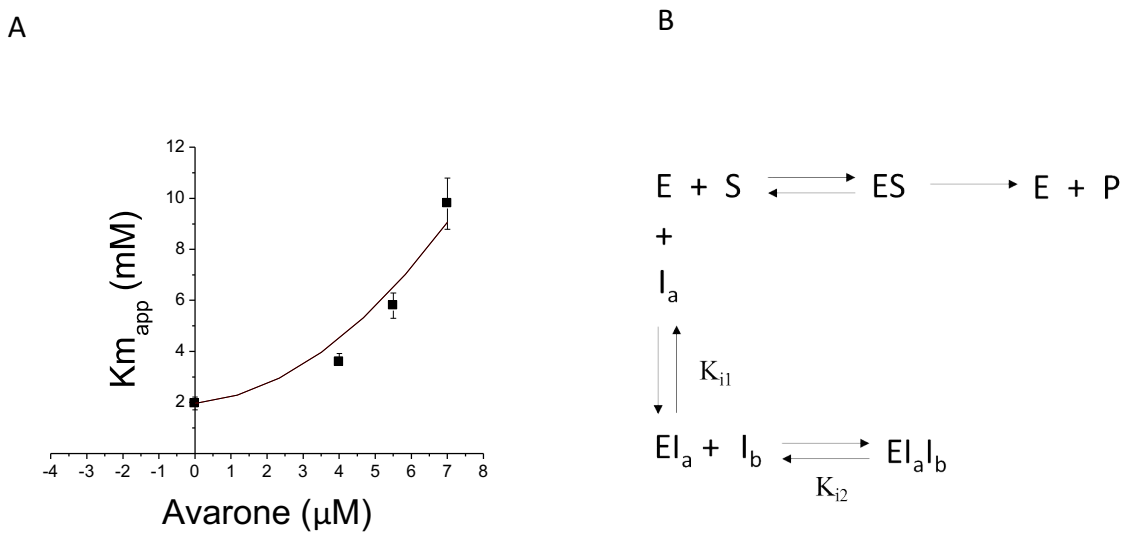

Fig. 28. Determination of K_i for avarone. **A**, dependence of K_m from the avarone concentration. Data fitting was obtained using OriginPlus 2021 software. **B**, Inhibition mechanism of avarone. **E** represents the free enzyme; **ES** the Michaelis-Menten complex; **P** the product of reaction, $\mathbf{I_a}$ and $\mathbf{I_b}$ represent the molecules of the inhibitor, $\mathbf{EI_a}$ and $\mathbf{EI_aI_b}$, the enzyme-inhibitor complexes, $\mathbf{K_i1}$ and $\mathbf{K_i2}$ are the enzyme inhibition constants for $\mathbf{I_a}$ and $\mathbf{I_b}$, respectively.

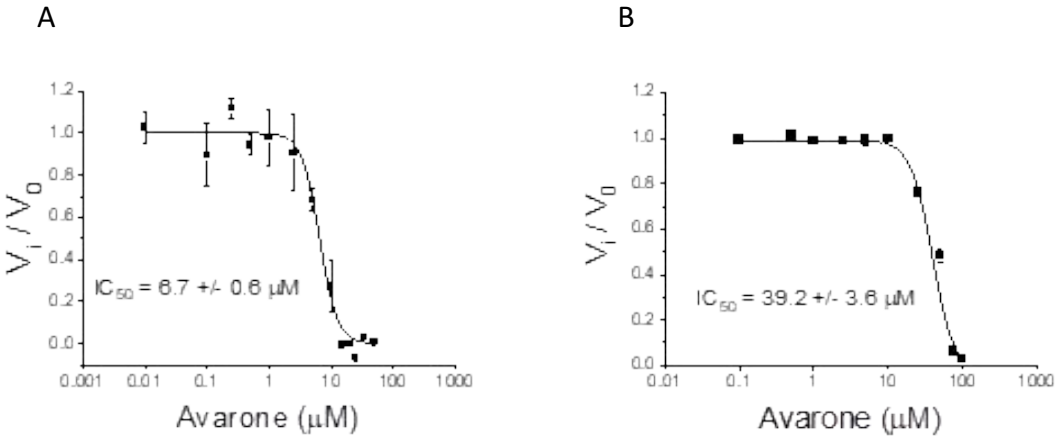

Fig. 29. Comparison between the IC_{50} of avarone. **A** PTP1B; **B** TC-PTP.

PTP1B docking experiments

In order to better evaluate the interaction modality of avarone with PTP1B, *in silico* docking analyzes were carried out. In accordance with the kinetic analyzes, the analyzes carried out identified three different binding sites for avarone on PTP1B surface, including the active site and other two region far from it (Figure 30).

A **B**

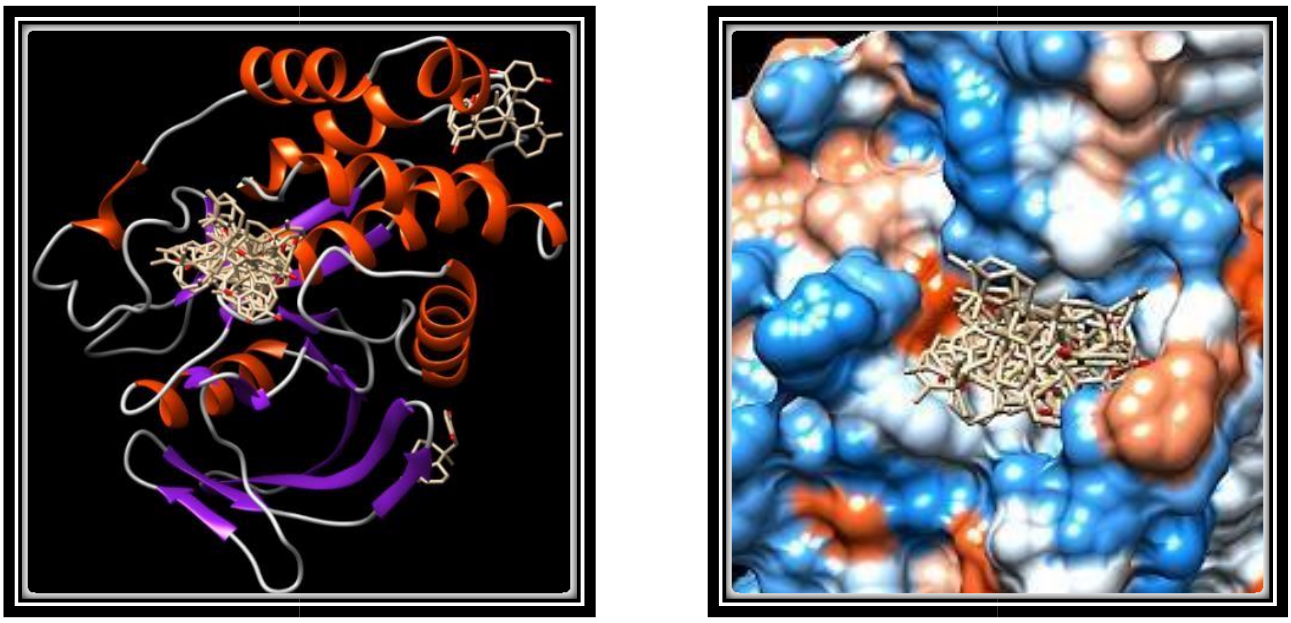

Fig. 30. Binding sites of avarone identified by docking analyses. **A**, General view of interaction sites of avarone on PTP1B surface. **B**, detail showing the molecules of avarone bound to the active site of PTP1B.

Interestingly, three of the most thermodynamically favorable poses see the avarone benzoquinone group bound in the active site of PTP1B. In the first (-7.8 kcal/mol) and third (-7.6 kcal/mol) poses, one oxygen atom of benzoquinone makes a hydrogen bond with one of the nitrogen atoms of the guanidine group of Arg 221, while the hexahydronaphthalen group is projected towards the outermost portion of the active site where it forms hydro-phobic bonds with the Tyr46, Val49, Glu115, Lys116, Lys120, Gly 220 and Gln262 (first pose showed in figure 31), or with Trp179, Gly183, Ala217, Gly220, Gln262 and Gln266 (third pose showed in figure 33).

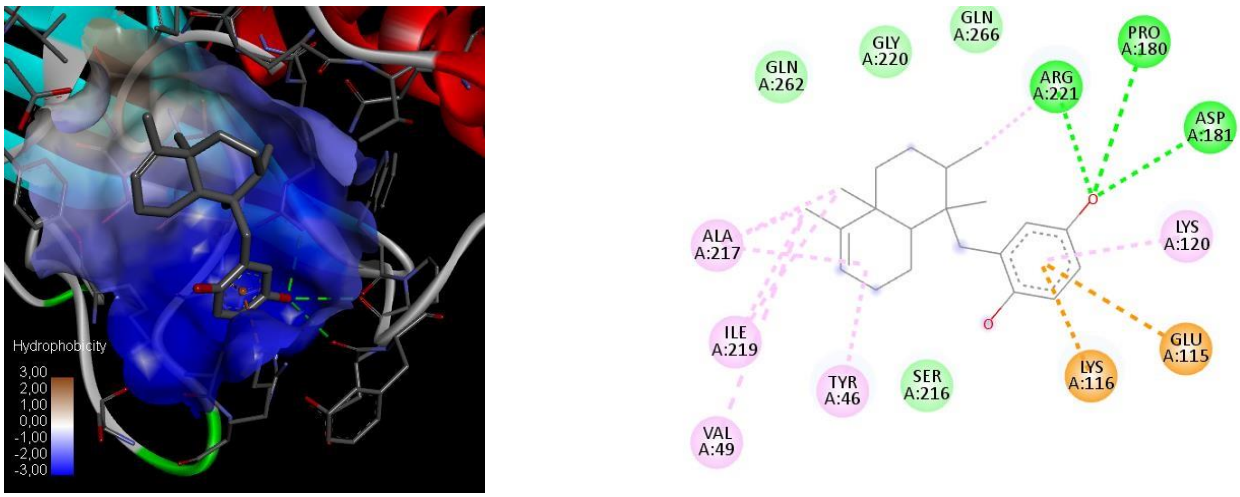

Fig. 31. First pose of avarone in the active site of PTP1B and 2d picture of interactions (on right). Conventional hydrogen bonds are shown in green dotted lines.

In the second pose (figure 32), the avarone is docked to PTP1B active site mainly through hydrophobic interactions. This is possible because methyl groups and hexahydronaphthalen moiety of molecule make hydrophobic interactions with phenyl ring of Tyr46, and with aliphatic chain of Arg221, Cys215, and Lys120 or the amino acid of active site crevice including Gly183, Ser216, Gly220, Gln262 and Gln266. Finally, in the fourth pose (figure 34) one oxygen atom of benzoquinone makes a hydrogen bond with the nitrogen atoms of main chain of Ala217 the surface mainly or with the NH group of main chain of Ala217 and the naphthalene group of avarone interacted with residues lining the active site of the enzyme such as Val49, A6c8, Cys215, Arg221, Gln262, Thr263, and Gln266. Based on results of kinetic analyses showing that the K_m hyperbolically increase as the concentration of avarone increase, and on the evidences that the avarone can acquire different position into the active site, we cannot exclude that the active site of PTP1B could host two molecules of avarone simultaneously.

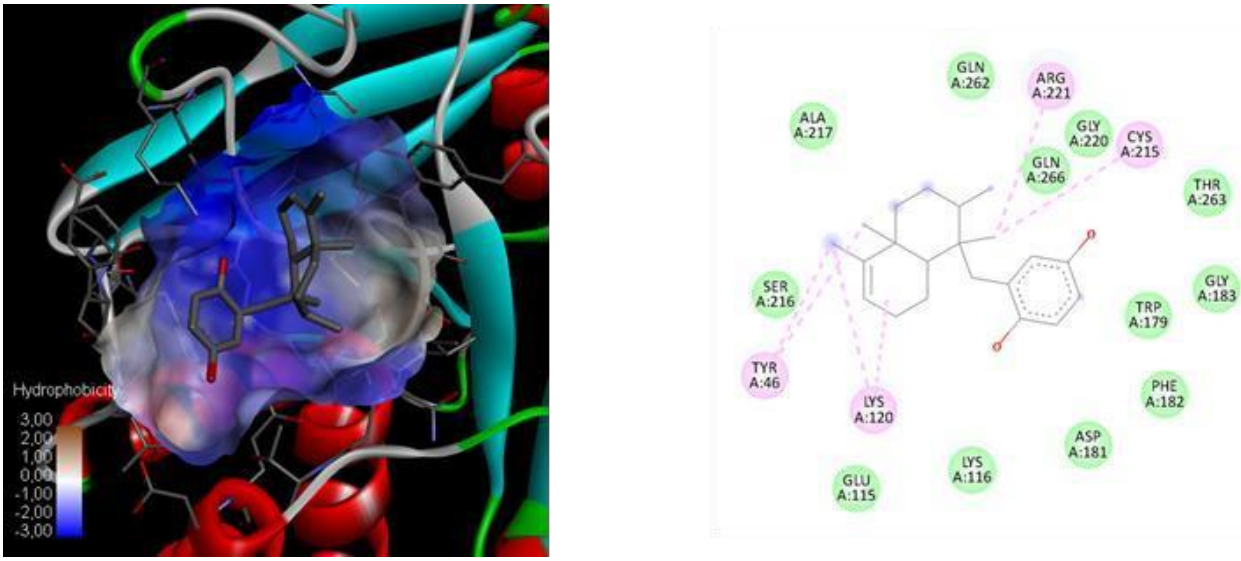

Fig. 32. Second pose of avarone in the active site of PTP1B and 2d picture of interactions (on right).

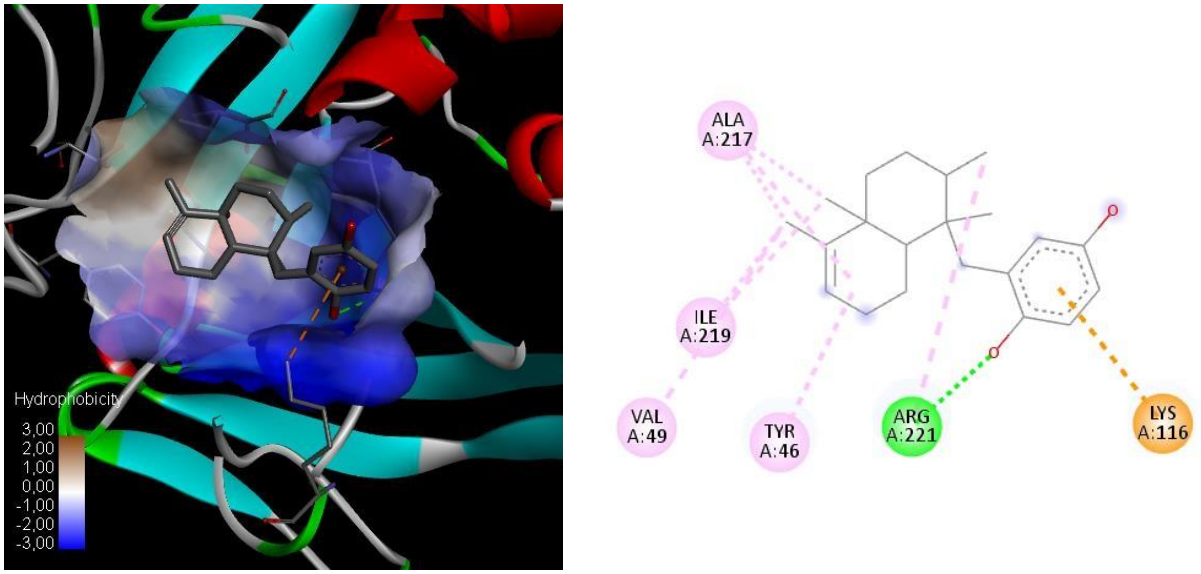

Fig. 33. Third pose of avarone in the active site of PTP1B and 2d picture of interactions (on right). Conventional hydrogen bonds are shown in green dotted lines.

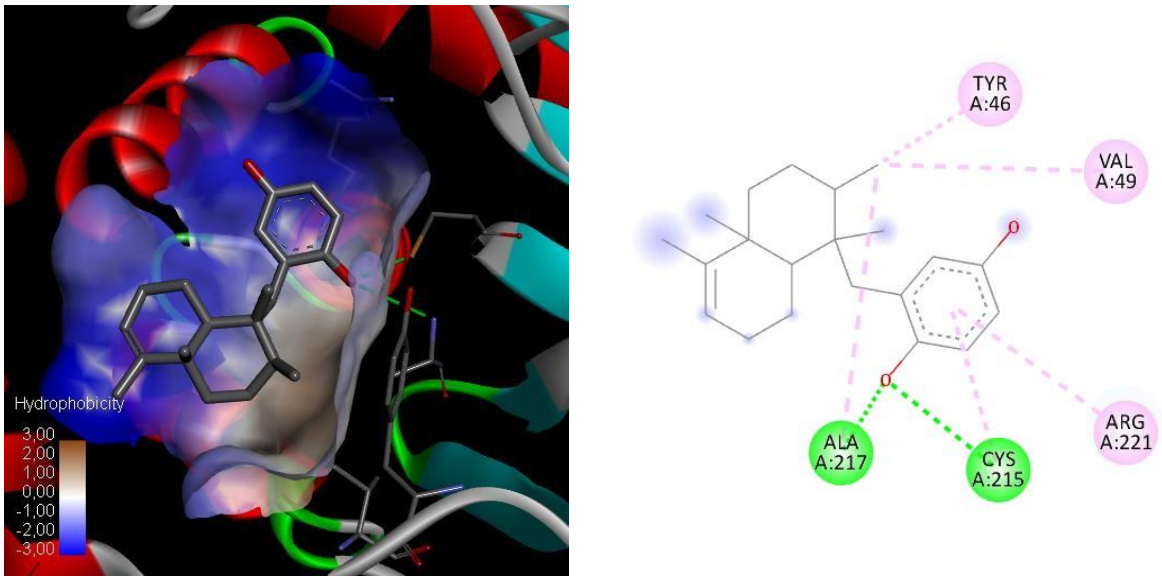

Fig. 34. Fourth pose of avarone in the active site of PTP1B and 2d picture of interactions (on right). Conventional hydrogen bonds are shown in green dotted lines.

Ex vivo assay

To evaluate the impact of avarone on insulin signalling pathway, further tests were carried out using C2C12 cells. Muscle cells were treated with insulin, avarone or combination of both. After 30 min, cells were lysed, and cells extracts analysed by western blot to evaluate the phosphorylation levels of Akt (Figure 35).

A

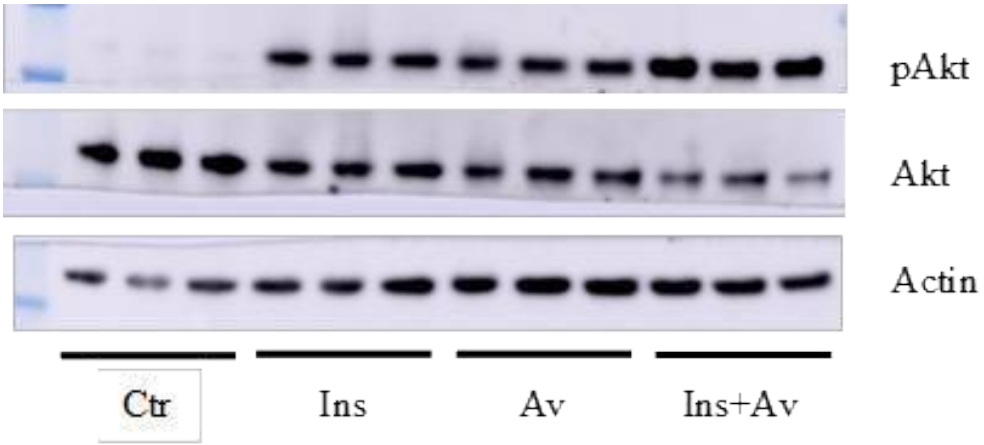

B

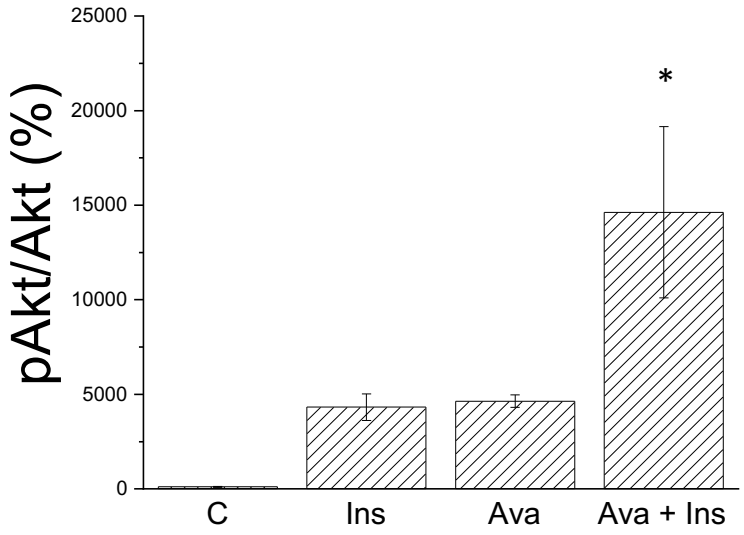

Fig. 35. Effects of avarone (2) on insulin signaling pathway. C2C12 cells were starved and stimulated with 10 nM insulin, 25 mM 2 or combination of both for 30 min at 37°C. After, cells were washed, lysed and analysed to evaluate phosphorylation levels of Akt. All test was carried out in triplicate. **A**, results of western blot analysis; **B**, quantitation of western blot. Data were normalized respect to control samples. Data reported in the figure, represent the mean value ± SD.

We observed that the treatment with avarone resulted in an increase of Akt phosphorylation levels similar to that observed after insulin stimulation, while the treatment with the Insulin-avarone combination results in phosphorylation levels of Akt higher than that observed after treatment with insulin alone. Such data suggest that avarone possesses both insulin-mimetic and insulin-sensitizing activity.

To confirm these results, we evaluated also the rate of glucose uptake. Starved C2C12 cells were treated as described above and then incubated with 2-NBDG; after 3 h, levels of fluorescent glucose incorporated by cells were evaluated using the flow cytometer (Figure 36).

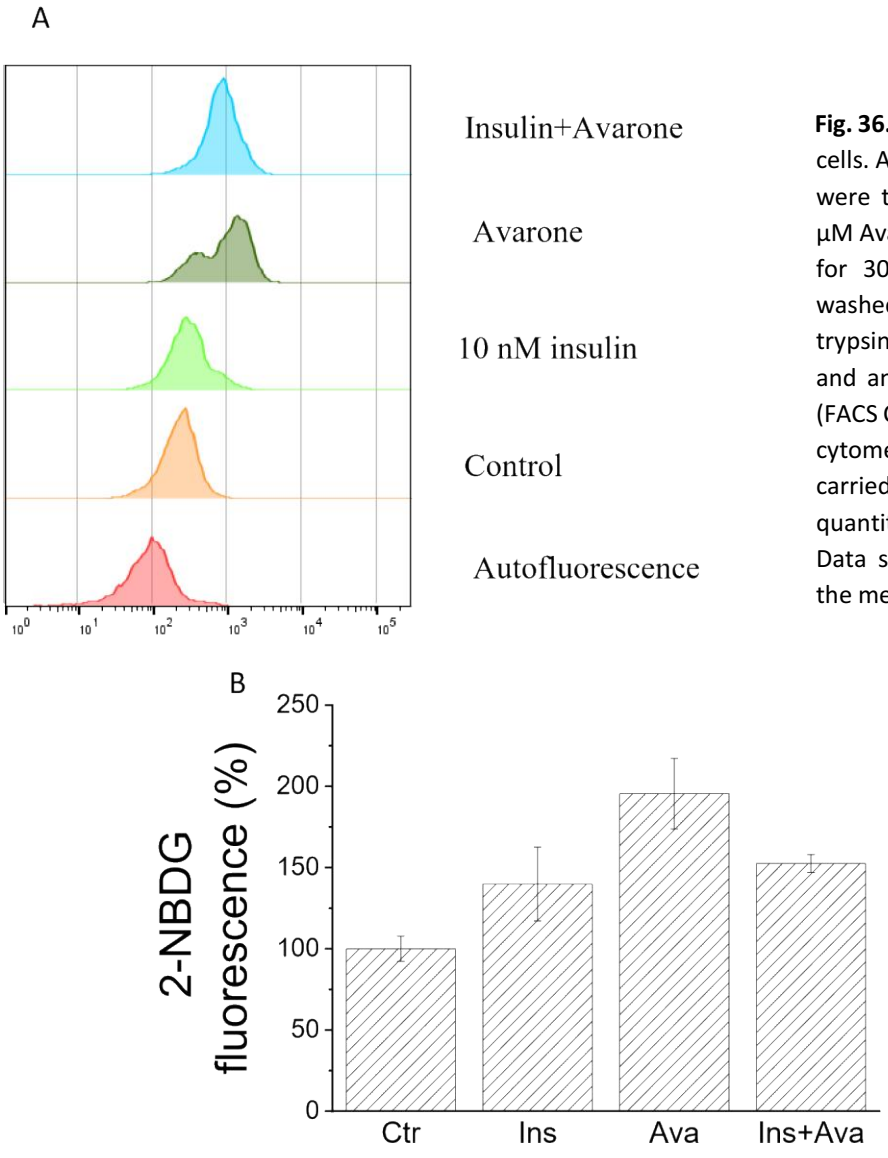

Fig. 36. Glucose uptake assay on C2C12 cells. After being starved for 24 h, cells were treated with 10 nM insulin, 25 µM Avarone alone and in combination for 30' at 37 °C. Later, cells were washed with PBS, detached using trypsin, collected by centrifugation and analyzed usign a flow cytometer (FACS Canto II, BD Biosciences). **A**, flow cytometer analysis. Each test was carried out in quadruplicate. **B**, quantitation of fluorescence levels. Data showed in the figure represent the mean value ± SD.

We observed that level of glucose incorporated significantly increase in cells treated with Insulin - avarone combination respect to cells treated with insulin, confirming that avarone acts as an insulin-sensitizing agent. However, a higher amount of fluorescent glucose was detected in cells treated with avarone alone, indicating that it is able to act as an insulin-mimetic compound when administered alone. It is well known that insulin promotes glucose uptake stimulating GLUT4 translocation to plasmamembrane of C2C12 cells[137]. Therefore, we speculate that avarone could favor translocation/activation of GLUT4. To confirm this hypothesis, we evaluate level of fluorescent glucose incorporated in C2C12 cells pretreated or not with cytocalasin B, a potent inhibitor of GLUT4 activity[138](Figure 37). We observed that preincubation with cytochalasin B strongly affects insulin-stimulated glucose uptake, and abolish the avarone-mediated glucose uptake. Taken together, these data suggest that Avarone promotes GLUT4 translocation/activation.

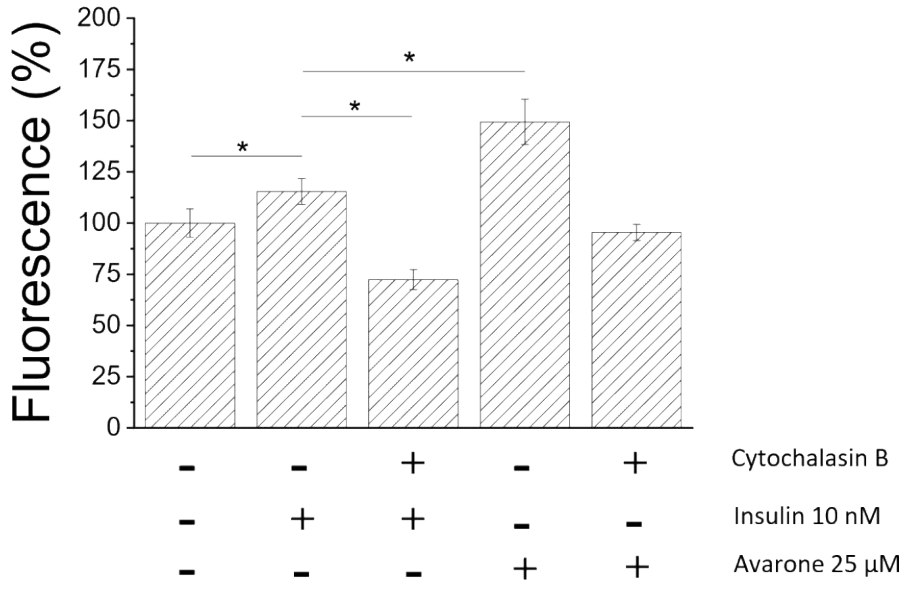

Fig. 37. Impact of Cytochalasin on avarone-induced glucose uptake. C2C12 cells were starved for 24 h and the incubated for 2 h in the presence of 10 mM cytochalasin B. Then cells were treated with 25 µM Avarore or 10 nM insulin for 30 min at 37°C. After, cells were washed, and incubated for 3 h with 40 µM 2-NBDG and then analysed using a flow cytometer (FACSCanto II, BD Biosciences). For each experiment, 10000 events were ana-lysed. Each test was carried out in quadruplicate. Data showed in the figure represent the mean value ± SD. Student's t-test was used to assess differences in experimental features. Statis-tical significance is annotated as follow: * $p \leq 0.05$.

Bioenergetic analysis of C2C12 cells treated with avarone

To evaluate whether 2 has an impact om mitochondrial metabolism, C2C12 cells treated with avarone were analyzed using the Seahorse XFe24 Analyzer to obtain further information about basal respiration, ATP production, maximal respiration, spare respira-tory capacity, non-mitochondrial respiration, and proton leak. To obtain more information about the mechanism of action of Avarone, a comparative analysis was carried out on C2C12 cells treated with UK5099, an inhibitor of

mitochondrial pyruvate carried[139] (Figure 38). We found that control and Avarone treated C2C12 cells had the same basal respiration, while C2C12 cells treated with Avarone showed a significant reduction of basal oxygen consumption destined to endogenous ATP production. On the other hand, UK5099 hindered pyruvate entry into the mitochondria thereby reducing NADH and FADH2 production, the flux of electrons through the mitochondrial electron transport chain, and consequently also of oxygen consumption. This finding indicates also that, differently from UK5099, the treatment with Avarone did not impair the oxygen-dependent ATP production. Moreover, we found that unlike the UK5099, treatment with avarone slight increased both spare capacity and maximal respiration, without affect the proton leak rate.

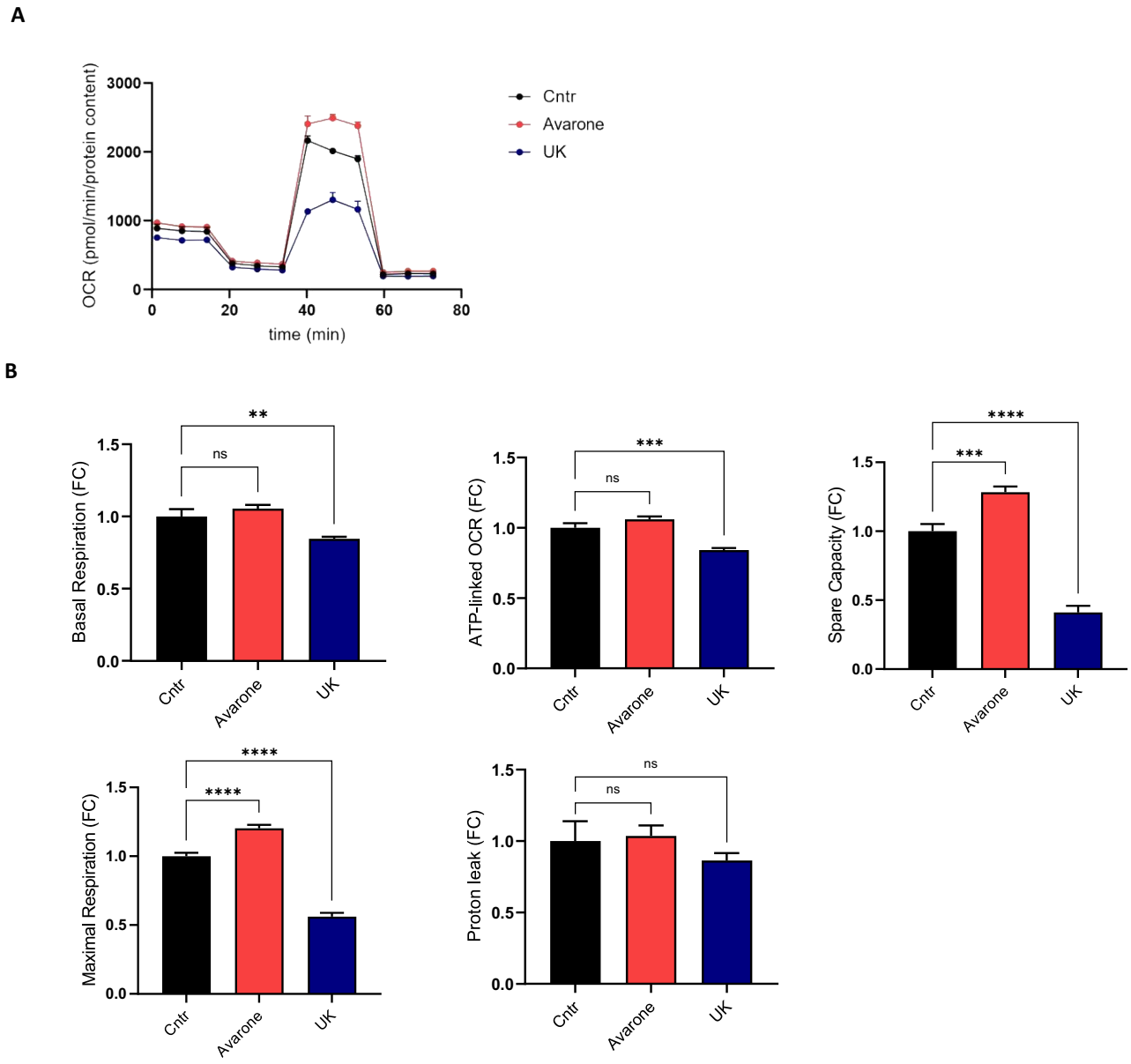

Fig. 38. Results of Mito Stress Test assay. **A**, Oxygen consumption rate (OCR) assay on C2C12 cells treated with 20 µM avarone, of 20 µM UK5099. **B**, the histograms showed the calculated basal respiration, the oxygen-dependent ATP production, the spare (reserve) respiratory capacity, the rates of maximal respiratory capacity, and the proton leak. All

metabolic parameters were calculated for each well using the data obtained from OCR plot. Each point reported in the OCR plot represent the medium value ± SD obtained from three of four independent analysis (n = 3, or 4). Alla data were normalized respect the protein content of each well. Student's t-test was used to assess differences in experimental features by using Prism 6 software (GraphPad). Statistical significance is annotated as follow: * $p \leq 0.05$, ** $p \leq 0.01$, *** $p \leq 0.001$, or **** $p \leq 0.0001$ (t-test).

We investigated the inhibitory effects of four secondary metabolites (compounds 1−4) from *D. avara* against PTP1B and AR, key targeting enzymes involved in the onset of insulin resistance in T2DM disease.

Among all tested compounds, avarone is the most active, acting as acompetitive inhibitor of PTP1B. We found that PTP1B can host two molecules of inhibitor in its active site, and that the binding of the second is favoured over the first one. We think that the binding of the first molecule could slightly modify the structure of the active site of the enzyme, thus creating a more favourable site for the second molecule. Moreover, we observed that avarone shows greater specificity for PTP1B than TC-PTP. This is very interesting considering that these enzymes share a high degree of similarity of the primary and tertiary structure of the active site[140]. At present, it is not simple to explain the differences in IC_{50} values over PTP1B and TC-PTP. We suppose that, although the highly similarity level, the active site of enzymes could assume a conformation slightly different, which influence the positioning of inhibitor in the active site of enzyme, being more comfortable for avarone binding on PTP1B. This hypothesis was supported by docking analyses showing that the free energy values relating to the PTP1B inhibitor complex are on average lower respect those calculated for the TCPTP inhibitor complex. Moreover, it is interestingly to note that avarone, as opposed to many competitive inhibitors synthesized in recent years, does not possess negative charged groups, such as phosphonates, sulphonates or carboxylates. Such groups are generally inserted for driving the inhibitor into the positively charged active site of the PTPs. However, the presence of negatively charged groups is a detrimental factor as it prevents the molecules from crossing the plasma membrane and allows them to cross-inhibit many members of the PTP family, thus being highly toxic. These results suggest that avarone represents an innovative scaffold molecule to design novel potent, specific and bioavailable competitive inhibitors of PTP1B, abandoning the idea that PTPs are undruggable targets.

Cellular assays revealed that avarone is able to activate the kinase Akt and stimulates glucose uptake in C2C12 cells either when administered alone or in combination with insulin. The kinase Akt acts downstream insulin receptor and is activated following the binding of insulin to its cognate receptor[141]. However, degree of activation of insulin receptor depends also by PTP1B activity, which dephosphorylates insulin receptor contributing to switch off the signal activated by insulin. Therefore, PTP1B is a key regulator of insulin signaling pathway and its overexpression or unusual activation contribute to the onset of insulin resistance[142]. Thus, treating diabetic mice with PTP1B inhibitors it is possible to boost insulin receptor activation, to increase insulin sensitivity and reduceblood glucose levels both in fasting conditions and after a meal[143]. Avarone seems to show both insulin sensitizer and mimetic activities, confirmed by inducing the phosphorylation of Akt just like insulin when administered alone. So we think that it is capable to trigger GLUT4 translocation to plasmamembrane also without insulin. Tests carried out with C2C12 cells confirmed that pretreatment with Cytochalasin B, a potent inhibitor of GLUT4 translocation, abolish glucose uptake,

confirming that Avarone alone is able to boost migration of GLUT4 on the plasmamembrane. However, it is interesting to note that avarone stimulates glucose uptake more efficiently than insulin. This evidence suggested that it acts through a complex mechanism that could include also the direct activation of GLUT4. In accordance with this hypothesis, previous studies reported that GLUT4 undergo activation after its translocation on plasmamembrane of cells, and that both mechanisms contribute to the full stimulation of glucose uptake by insulin[144]. There-fore, to date we cannot exclude that avarone may also act as a GLUT4 activator, enhancing, after exposure to the plasma membrane, the transporter's ability to import glucose in-to muscle cells.

The treatment with avarone increases the spare respiratory capacity (SRC) and the maximum respiration (MR) of mitochondria of C2C12 cells. The increase of both spare capacity and maximal respiration represents positive events because witnesses the increased ability of cells to respond to stress stimuli increasing the ATP production[145]. Based on literature data we suppose that this effect can be another consequence of Akt activation as both SRC and MR are modulated by PI3K/AKT/mTOR signaling pathway. According with this evidence, it has been reported that pharmacological inhibition of this pathway leads to significant reduction of SRC; on the other hand, the activation of PI3K/AKT/mTOR signaling pathway triggered by stimulation with different growth factors or through PTEN knock down, results in an enhancement of glycolytic flux and of the SRC[146]. Therefore, we hypothesize that treatment with avarone not only could improve insulin sensitivity, and decrease blood glucose levels, but have a positive impact on mithocondrial activity. The mitochondrial activity of muscle cells resulted impaired in diabetic patients, leading to reduction of fatty acid oxidation, promoting lipid accumulation in muscle cells, and favouring the development of insulin resistance[147]. According with this finding, we hypothesize that avarone could contribute to revert the insulin resistance condition improving mitochondrial activity in diabetic patients' muscle cells.

Finally, we demonstrated that avarone is able to inhibit aldose reductase, the enzyme responsible of conversion of glucose in sorbitol through the polyol's pathway The overexpression of aldose reductase in lens epithelial cells has been described in most of diabetic patients. Blood glucose fluctuations and aldose reductase expression favour GSH depletion, apoptosis and the increase of polyol level, thereby promoting the onset of retinophaty, and other diabetes-related complications[148]. Surprisingly, we found that avarone shows an elevate affinity for AKR1B1 (nanomolar range) and for this reason can be considerd an tight binding inhibitor. It is interesting to note that chemical structure of Avarone differ from aldose reductase inhibitor synthesized to date showing a quinone-like structure. Few informations are available on biological activity of avarone, but its features make it an interesting scaffold for aldose reductase inhibitors development. Recent studies report that activated polyol pathway contribute to elevate ROS levels and trigger inflammatory response. These are considered two important risk factors for development of diabetic retinopathy[149]. Therefore, in the future it will be interesting to evaluate whether avarone treatment can prevent oxidative stress as well as normalize sorbitol levels.

In conclusion, our data showed that avarone is an interesting molecule able to act as multitarget drug and could be used for treatment of type 2 diabetes and diabetes-related complications.

Results and brief discussion

Chemistry

Phosphoeleganin (PE) was obtained in pure form by extraction of a sample of the Mediterranean ascidian *S. elegans* from the existing collection of natural sources available at the Department of Pharmacy of University of Naples Federico II. PE was isolated and purified according to the previously described procedure[150] and unequivocally identified by comparison of its HRMS and NMR data with those reported in literature[151].

Preliminary screening on PTP1B and AR *in vitro*

To assess the effect of PE on PTP1B and AR catalytic activities, a preliminary evalua-tion of IC50 was performed. The obtained results confirm the ability of PE to inhibit PTP1B and highlight that PE can act also as AR inhibitor despite with a minor efficiency (IC50: 28.7 ± 1.1 μM). The IC_{50} value determined for PTP1B (1.3 ± 0.04 μM) is almost 8 times lower than that previously determined[150]. We think that such differences may be attributable to the different experimental conditions used to perform the activity assays, such as a differ-ent pH value, and the use of a GST-PTP1 fusion protein instead of purified PTP1B alone (1-302 aa).

Definition of PTP1B and AR inhibition mechanism by PE

The mechanism of the enzymes inhibition by PE was investigated and it was shown that it behaves as a reversible inhibitor of both AR and PTP1B. As far as AR is concerned, indeed, we found that 100% of enzyme activity was recovered after the inhibitor has been removed by extensive dialysis. Analogously, dilution assay test showed that PTP1B recovered almost completely its activity after incubation with satu-rating concentration of PE, thereby confirming that PE behaves as reversible inhibitor of PTP1B. Kinetic characterization of PE as AR and PTP1B inhibitor was carried out. Kinetic analysis revealed that PE acts as a mixed inhibitor of AR (Figure 39A), being able to affect at a different extent both V_{max} and K_M. The analysis of the dependence of V_{max} and K_M/V_{max} on the inhibitor concentration allowed the measurement of K'_i (36 ± 1 μM, Figure 39B) and K_i (47 ± 1 μM, Figure 39C).

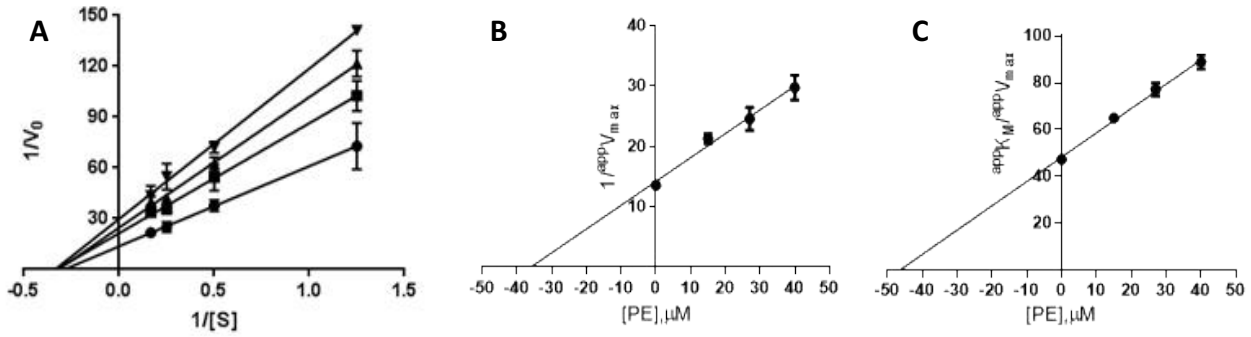

Fig. 39. Kinetic characterization of PE as AR inhibitor. Panel **A,** AR activity (10 mU) at the indicated L-idose concentrations in the presence of PE at concentrations: zero (●), 15 (■), 27 (▲) and 40 μM (▼). Data are reported as Lineweaver-Burk plot. Bars (when not visible are within the symbols size) represent the standard deviations of the means from at least three independent measurements. Panels **B** and **C** Secondary plots of the ordinate intercepts ($1/V_{max}$) and of the slopes (K_M/V_{max}), respectively, of the primary plot as a function of PE concentration. Bars (when not visible are within the symbols size) represent the standard error of the ordinate in-tercepts and of the slopes obtained from data of Panel **A**.

These values indicated a slight, but significant ($p < 0.001$), preference of PE toward the ES complex with respect to the free enzyme. On the other hand, PE acts as a pure non-competitive inhibitor of PTP1B; the analysis of Lineweaver-Burk plot, indeed, indicated that only V_{max} is affected by the presence of the inhibitor (Figure 40). In fact, the analysis of the dependence of appVmax and K_M/V_{max} on the inhibitor concentration allowed the measurement of an identical value of 0.7 ± 0.1 μM for K_i and K'_i.

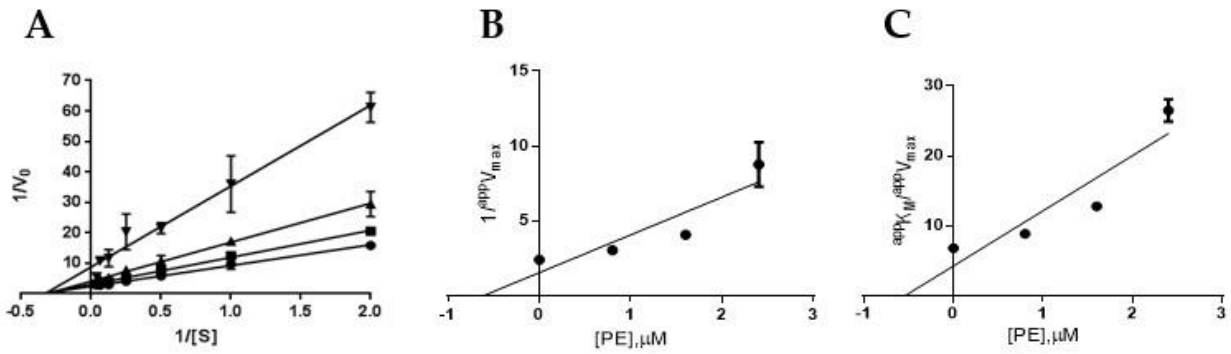

Fig. 40. Kinetic characterization of PE as PTP1B inhibitor. **A**, PTP1B activity (8 mU) at the indicated p-NPP concentrations in the presence of PE at concentrations: zero (●), 0.8 (■), 1.6 (▲) and 2.4 μM (▼). Data are reported as Lineweaver-Burk plot. Bars (when not visible are within the symbols size) represent the standard deviations of the means from at least three independent measurements. **B**, and **C**, Secondary plots of the ordinate intercepts ($1/V_{max}$) and of the slopes (K_M/V_{max}), respectively, of the primary plot as a function of PE concentration. Bars (when not visible are within the symbols size) represent the standard error of the ordinate intercepts and of the slopes obtained from data of Panel **A**.

Dissecting the interaction of PE with PTP1B and AR by *in silico* docking analyses

To evaluate the interaction mode of PE with PTP1B, *in silico* docking analysis was carried out using AutoDock software. The compound was docked to the whole protein surface of PTP1B. We found that PE was able to fit to different sites that can be categorized depending on the docking energy.

The most favourable position places PE between the ac-tive site and the region that define the “C” site[152], which differs from the secondary aryl phosphate site (identified by Arg24 and Arg254) previously described as docking site for aryldifluorophosphonate groups (Figure 41)[153].

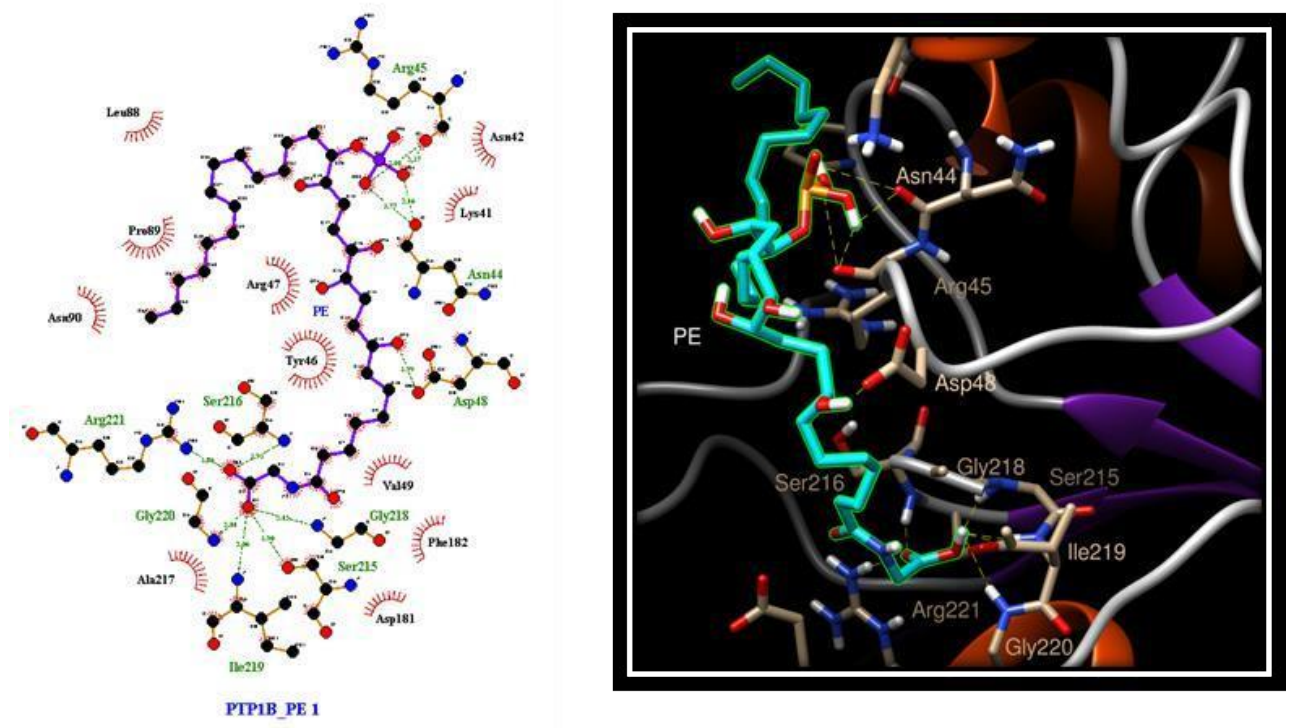

Fig. 41. Docking analysis revealing the most favourable interaction of PE with PTP1B. 2D representation of interactions are shown on left, green dotted lines represent conventional hydrogen bonds.

Interestingly, the phosphate group of PE creates hydrogen bonds with the carbonyl groups of Asn44 and Arg45 that lie beyond the residues forming the "C" site. This suggested an alternative bonding mode of PE on the surface of PTP1B compared to fluo-rine-bisphosphonates. Further hydrogen bonds involve the A6c8 residue belonging to the “C” site and a hydroxyl group present on the aliphatic chain (C12) of PE. Finally, the carbon chain of PE extends to the active site where the carboxyl group of PE forms several hydrogen bonds with the side chain of Arg221 and the nitrogen atoms of the main chains of Ser215, Ser216, Gly218, Ile219 and Gly220. The docking analysis carried out in the absence of substrate (Figure 43) localize PE in the active site of AR (Figure 42).

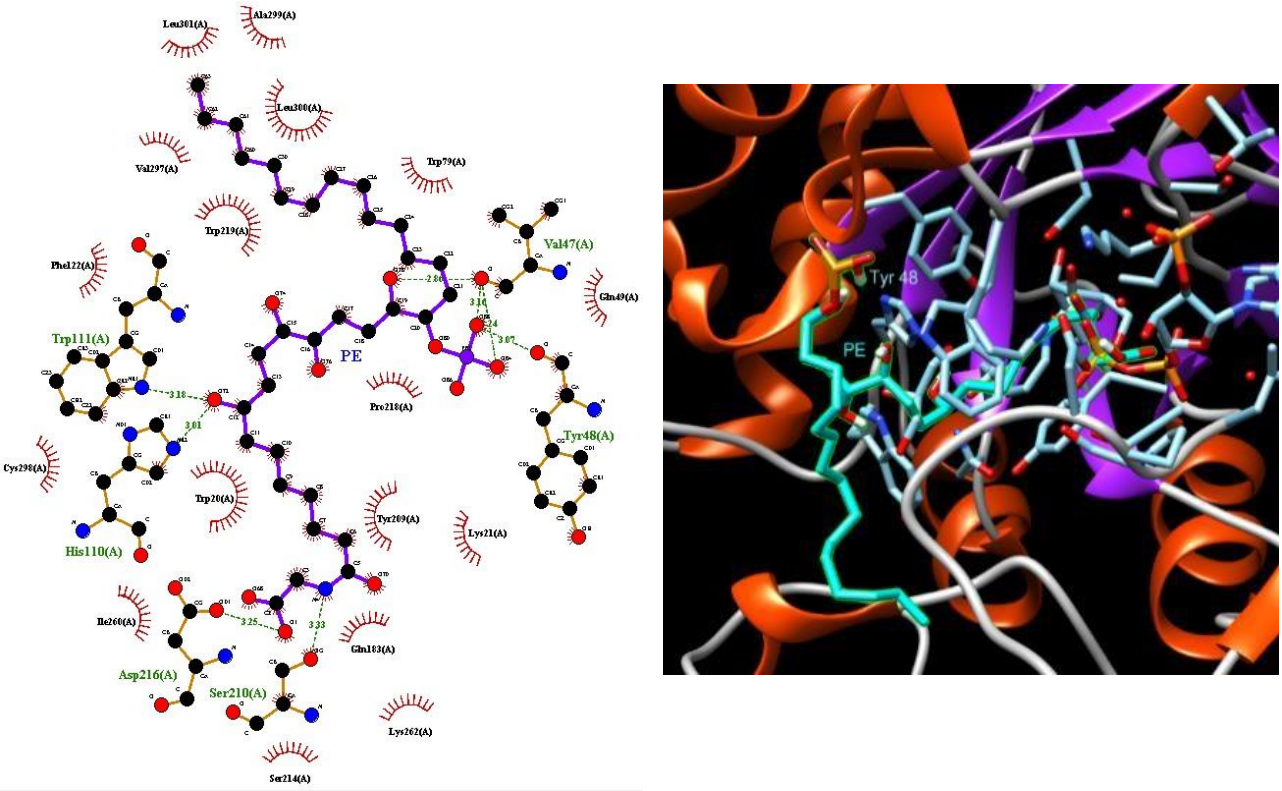

Fig. 42. Docking analysis revealing the most favourable interaction of PE with AR. 2D representation of interactions are shown on left, green dotted lines represent conventional hydrogen bonds.

Here, the OH group at C8 forms hydrogen bonds with nitrogen atoms of His110 and Trp111, whereas the OH at C15 as well as the phosphate group form hydrogen bonds with carbonyl groups of main chain of Val47 and Tyr48. In addition, aliphatic portion of PE (C17-30) is firmly anchored to the selectivity pocket, where makes several hydrophobic interactions with Trp79, Trp219, Val297, Ala299, Leu300, and Leu301. Finally, the portion from carboxyl group at C7 interacts with Trp20, Tyr209 and extends up to a more hydro-philic region where carboxyl group forms hydrogen bonds with side chains of Asp216 and Ser210. When PE was docked in the AR-substrate complex, the interaction with the enzyme appears different, since it involves amino acids located in the external portion of the active site (Figure 43).

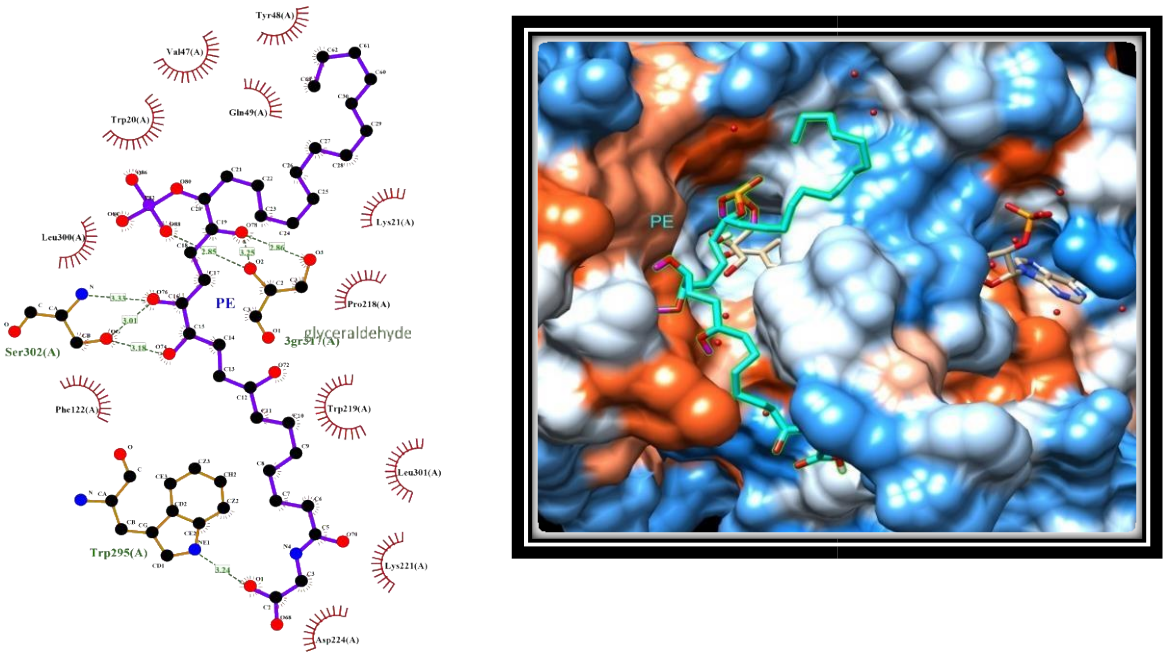

Fig. 43. Docking analysis revealing the most favourable interaction of PE with AR in the presence of substrate (glyceraldehyde) and NADPH. 2D representation of interactions are shown on left, green dotted lines represent conventional hydrogen bonds.

In this arrangement, the terminal carboxyl portion of PE (C7-C1') extended out of the active site making hydrophobic interaction with Trp219, Leu301, and Lys221, while car-boxyl group of PE form a hydrogen bond with nitrogen atom of Trp295. On the other side, the hydroxyl groups at both C15 and C16 face the mouth of the active site where they form hydrogen bonds with oxygen atom of Ser302. In addition, phosphate moiety moves into the active site where it forms hydrogen bonds with glyceraldehyde. Finally, the C17-C30 portion of PE remains excluded from the active site, interacting with amino acids sur-rounding the entrance to the active site, including aliphatic chain of Lys21, Tyr48 and Gln49.These data concur with kinetic analysis in confirming the ability of PE to efficiently interact with AR.

Analysis of insulin signaling pathway in liver cells treated with PE

To evaluate whether PE is able to improve insulin-signalling pathway *in vitro*, we analysed the effect of the compound on HepG2 cell line. To this purpose, we treated HepG2 cells with PE (25 µM final concentration), for 30 minutes, in the presence or not of insulin (10 nM). After treatment, cells were lysed and cellular extracts were analysed to evaluate the phosphorylation status of insulin receptor (IR) and Akt, a kinase downstream IR (Figure 44).

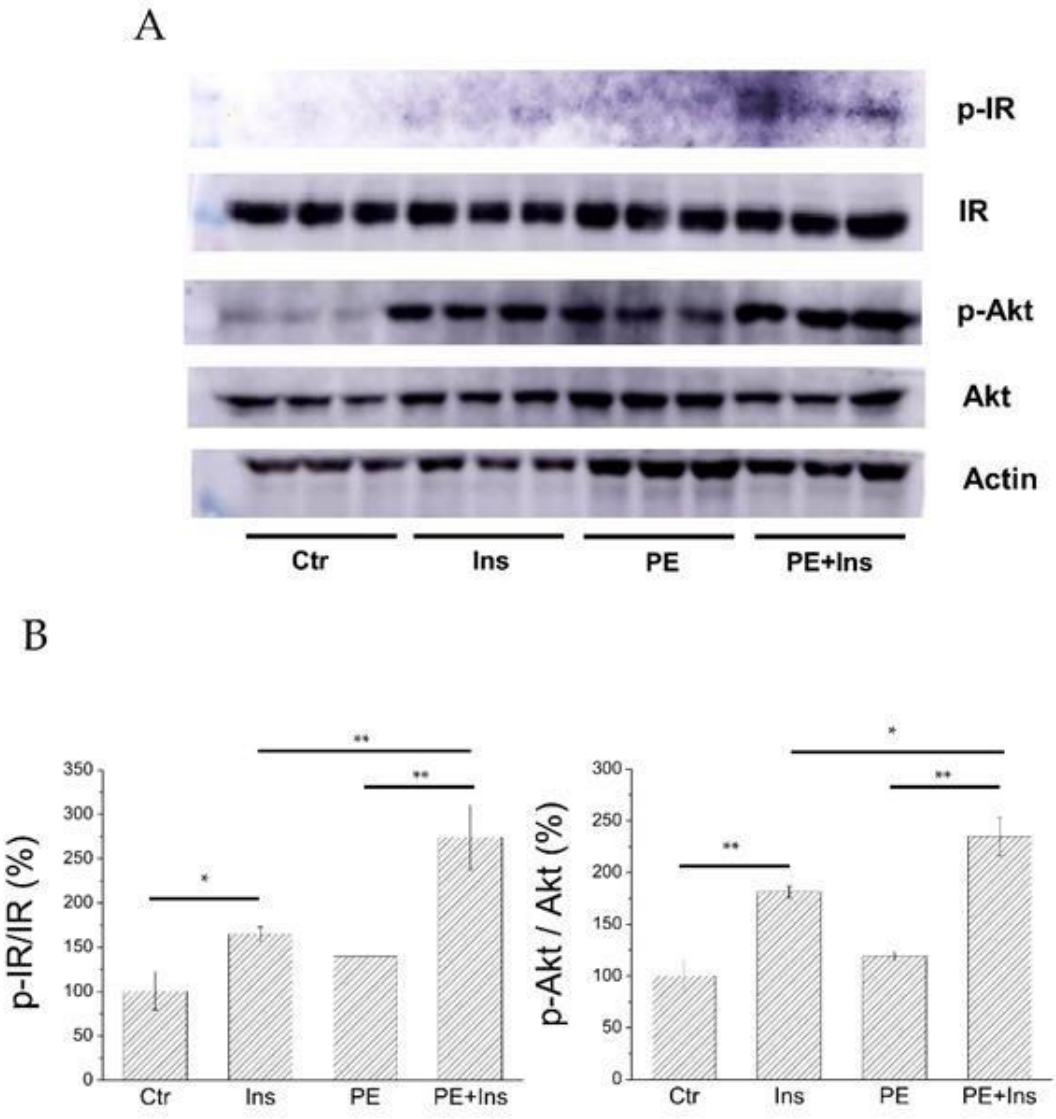

Fig. 44. Effect of PE on insulin signalling pathway. **A**, western blot image; **B**, quantitation of western blot carried out using Kodak MI software. Data showed were normalized respect to control sample. All tests were carried out in triplicate. Statistical analysis was repeated using ANOVA followed by Tukey HSD. Data was checked for appropriate normality and homoscedasticity using the Shapiro-Wilk normality test and the Levene's test, respectively. Ctr: control experiment; Ins: cells treated with 10 nM insulin; PE: cells treated with compound PE (25 µM); *p < 0.05; ** p < 0.01.

We found that in liver cells treated with PE alone the phosphorylation levels of both IR and Akt are similar that detected in control cells, suggesting that PE did not behave as an insulin insulin-mimetic agent. Nevertheless, a significant increase of IR and Akt phosphorylation levels were observed combining insulin stimulation with PE treatment. Taken together, these results demonstrated that PE acts as an insulin-sensitizing agent.

We demonstrated that PE, a phosphorylated polyketide isolated from the Mediterranean ascidian S. elegans, behaves as a multitarget ligand, targeting both PTP1B and AR. The ability of PE to inhibit PTP1B was previously described[151]; however, its mechanism of action and its *in vitro* activity, had

not yet been studied. Being endowed with a phosphate group, we expected that PE could bind to the active site of PTP1B, acting as a classical competitive inhibitor. However, unexpectedly, our results showed that PE acts as a pure non-competitive inhibitor of PTP1B, showing a K_i value of 0.7 µM. Interestingly, *in silico* docking analyses suggested that the not functionalized aliphatic portion of PE structure interacts with various hydrophobic residues present on the surface of the enzyme, where-as the phosphate group binds firmly to some amino acids close to the "C" site, a region previously described to act as a binding site for negatively charged difluorophenyl-methylene phosphonates[152].

The other functionalized part of the molecule forms hydrogen or hydrophobic bonds with numerous other amino acids, extending to the area of the active site, where the carboxyl group of the PE forms further bonds with the residues of the P-loop. Therefore, for the first time, we investigated the way in which PE interacts with PTP1B, also clarifying the role of the phosphate group in stabilizing the enzyme-inhibitor complex.

We showed for the first time that PE acts as a mixed type inhibitor of AR (IC_{50} of 28.7 µM), being able, in the absence of substrate, to move inside the active site of enzyme or, in presence of substrate, to interact on the upper part of the AR active site, positioning phosphate group at the entry of the active site. In this position, the phosphate can interact with substrate, thereby interfering with the catalytic process.

Tests performed on liver cells showed that after short-term PE treatment the phosphorylation levels of IR and Akt kinase increased in hormone-stimulated but not in non-stimulated cells. Akt kinases is an essential effector of insulin signalling pathway and its enhanced phosphorylation is an expected/essential event to propagate the signalling wave trigger by insulin[154]. Similarly, a plethora of study demonstrated that the enhancement of Akt phosphorylation is a common landmark observed in both muscle, liver cells treated with PTP1B inhibitors[42,155–157]. In analogy with these evidences, the data re-ported in this study show that treatment of liver cells with PE enhances insulin activity, suggesting that it act as an insulin-sensitizing agent. Moreover, our data indicate that PE, despite the presence of a charged phosphate group, can cross the plasma membrane and move within the cytoplasm of cells where it inhibits PTP1B, thus enhancing the insulin signalling pathway. This finding is quite surprising, considering that most low molecular weight inhibitors with a phosphate group show poor permeability across the cell membrane[158]. Although no information is currently available on the mechanisms promoting PE internalization in liver cells, it can be hypothesized that its entry into cells may be mediated by fatty acid transporters present on the cell surface or, alternatively, by the process of endocytosis. Further tests will be needed in the future to confirm this hypothesis.

In the past, many marine-derived molecules have been catalogued as PTP1B inhibitors[159], but very few of them have also been evaluated for their ability to inhibit AR, and none of those identified belong to the polyketide family. To our knowledge, this is the first study showing that a polyketide extracted from a marine organism exhibits significant inhibitory activity towards PTP1B and AR. The evidence that PE possess an intrinsic PTP1B/AR inhibitory activity suggests that it could be used as a natural lead to design multitarget drugs able to overcome insulin resistance and to counteract the onset of dia-betic complications induced by the increased polyol pathway flux. In conclusion, our data suggested that polyketides could be used as versatile scaffold structures for the synthesis of a

new generation of potent and safe multitarget antidiabetic drugs. Considering the enormous biodiversity of the marine world, it cannot be excluded that further polyketide-like molecules will be identified in the future, enriching the database of marine molecules that act as inhibitors of PTP1B and AR.

Designed multiple ligands for the treatment of type 2 diabetes mellitus and its complications: discovery of (5-arylidene-4-oxo-2-thioxothiazolidin-3-yl) alkanoic acids active as novel dual-targeted PTP1B/AKR1B1 inhibitors

Results and brief discussion

AR and PTP1B Inhibition

The *in vitro* evaluation of inhibitory ability of compounds 6a-f, 7a-f was assessed against both human recombinant PTP1B, by using p-nitrophenylphosphate as substrate and sodium metavanadate as the reference drug and against human recombinant AR, by using L-idose as substrate and epalrestat as the reference drug (Table 9).

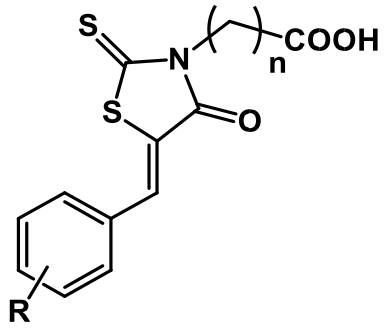

	n	R	AR IC_{50} (μM)	PTP1B IC_{50} (μM)
6a	1	4-$OCH_2CH_2CH_2Ph$	0.25 (0.13-0.62)	(79.0)*
6b	1	4-$OCH_2CH_2CH_2OPh$	0.22 (0.19-0.25)	(87.6)*
6c	1	4-$OCH_2CH_2CH_2CH_2Ph$	0.32 (0.25-0.43)	4.0±0.2 (51.7)*
6d	1	3-$OCH_2CH_2CH_2Ph$	0.05 (0.03-0.06)	(81.0)*
6e	1	3-$OCH_2CH_2CH_2OPh$	0.08 (0.06-0.10)	(100)*
6f	1	3-$OCH_2CH_2CH_2CH_2Ph$	0.06 (0.05-0.07)	4.3 ± 0.5 (61.0)*
7a	2	4-$OCH_2CH_2CH_2Ph$	38.21 (30.36-48.07)	(99.8)*
7b	2	4-$OCH_2CH_2CH_2OPh$	3.93 (3.16-4.89)	(74.4)*
7c	2	4-$OCH_2CH_2CH_2CH_2Ph$	60.75 (38.78-98.22)	2.9±0.6 (4.4)*
7d	2	3-$OCH_2CH_2CH_2Ph$	1.16 (0.91-1.48)	(67.6)*
7e	2	3-$OCH_2CH_2CH_2OPh$	2.15 (1.06-5.12)	(77.0)*
7f	2	3-$OCH_2CH_2CH_2CH_2Ph$	2.08 (1.78-2.43)	3.2 ± 0.2 (27.4)*
Epalrestat	/	/	0.102 ± 0.005	/
Vanadate	/	/	/	0.4 ± 0.01

Table 9. Inhibitory activities of compounds 6a-f, 7a-f against human AR and human PTP1B, expressed as IC_{50}. * Residual activity of PTP1B determined in the presence of 5 μM of each inhibitor.

All tested compounds 6a-f, 7a-f proved to be generally interesting inhibitors of human AR, with IC_{50} values in a range from low-micromolar to nanomolar concentrations and, in some cases, they proved to be more active than Epalrestat. By comparing the AR inhibitory potency of compounds 6a-f, 7a-f, it emerges that (5-arylidene-4-oxo-2-thioxothiazolidin-3-yl) acetic acids are better inhibitors than propionic acid analogues. The elongation of the carboxylic acid chain on N-3 appeared to be disadvantageous for the interaction with the enzyme; such results are in agreement with SARs that had previously been acquired for some analogues (5-arylidene-4-oxo-2thioxothiazolidin-3-yl) carboxylic acids. Moreover, among acetic acid derivatives, the influence of the 5-arylidene moiety on the AR inhibitory ability appeared negligible since IC_{50} values are within a narrow range, although the meta substituted derivatives appeared to be better inhibitors of AR than para substituted analogues. Significant differences in AR inhibition ability appeared between propanoic acid derivatives, among which the effect of substitution in the 5-arylidene position induced remarkable increases in IC_{50} values (from 23 to 189-fold); once again the 3-substituted derivatives turned out to be the best inhibitors.

It is worth pointing out that among 3-(5-arylidene-4-oxo-2-thioxothiazolidin-3-yl) propanoic acids, 3-phenoxypropoxyphenyl substituted compound 7b, obtained by the replacement of a methylene group with an oxygen atom, proved to be 15-fold more active than 4-buthylphenyl derivative 7c, suggesting that in this case the oxygen atom can establish additional bonds with the enzyme. On the contrary, in the other phenoxyalkoxy substituted derivatives (6b, 6e, 7e) this improvement of the inhibitory activity was not observed.

Regarding PTP1B, we did not observe strong differences in terms of IC_{50} values neither between compounds carrying the acetic acid group (6a-f) or the compounds presenting propionic groups (7a-f), nor between meta and para-analogues. Indeed, compounds 6c, 6f, 7c and 7f, which exhibited a 4-butylphenyl group, were found to be the most potent inhibitors of PTP1B, regardless of the para or meta position of the 4-butylphenyl group. It is worthless that the removal of a methylene group from the butyl chain strongly influenced the inhibitory activity of both acetic analogues (6a versus 6c, or 6d versus 6f) and propionic derivatives (7a versus 7c or 7d versus 7f). Finally, the replacement of a methylene group with an oxygen atom did not improve the inhibitory activity of the acetic (6b and 6e) and propionic (7b and 7e) analogs suggesting that the oxygen atom does not contribute to stabilize the compound complex. PTP1B through the formation of additional hydrogen bonds.

Kinetics analyses

Based on the data above, further studies were carried out to define the mechanism of action of compounds 6c, 6f, 7c and 7f. First, we evaluated whether these compounds behaved as reversible or irreversible inhibitors. Using the dilution assay method, we confirmed that 6c. 6f, 7c and 7f acted as reversible inhibitors of PTP1B (Figure 45).

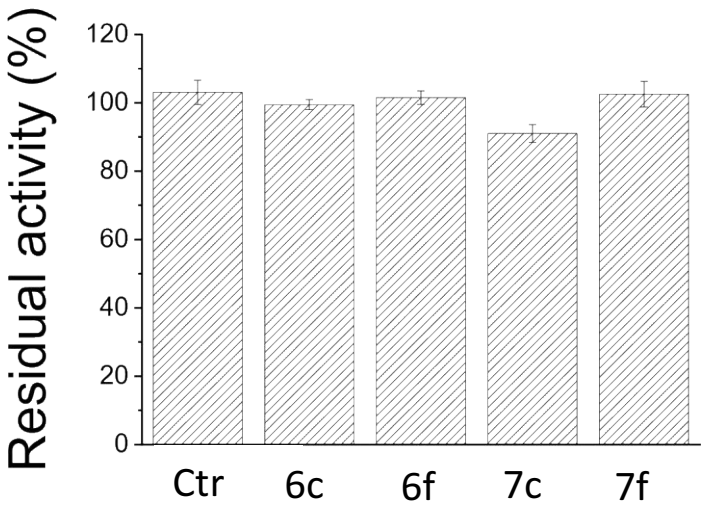

Fig. 45. Dilution assay. An aliquot of PTP1B was incubated in the presence of saturating concentration (25 μM) of each compound for 1 h at 37°C. After this time, 2.5 mL of each enzyme solutions was withdrawn and diluted in the enzymatic assays solution to evaluate the residual activity of the enzyme. Each test was carried out in triplicate. All data were normalized respect to control tests. Data showed in the figure represent the mean value ± SD.

Further kinetic analyses were carried out to investigate the mechanism of inhibition of each compound. In particular, we evaluate the impact of increasing concentrations of inhibitors on main kinetic parameters (K_m and V_{max}) of PTP1B and AR (Figure 46). Results obtained indicated that 6f behaved as a non-competitive inhibitor of PTP1B, while 7f, 7c and 6c as mixed-type noncompetitive inhibitors. The values of Ki and Ki'of compound for PTP1B, calculated using the appropriate equations, were reported in the Table 10 calculated.

	AR		**PTP1B**	
Inhibitor	K_i (mM)	K'_i (mM)	K_i (μM)	K'_i (μM)
6f	0.076 ± 0.015	0.034 ± 0.006	4.6 ± 0.9	4.3 ± 0.5
7f	4.00 ± 0.03	1.11 ± 0.10	0.9 ± 0.1	6.6 ± 3.5
7c	/	/	0.6 ± 0.2	2.4 ± 0.4
6c	/	/	12.1 ± 0.5	17.5 ± 2.4

Table 10: inhibition constants, K_i and K_i' calculated for PTP1B and AR.

A

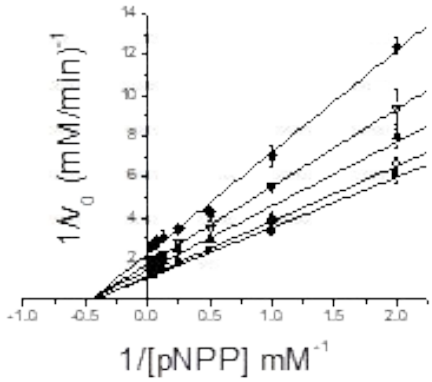

B

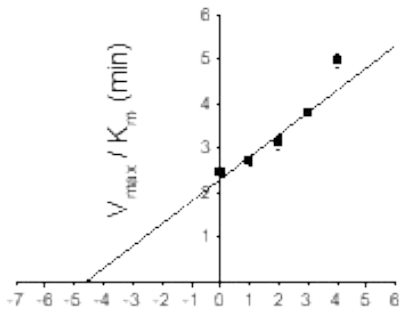

6f (μM)

C

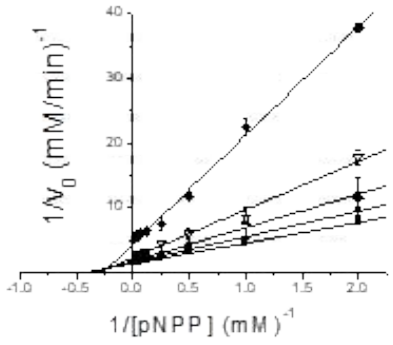

D

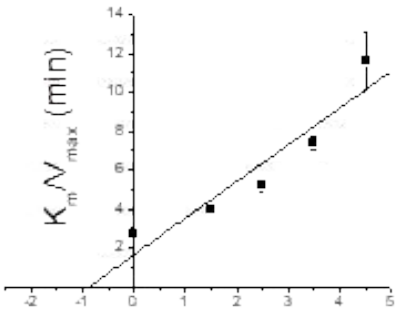

7f (μM)

E

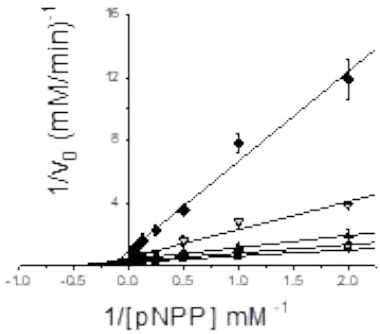

F

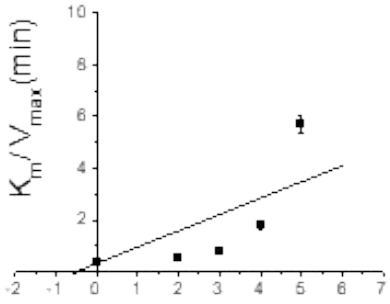

7c (μM)

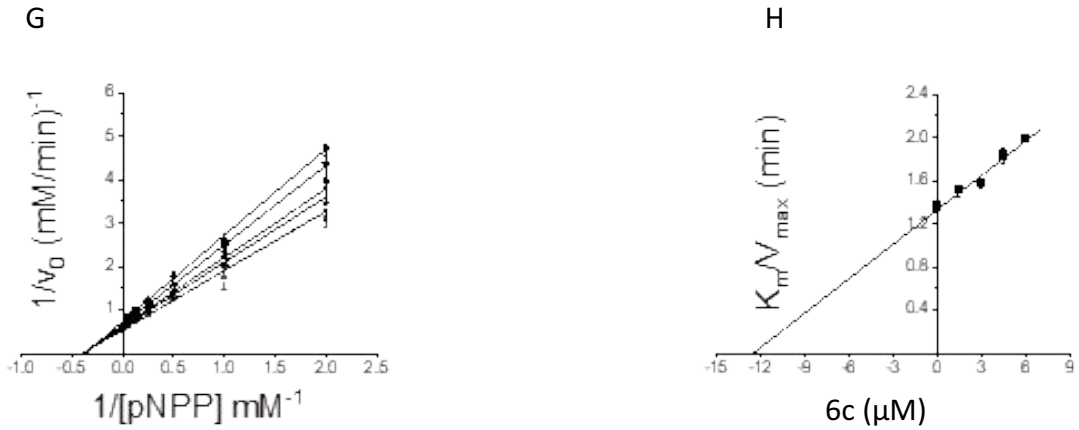

Fig. 46. Definition of mechanism of action of the inhibitors. Lineweaver-Burk plots (A, C, E, G); secondary plots (B, D, F, H). A, B, compound 6f; C, D, compound 7f; E, F, compound 7c; G, H, compound 6c. Concentration of inhibitors used were: 6f, 0 µM, (■); 1 µM, (○); 2 µM, (▲); 3 µM, (▽); 4 µM, (◆); 7f, 0 µM, (■); 1.5 µM, (○); 2.5 µM, (▲); 3.5 µM, (▽); 4.5 µM, (◆); 7c, 0 µM, (■); 2 µM, (○); 3 µM, (▲); 4 µM, (▽); 5 µM, (◆); 6c, 0 µM, (■); 1.5 µM, (○); 3 µM, (▲); 4.5 µM, (▽); 6 µM, (◆).

AR and PTP1B Docking Experiments

PTP1B kinetic studies showed that 6f and 6c act as pure non-competitive inhibitors, whereas 7f and 7c display mixed-type non-competitive inhibition. Therefore, docking studies into both the catalytic binding site and the previously described allosteric binding site of PTP1B[74,83] were performed.

The obtained docking poses of 6f, 7f, 7c and 6c into the allosteric site of PTP1B (Figure 47) showed comparable lipophilic contacts of the terminal phenyl ring with residues Arg79, Pro206 and Pro210. Docking poses of 6f, 7c and 6c display ionic interactions of carboxylic groups to residues Lys103, Arg 105 and Arg169. The orientation of the thioxothiazolidinone moiety of 7c is different from the one observed in 7f, thus preventing the propionic acid moiety from forming hydrogen bonding interactions with Lys103 and Arg169 displayed in the docking pose of 7f and only showing a hydrogen bonding interaction of the propionic moiety with Arg105, explaining the lower inhibitory potency of 7c (IC_{50}: 3.6 µM) compared to 7f (IC_{50}: 3.2 µM).

Docking studies of 6f, 7f, 7c and 6c in the catalytic site of PTP1B (Figure 48) displayed hydrogen bonding of acetic and propionic acid moieties with the side chain of Arg 221 and the backbones of Phe182 and Ser216. The terminal phenyl ring of 6f, 7f, 7c and 6c exhibits equivalent lipophilic contacts with residues Ala27, Met258 and Arg24 in the non-catalytic aryl phosphatase binding site. Lipophilic contacts of the butoxyphenyl substituent in position 3 of the 5-benzylidene ring of 6f and 7f with Tyr46 and Val49 were observed in the docking studies, which were comparable to the lipophilic contacts of the butoxyphenyl substituent in position 4 of the 5-benzylidene of 7c and 6c with the above-named residues. The propionic moiety allows 7f and 7c to progress further into the catalytic binding pocket, which reduces the hydrogen bonding interaction distance of the propionic moiety with the previously mentioned residues Phe182, Arg221 and Ser216 and minimizes the distance between the propionic moiety and key residue Phe182, favouring a crucial lipophilic

contact. This lipophilic interaction was not observed in the docking poses of 6f and 6c, which act as pure non-competitive inhibitors and showcases the importance of the propionic moiety in the mixed-type inhibition of 7f and 7c.

The difference in the surface shape of the polar head of 7c and 6c (Figure 49) proved that the propionic acid moiety for the affinity in the catalytic binding site, since a smaller distance to Phe182 was observed for the propionic moiety of 7c compared to the acetic moiety of 6c. The docking studies were in accordance with the kinetic studies and allowed to further describe the different inhibitory potency between 6f, 7f, 7c and 6c.

The obtained docking poses of 6f and 7f within the AR-idose complex (Figure 50) showed consistent ionic and hydrogen bonding interactions with residues Arg217 and Lys221. The thioxothiazolidinone moiety of 6f and 7f displays a hydrogen bond with the backbone of Ala299. The acetic moiety of 6f enables the 5-nenzylidene ring to showcase lipophilic contacts with residues Trp219 and Leu302, whereas the propionic moiety of 7f leads to a rotation of the 5benzylidene ring, which is more exposed to solvent and a further distance from residue Leu302 compared to 6f, thus displaying only a lipophilic contact with residue Trp219. The different conformation of the 5-benzylidene ring enables 6f to advance further into the binding pocket, thus allowing 6f to establish a lipophilic contact with residue Trp20 in addition to lipophilic interactions to residues Val49 and Phe122 present in both 6f and 7f docking poses. These additional lipophilic contacts account for the increase of the potency of 6f in comparison to 7f (IC_{50}: 0.076 µM vs IC_{50}: 4.00 µM).

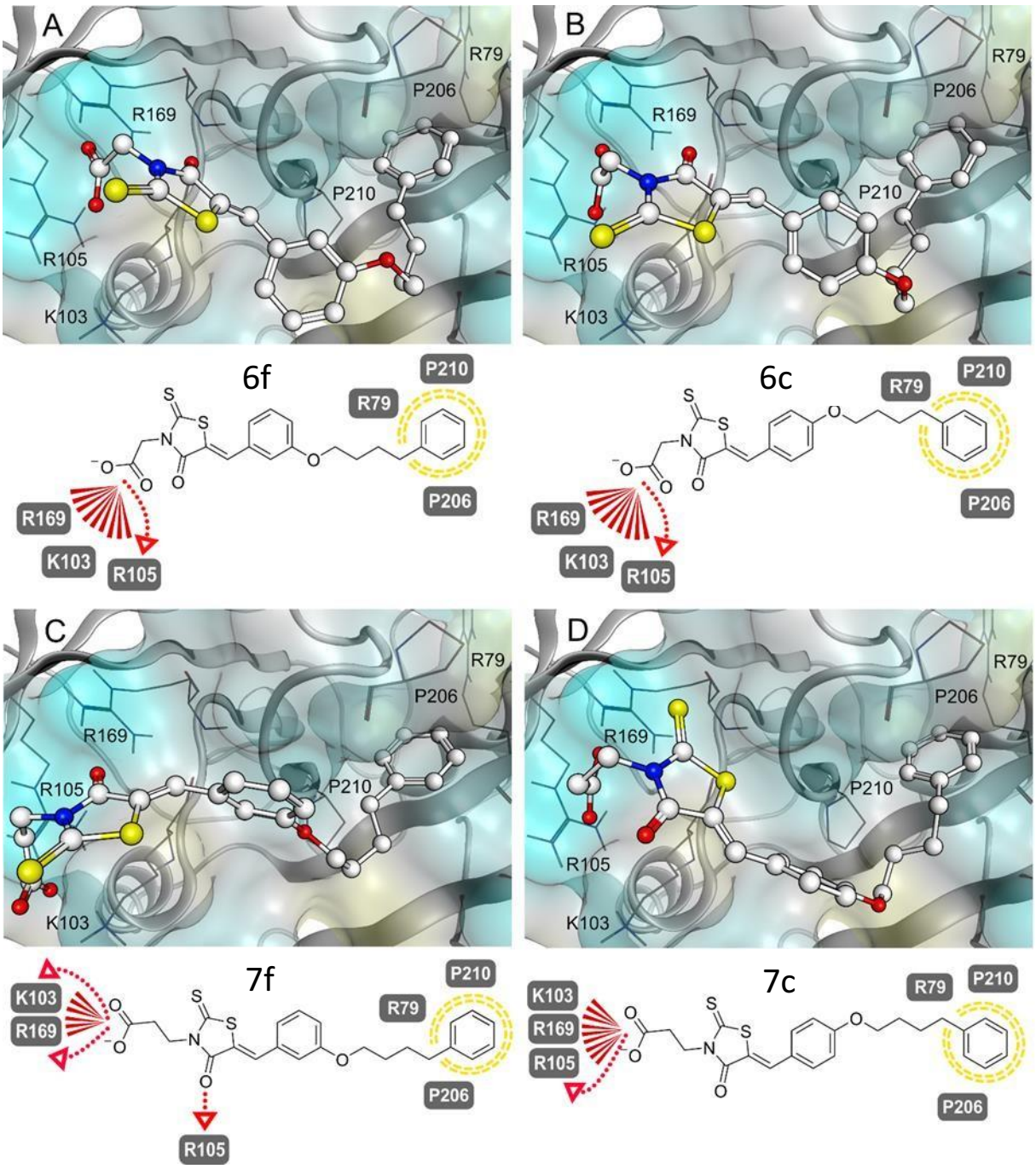

Fig. 47. 3D and 2D depictions of 6f, 7f, 7c and 6c in the PTP1B allosteric binding site. **A**, 3D and 2D depiction of selected 6f pose. **B**, 3D and 2D depiction of selected 6c pose. **C**, 3D and 2D depiction of selected 7f pose. The rotation of thioxothiazolidinone is more favorable and allows 7f to move further into the binding pocket and establish a hydrogen bonding interaction with residues Lys103, Arg105 and Arg169. **D**, 3D and 2D Depiction of selected 7c pose. The rotation of thioxothiazolidinone is less favorable and prevents 7f from forming hydrogen bonding interactions with residues Lys103 and Arg169. Blue surface visualizes hydrophilic regions and yellow surface lipophilic regions. Yellow dotted lines indicate lipophilic contacts, red arrows hydrogen bonding interactions and red lines anionic interactions.

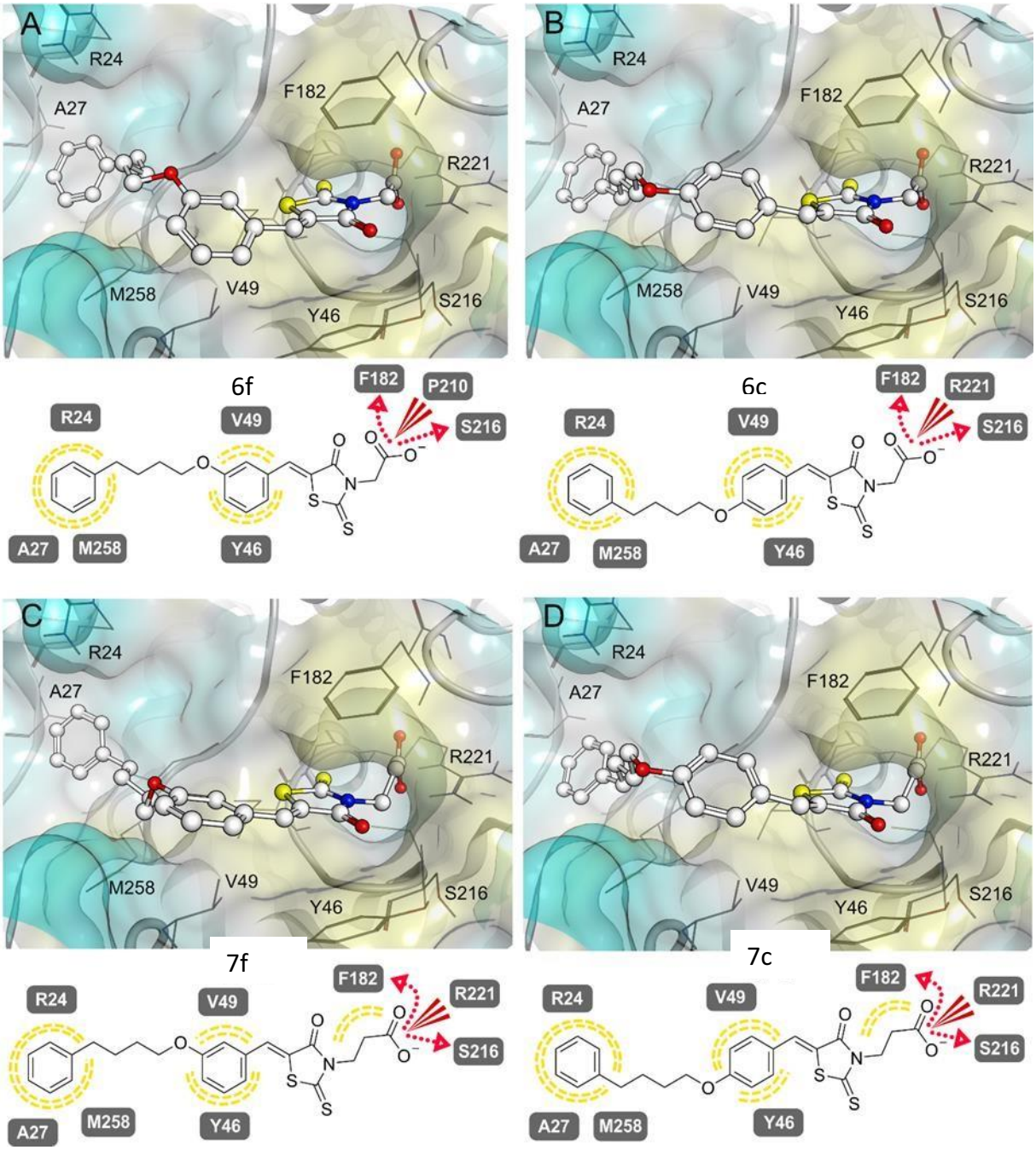

Fig. 48. 3D and 2D depictions of 6f, 7f, 7c and 6c in the PTP1B catalytic binding site. **A**, 3D and 2D depiction of selected 6f pose. **B**, 3D and 2D depiction of selected 6c pose. **C**, 3D and 2D depiction of selected 7f pose. **D**, 3D and 2D depiction of selected 7c pose. The propionic moiety of 7f and 7c permits the ligand to advance further into the catalytic binding pocket and obtain a crucial lipophilic contact with residue Phe182. Yellow dotted lines indicate lipophilic contacts, red arrows hydrogen bonding interactions and red lines anionic interactions.

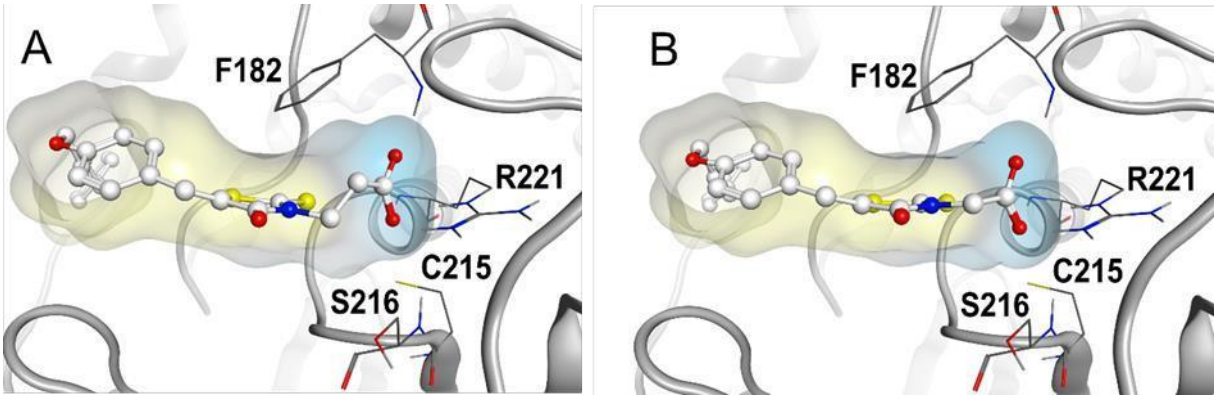

Fig. 49. Ligand surface shapes of 7c and 6c in the PTP1B catalytic binding site. **A**, Binding site of 7c showcases a complementary ligand surface and displays a lipophilic contact with Phe182. **B**, Binding site of 7c displays a more distanced ligand surface from Phe182 and no lipophilic contact can be observed.

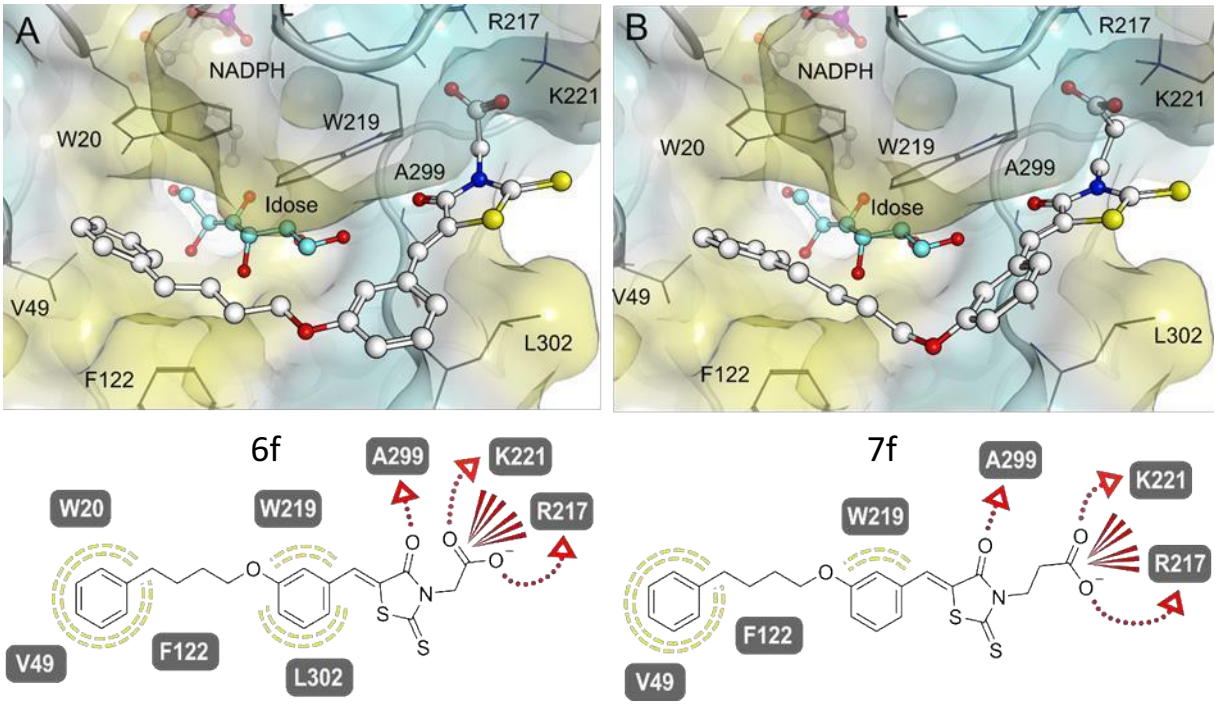

Fig. 50. 3D and 2D depictions of 6f and 7f within the AR-Idose complex. **A**, 3D and 2D depiction of the selected 6f pose. **B**, 3D and 2D depiction of the selected 7f pose. The rotation of the 5-benzylidene ring of 6f reduces the distance to residue Leu302 and allows the ligand to advance further into the binding pocket, granting two additional lipophilic contacts. Yellow dotted lines indicate lipophilic contacts, red arrows hydrogen bonding interactions and red lines anionic interactions.

Cytotoxic activity of 6f, 7f, 7c and 6c compounds

Toxicity of compounds was evaluated measuring viability of differentiated C2C12 cells incubated for 24 h with each compound (20 µM, final concentration). The results of toxicity assay are showed in the Figure 51. Interestingly, we observed that none of compounds caused a significant reduction of cell viability at 20 µM concentration.

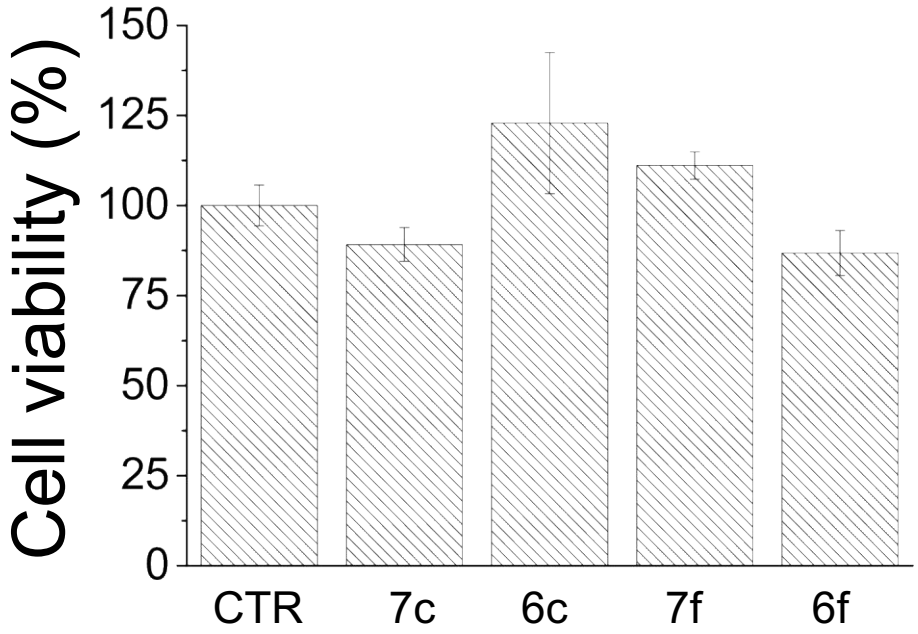

Fig. 51. Cell viability assay. Differentiated C2C12 cells were incubated in the presence of 20 mM of each compound for 24 h in complete medium. After this time, medium was withdrawn and cells washed with PBS. Then, cells were incubated for 60 min with 500 µL of complete medium containing 0.5 mg/mL of MTT salt. After 30 min, cells were recovered, washed with PBS, and the lysed with 400 uL of DMSO to ensure cell lysis and the solubilization of formazane crystal present inside the cells. The absorbance of each sample was determined measuring the absorbance of samples using a microplate reader. Each test was carried out in quadruplicate. Data reported in the figure represent the mean value ± SD (n: 4). Data were normalized respect to control samples, that consist in differentiated C2C12 cells incubated with the same volume of DMSO, the solvent used to solubilize each compound.

Effects of compounds 6f, 7f, 7c and 6c on insulin signalling pathway

To evaluate the ability of compounds to improve insulin signaling, further tests were carried out on C2C12 cell lines. Differentiated C2C12 cells were starved for 24 h and then incubated at 37°C for 15' with insulin (10 nM), 6f, 7f, 7c or 6c both alone and in combination with insulin. After this time, cells were washed and lysed to evaluate phosphorylation levels of kinase Akt. Western blot was showed in Figure 52-55.

A

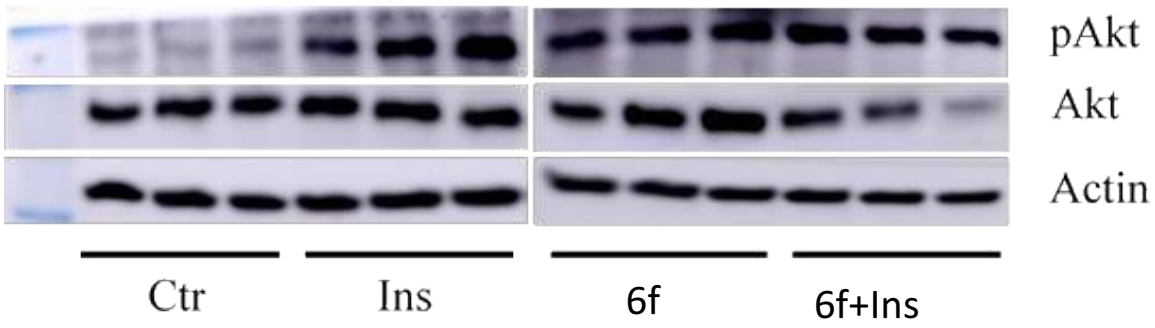

B

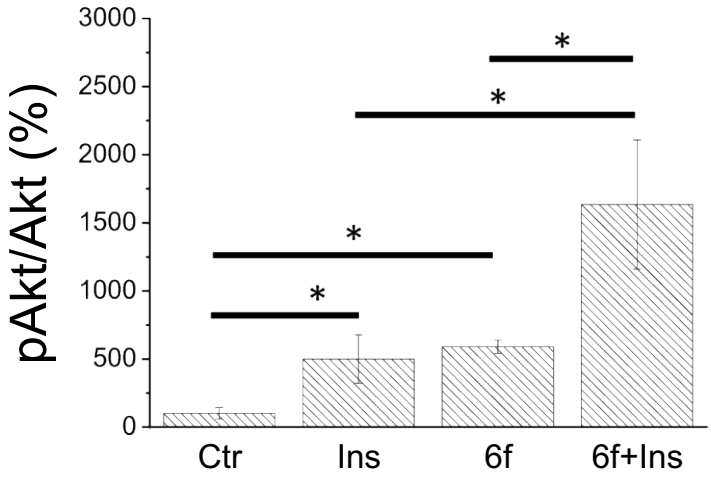

Fig. 52. Effect of 6f on insulin signalling pathway. C2C12 cells were starved and then stimulated for 15 min with 10 nM insulin, 20 µM 6f or Insulin-6f combination. After time, cells were washed with cold PBS and lysed using 1X Laemmli sample buffer solution. Proteins of the extracts were separated by SDS-PAGE electrophoresis and then transferred on a PVDF membrane by western blotting. Phosphorylation status and total expression levels of kinase Akt were determined using specific antibodies for phosphorylated and unphosphrylated form of Akt (**A**). Levels of actin were detected to evaluate the number of samples loaded on gel. Each test was carried out in triplicate. (**B**) Quantification of the intesity of western blot bands. Data reported in the figure represent the mean value ± SD (n: 3). * $p < 0.05$

A

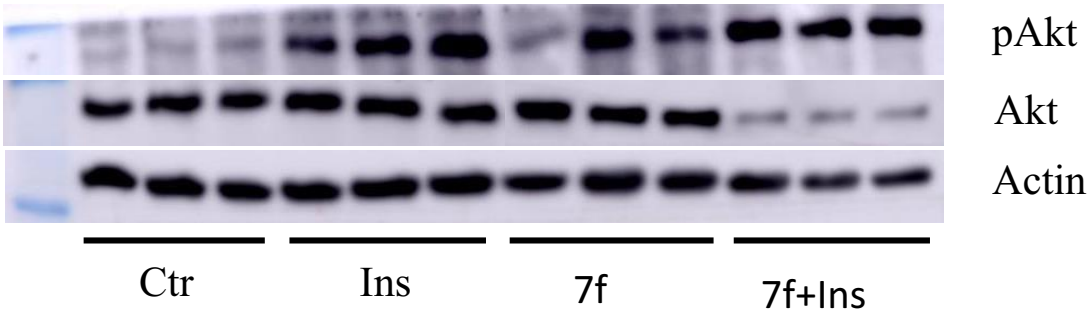

B

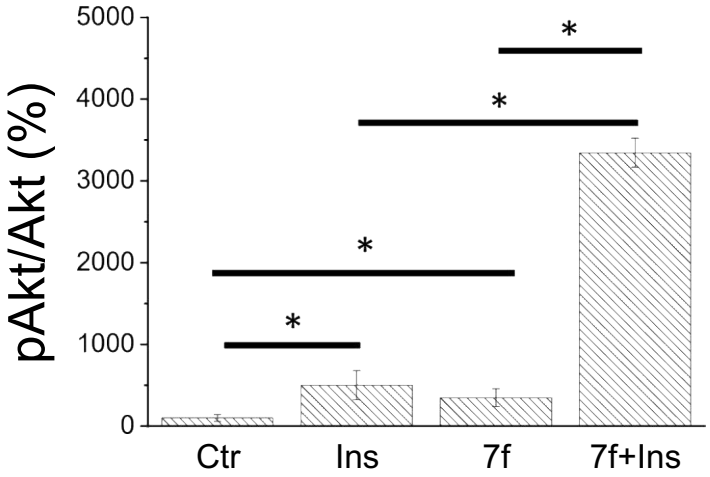

Fig. 53. Effect of 7f on insulin signalling pathway. C2C12 cells were starved and then stimulated for 15 min with 10 nM insulin, 20 µM 7f or Insulin-7f combination. After time, cells were washed with cold PBS and lysed using 1X Laemmli sample buffer solution. Proteins of the extracts were separated by SDS-PAGE electrophoresis and then transferred on a PVDF membrane by western blotting. Phosphorylation status and total expression levels of kinase Akt were determined using specific antibodies for phosphorylated and unphosphrylated form of Akt (**A**). Levels of actin were detected to evaluate the number of samples load on gel. Each test was carried out in triplicate. (**B**) Quantification of the intesity of western blot bands. Data reported in the figure represent the mean value ± SD (n: 3). * $p < 0.05$

A

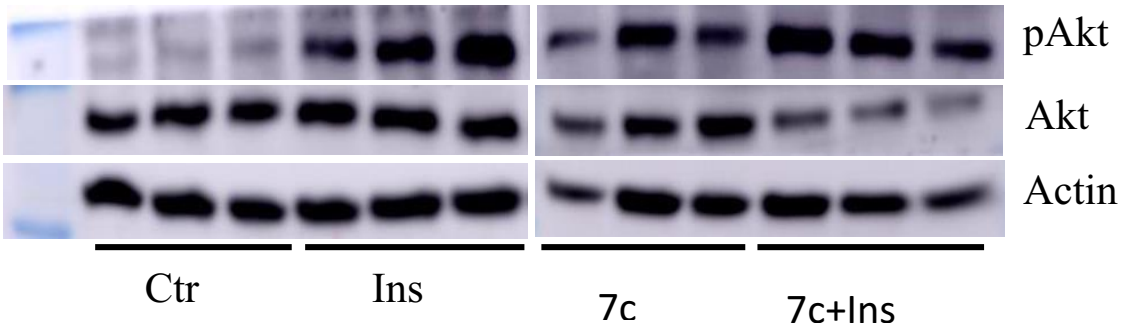

B

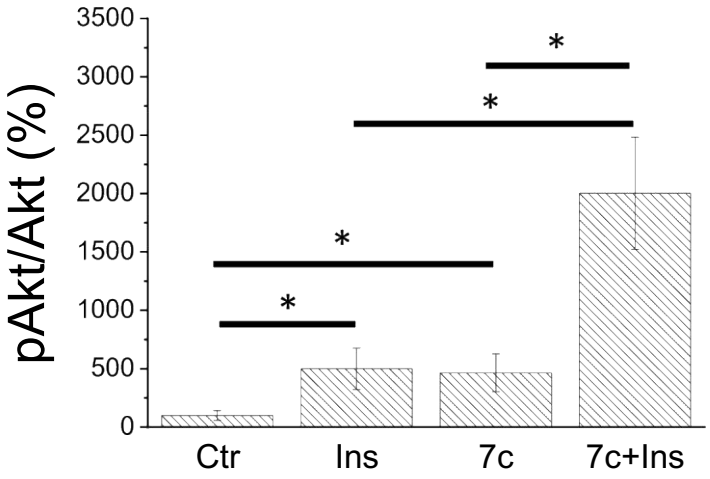

Fig. 54. Effect of 7c on insulin signalling pathway. C2C12 cells were starved and then stimulated for 15 min with 10 nM insulin, 20 µM 7c or Insulin-7c combination. After time, cells were washed with cold PBS and lysed using 1X Laemmli sample buffer solution. Proteins of the extracts were separated by SDS-PAGE electrophoresis and then transferred on a PVDF membrane by western blotting. Phosphorylation status and total expression levels of kinase Akt were determined using specific antibodies for phosphorylated and unphosphrylated form of Akt (**A**). Levels of actin were detected to evaluate the number of samples load on gel. Each test was carried out in triplicate. (**B**) Quantification of the intesity of western blot bands. Data reported in the figure represent the mean value ± SD (n: 3). * $p < 0.05$

A

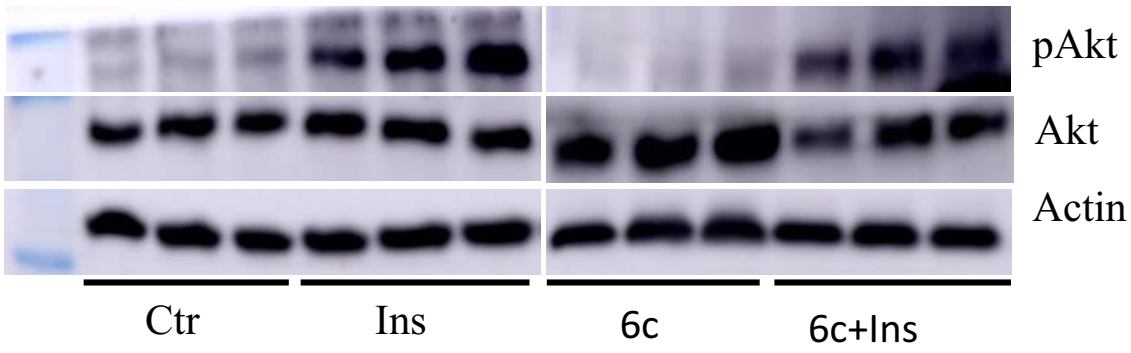

B

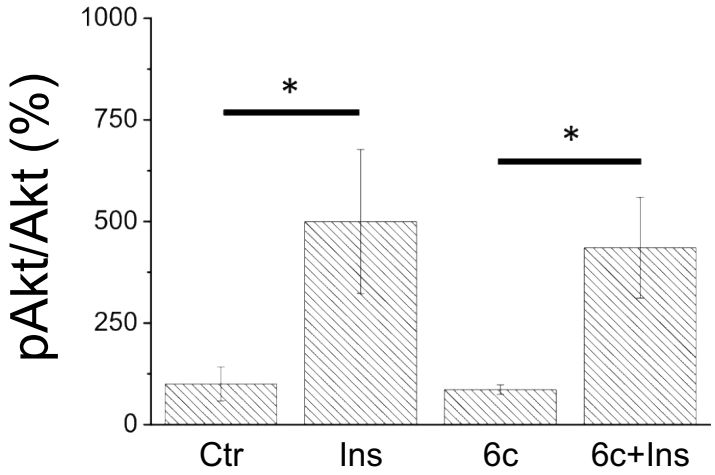

Fig. 55. Effect of 7c on insulin signalling pathway. C2C12 cells were starved and then stimulated for 15 min with 10 nM insulin, 20 µM 7c or Insulin-7c combination. After time, cells were washed with cold PBS and lysed using 1X Laemmli sample buffer solution. Proteins of the extracts were separated by SDS-PAGE electrophoresis and then transferred on a PVDF membrane by western blotting. Phosphorylation status and total expression levels of kinase Akt were determined using specific antibodies for phosphorylated and unphosphrylated form of Akt (**A**). Levels of actin were detected to evaluate the number of samples load on gel. Each test was carried out in triplicate. (**B**) Quantification of the intesity of western blot bands. Data reported in the figure represent the mean value ± SD (n: 3). * $p < 0.05$.

Glucose uptake assay

To better evaluate the impact of compounds on insulin signaling pathway, the ability of 6f and 7f to stimulate glucose uptake was also investigated. Myoblast were starved for 24 h and then stimulated with 10 nM insulin or 20 µM compounds 6f and 7f for 15 min. Then, the medium was removed, cells were washed with PBS and then incubated for 3 h at 37°C with starvation medium containing 40 µM 2-NBDG. The amount of fluorescent glucose incorporated into myoblasts was quantified analysing cells by using a flow cytometer. Data obtained were reported in the Figure 56.

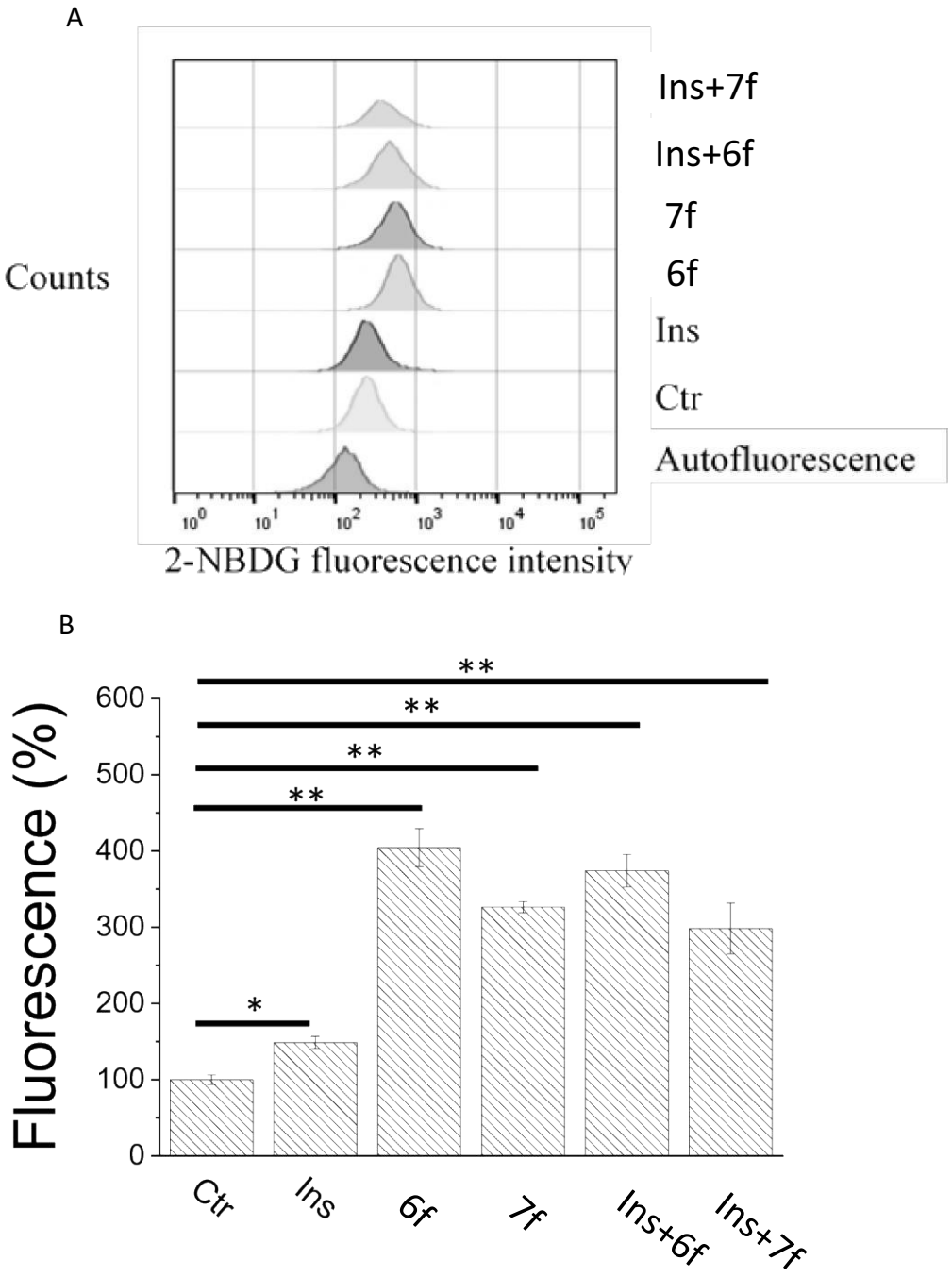

Fig. 56. Glucose uptake assay. C2C12 myoblasts were starved for 24 h and then stimulated with 10 nM insulin, 20 µM 6f and 7f, or with Ins-6f, Ins-7f combination for 15 min. After, the starvation medium was removed and cells were washed with PBS before to add starvation medium containing 40 µM of 2-NBDG. After 3 h, medium was removed, cells washed with PBS and trypsinized. Cells were collected and analysed using a FACS Canto II flow cytometer (BD Bioscence). **A**, representative flow plots of 2-NBDG uptake in C2C12 myoblasts obtained using FlowJo software. **B**, quantitative analysis of data obatined. All tests were carried out in quadruplicate. Data reported represent the mean fluorescence value ± SD. * $p < 0.05$, ** $p < 0.01$

Western blot analysis revealed that treatment with 6f, 7c and in lesser extent 7f enhanced the phosphorylation levels of kinase Akt, while 6c compound resulted completely ineffective. Interestingly, the highest values of pAkt/Akt ratio were observed for cells treated with insulincompound combinations, suggesting that 6f, 7c, 7f act as potent insulin-sensitizing agents. However, the results of the glucose incorporation assay showed that levels of fluorescent glucose incorporated into the cells treated with 6f, 7f, and the combination insulin-compounds are very similar one each other. These data indicated that 6f and 7f compounds alone act as potent insulin-mimetic agent and that combined treatment did not increase the amount of glucose incorporated respect to single compound treatments. All together, these data suggested that compounds behave as insulin-mimetic compounds more that insulin-sensibilizing agents.

Although western blot analyzes showed that the combined treatment (insulin + 6f or 7f) strongly increased Akt phosphorylation, however, glucose incorporation tests did not confirm these data showing that treatment with the compounds alone was as effective as the combined treatment. We hypothesized that these differences are mainly due to the low levels of Akt expression detected by the western blot after co-stimulation with insulin plus 6f or 7f. Based on the data, we speculated that a lower Akt expression level could be the result of an increase in the degradation rate or, alternatively, due to the inability of antibodies used to recognize their target. To assess whether costimulation resulted in increased protein degradation, we analyzed the total protein content of the samples using the SDS-PAGE method. After staining the gel with colloidal Coomassie, we observed that neither treatment with compounds 6f and 7f alone nor combined treatment with insulin and compounds caused a decrease in the overall cellular protein content (Figure 57). Therefore, we concluded that low detection levels of Akt after co-stimulation could result from the inability of antibodies to recognize this target after combined treatment rather than from increased protein degradation.

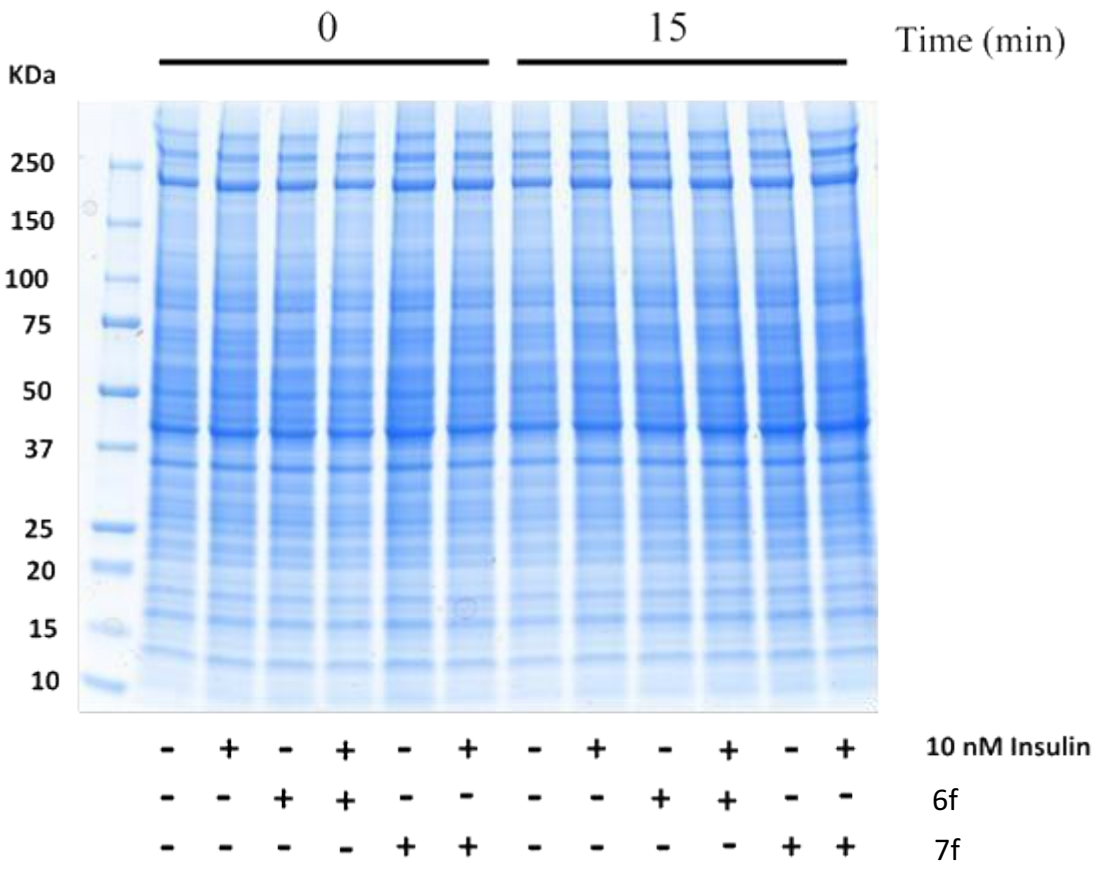

Fig. 57. SDS-PAGE of protein extracts. Myotubes were starved and then stimulated with 10 nM insulin, 20 µM 6f and 7f alone and in combination with insulin for 15 min. After stimulation, cells were lysed using 1X Laemmli sample buffer solution. Then, protein extracts were collected, transferred in eppendorf tubes and boiled for 5 min. The same volumes of protein samples (10 µL) were loaded in each lane. After the run, cellular proteins were highlighted by staining the gel with colloidal Coomassie.

Explaining the discrepancy between western blot analyses and glucose incorporation tests observed during co-stimulation experiments is not straightforward. Western blot analysis showed that cotreatment (Ins + compounds) did not enhance the phosphorylation level of Akt, even if a decrease of total Akt levels was observed, in particular in the case of 6f, 7f and 7c. Therefore, when we calculate the pAkt/Akt ratio, we obtained a strong increase of the value, which prompted us to hypothesize that such compounds possess a strong insulin-sensitizing activity. However, any change in Akt protein levels were observed after treatment of cells with 6f, 7f, 7c and 6c compounds or with insulin alone. This evidence suggested that the increase of insulin sensitivity is the result of an experimental artifact due to decreased level of Akt detected by western blot. We can speculate that the decrease of Akt levels observed after co-stimulation may be the result of an increased degradation of Akt, or the inability of antibodies to recognize their own molecular target. Indeed, the antibodies used to assess total Akt levels bind to the carboxy terminal sequence of Akt, a domain that has several phosphorylation sites in addition to Ser473. Based on this evidence, we speculated that the ability of 6f and 7f to inhibit PTP1B or other phosphatases could strongly stimulate insulin pathway, resulting in an enhanced phosphorylation of residues located in carboxy-terminal region

of Akt, thereby hindering the binding of antibodies capable of recognizing the nonphosphorylated form of this protein.

Our results demonstrated that compounds 6f and 7f possess strong insulin-mimetic activity rather than insulin-sensitizing activity. This finding might seem contrary to the idea that an inhibitor capable of targeting PTP1B, an enzyme that acts as a negative regulator of the activated form of the insulin receptor, should enhance insulin activity, and not act as an insulin-mimetic agent by itself.

However, the insulin mimetic activity of PTP1B inhibitors could be explained by considering the peculiar structure of the insulin receptor. In fact, unlike most hormone or growth factor receptors, the insulin receptor is naturally dimeric and possesses a low intrinsic (constitutive) tyrosine kinase activity, even in the absence of insulin[160]. Based on this evidence, it is reasonable to think that under starvation, the activity of PTP1B is necessary to dampen the spontaneous phosphorylation of the insulin receptor, thus contributing to its complete inactivation. According to this hypothesis, the exposure on the membrane of the glucose transporter GLUT4 is decreased in adipocytes that overexpress PTP1B, both during fasting and after a meal[161]. Together these findings suggest that PTP1B damped basal phosphorylation levels of insulin receptor during fasting and that the inhibition of PTP1B activity would be expected to increase the basal level of IR phosphorylation, leading to the activation of insulin signaling.

In the past, several examples of small PTP1B inhibitors showing *in vivo* an insulin-mimetic activity have been described. John E. Bleasdale et al. showed that some cholecystokinin (CCK)-derived peptidomimetic compounds act as potent and specific inhibitors of PTP1B and promote IR activation. Indeed, they observed that in rat skeletal (L6) myoblast cells, one of these compounds increased the magnitude of tyrosine phosphorylation of IR and the rate of absorption of 2-[3H] deoxyglucose (2-DOG) even in the absence of insulin. This finding suggested that this molecule behaved like an insulin-mimetic compound[162].

In 2003 Laiping Xie et al., studied the effect of new small molecules PTP1B inhibitors on insulin signalling pathway in different insulin-sensitive cell lines. They observed that the most potent molecules acted as both insulin mimetics and sensitizers, thereby validating the notion that small molecule PTP1B inhibitors could be used as antidiabetes drugs[154]. In 2004, Christian Wiesmann et al. reported that some benzbromarone derivatives behaved as potent and specific allosteric PTP1B inhibitors and were able to enhance insulin signalling in chinese hamster ovary cells (CHO cells). Interestingly, the authors of this study demonstrated that such compounds not only acted as insulin sensitizing agents, but also were able to activate the insulin signalling pathway also in the absence of insulin co-stimulation. Based on these evidences, the authors concluded that these allosteric inhibitors also can act as insulin mimetic agents[42]. It is thus evident that the ability of PTP1B inhibitors to act as insulin-mimetic compounds is not a peculiarity of our compounds but rather a common property of other PTP1B inhibitors, as those above reported.

As shown in results, 6f and 7f seem to be the most effective molecules capable to enhance glucose uptake through PTP1B inhibition. Meanwhile, their activity on AR is also very effective suggesting their potential use as scaffolds for drug development.

Conclusion

In this PhD program, several compounds (natural and synthetic) were evaluated for their potential use as scaffolds for antidiabetic drug development.

The driving idea was to investigate their inhibition effect on protein tyrosine phosphatase 1B (PTP1B), one of the main negative regulators of insulin-signalling pathway. Many of tested molecules showed strong inhibition effect and, by comparing their characteristics and thanks to *in silico* simulations, we evidenced important structural features that could inspire the development of specific antidiabetic drugs.

Among tested molecules, the most promising were the natural Epigallocatechin gallate, Gossypetin, Avarone, Phosphoeleganin and synthetic 6f and 7f. They showed strong specific inhibition activity, they enhanced glucose uptake in cells and, moreover, some of them showed strong inhibition on Aldose reductase (AR), target of great interest for the treatment of type 2 diabetes associated pathologies. These findings support the 'multi-targeting' approach focused on the development of a drug that specifically target several factors involved in the same disease, improving the treatment outcome and reducing side-effects.

We hope that our results give interesting starting points for type 2 diabetes drug development and that can rise awareness on how natural world could still inspire us and suggest strategies against chronic diseases.

Bibliography

(1) World health organization. About Diabetes. *WHO* **2014**. https://web.archive.org/web/20140331094533/http://www.who.int/diabetes/action_online/basics/en/.

(2) Kitabchi, A. E.; Umpierrez, G. E.; Miles, J. M.; Fisher, J. N. Hyperglycemic Crises in Adult Patients With Diabetes. *Diabetes Care* **2009**, *32* (7), 1335–1343. https://doi.org/10.2337/dc09-9032.

(3) Masharani, U.; German, M. S. Chapter 17. Pancreatic Hormones and Diabetes Mellitus. 120.

(4) National Institute of Diabetes and Digestive and Kidney Diseases. What Is Diabetes? *NIDDK* **2022**. https://www.niddk.nih.gov/health-information/diabetes/overview/what-is-diabetes.

(5) Associazione Medici Diabetologi (AMD). Standard Italiani per La Cura Del Diabete Mellito 2018.

(6) Daneman, D. Type 1 Diabetes. *The Lancet* **2006**, *367* (9513), 847–858. https://doi.org/10.1016/S01406736(06)68341-4.

(7) World health organization. Diabetes Causes. *WHO*. https://web.archive.org/web/20130826174444/http://www.who.int/mediacentre/factsheets/fs312/en/.

(8) Lippincott Williams & Wilkins. *Diabetes Mellitus a Guide to Patient Care.*; 2007.

(9) Melmed S, Polonsky KS, Larsen PR, Kronenberg HM, eds. *Williams Textbook of Endocrinology*, 12th ed.; 2011.

(10) Sun, T.; Han, X. Death versus Dedifferentiation: The Molecular Bases of Beta Cell Mass Reduction in Type 2 Diabetes. *Seminars in Cell & Developmental Biology* **2020**, *103*, 76–82. https://doi.org/10.1016/j.semcdb.2019.12.002.

(11) Lascar, N.; Brown, J.; Pattison, H.; Barnett, A. H.; Bailey, C. J.; Bellary, S. Type 2 Diabetes in Adolescents and Young Adults. *The Lancet Diabetes & Endocrinology* **2018**, *6* (1), 69–80. https://doi.org/10.1016/S2213-8587(17)30186-9.

(12) Stumvoll, M.; Goldstein, B. J.; van Haeften, T. W. Type 2 Diabetes: Principles of Pathogenesis and Therapy. *The Lancet* **2005**, *365* (9467), 1333–1346. https://doi.org/10.1016/S0140-6736(05)61032-X.

(13) Robertson, R. P.; Harmon, J.; Tran, P. O.; Tanaka, Y.; Takahashi, H. Glucose Toxicity in ␢-Cells: Type 2 Diabetes, Good Radicals Gone Bad, and the Glutathione Connection. **2003**, *52*, 7.

(14) International Diabetes Federation (IDF). Diabetes ATLAS. **2019**.

(15) endocrinologist Yogish Kudva. What Is Type 1 Diabetes? A Mayo Clinic Expert Explains.

(16) Colberg, S. R.; Sigal, R. J.; Fernhall, B.; Regensteiner, J. G.; Blissmer, B. J.; Rubin, R. R.; Chasan-Taber, L.; Albright, A. L.; Braun, B. Exercise and Type 2 Diabetes. *Diabetes Care* **2010**, *33* (12), e147–e167. https://doi.org/10.2337/dc10-9990.

(17) Holman R. Metformin as First Choice in Oral Diabetes Treatment: The UKPDS Experience. *Journ Annu Diabetol Hotel Dieu.* **2007**. https://doi.org/PMID: 18613325.

(18) Kim, Y. D.; Park, K.-G.; Lee, Y.-S.; Park, Y.-Y.; Kim, D.-K.; Nedumaran, B.; Jang, W. G.; Cho, W.-J.; Ha, J.; Lee, I.-K.; Lee, C.-H.; Choi, H.-S. Metformin Inhibits Hepatic Gluconeogenesis Through AMP-Activated Protein Kinase– Dependent Regulation of the Orphan Nuclear Receptor SHP. *Diabetes* **2008**, *57* (2), 306–314. https://doi.org/10.2337/db07-0381.

(19) Hundal, R. S.; Inzucchi, S. E. Metformin: New Understandings, New Uses. *Drugs* **2003**, *63* (18), 1879–1894. https://doi.org/10.2165/00003495-200363180-00001.

(20) DeFronzo, R. A.; Ferrannini, E.; Groop, L.; Henry, R. R.; Herman, W. H.; Holst, J. J.; Hu, F. B.; Kahn, C. R.; Raz, I.; Shulman, G. I.; Simonson, D. C.; Testa, M. A.; Weiss, R. Type 2 Diabetes Mellitus. *Nat Rev Dis Primers* **2015**, *1* (1), 15019. https://doi.org/10.1038/nrdp.2015.19.

(21) Proks, P.; Reimann, F.; Green, N.; Gribble, F.; Ashcroft, F. Sulfonylurea Stimulation of Insulin Secretion. *Diabetes* **2002**, *51* (suppl_3), S368–S376. https://doi.org/10.2337/diabetes.51.2007.S368.

(22) Wu, Y.; Ding, Y.; Tanaka, Y.; Zhang, W. Risk Factors Contributing to Type 2 Diabetes and Recent Advances in the Treatment and Prevention. *Int. J. Med. Sci.* **2014**, *11* (11), 1185–1200. https://doi.org/10.7150/ijms.10001.

(23) McIntosh, C. H. S.; Demuth, H.-U.; Pospisilik, J. A.; Pederson, R. Dipeptidyl Peptidase IV Inhibitors: How Do They Work as New Antidiabetic Agents? *Regulatory Peptides* **2005**, *128* (2), 159–165. https://doi.org/10.1016/j.regpep.2004.06.001.

(24) Del Prato, S.; Felton, A.-M.; Munro, N.; Nesto, R.; Zimmet, P.; Zinman, B. Improving Glucose Management: Ten

Steps to Get More Patients with Type 2 Diabetes to Glycaemic Goal: Recommendations from the Global Partnership for Effective Diabetes Management. *International Journal of Clinical Practice* **2005**, *59* (11), 1345–1355. https://doi.org/10.1111/j.1742-1241.2005.00674.x.

(25) Abdelsalam; Korashy; Zeidan; Agouni. The Role of Protein Tyrosine Phosphatase (PTP)-1B in Cardiovascular Disease and Its Interplay with Insulin Resistance. *Biomolecules* **2019**, *9* (7), 286. https://doi.org/10.3390/biom9070286.

(26) Zhang, Z.-Y.; Lee, S.-Y. PTP1B Inhibitors as Potential Therapeutics in the Treatment of Type 2 Diabetes and Obesity. *Expert Opinion on Investigational Drugs* **2003**, *12* (2), 223–233. https://doi.org/10.1517/13543784.12.2.223.

(27) Verma, M.; Gupta, S. J.; Chaudhary, A.; Garg, V. K. Protein Tyrosine Phosphatase 1B Inhibitors as Antidiabetic Agents – A Brief Review. *Bioorganic Chemistry* **2017**, *70*, 267–283. https://doi.org/10.1016/j.bioorg.2016.12.004.

(28) Taylor, S. Inhibitors of Protein Tyrosine Phosphatase 1B (PTP1B). *CTMC* **2003**, *3* (7), 759–782. https://doi.org/10.2174/1568026033452311.

(29) Issad, T.; Boute, N.; Boubekeur, S.; Lacasa, D. Interaction of PTPB with the Insulin Receptor Precursor during Its Biosynthesis in the Endoplasmic Reticulum. *Biochimie* **2005**, *87* (1), 111–116. https://doi.org/10.1016/j.biochi.2004.12.008.

(30) Hussain, H.; Green, I. R.; Abbas, G.; Adekenov, S. M.; Hussain, W.; Ali, I. Protein Tyrosine Phosphatase 1B (PTP1B) Inhibitors as Potential Anti-Diabetes Agents: Patent Review (2015-2018). *Expert Opinion on Therapeutic Patents* **2019**, *29* (9), 689–702. https://doi.org/10.1080/13543776.2019.1655542.

(31) Kil, Y.-S.; Pham, S. T.; Seo, E. K.; Jafari, M. Angelica Keiskei, an Emerging Medicinal Herb with Various Bioactive Constituents and Biological Activities. *Arch. Pharm. Res.* **2017**, *40* (6), 655–675. https://doi.org/10.1007/s12272017-0892-3.

(32) Zhao, B. T. Protein Tyrosine Phosphatase 1B Inhibitors from Natural Sources. 32.

(33) Jiang, C. Natural Products Possessing Protein Tyrosine Phosphatase 1B (PTP1B) Inhibitory Activity Found in the Last Decades. *Acta Pharmacologica Sinica* 29.

(34) Ma, Q. Bioactive Alkaloids from the Aerial Parts of Houttuynia Cordata. *Journal of Ethnopharmacology* **2017**, 7.

(35) Gabber, A. A.; Samawi, K. A.; Mahdi, F. M. A Theoretical and Practical Study to Assess the Toxicity of Drugs Used in the Treatment of Chronic Myelogenous Leukemia. **2022**, *140* (01), 8.

(36) Shibata, E.; Kanno, T.; Tsuchiya, A.; Kuribayashi, K.; Tabata, C.; Nakano, T.; Nishizaki, T. Free Fatty Acids Inhibit Protein Tyrosine Phosphatase 1B and Activate Akt. *Cell Physiol Biochem* **2013**, *32* (4), 871–879. https://doi.org/10.1159/000354489.

(37) Huang, X.; Liu, G.; Guo, J.; Su, Z. The PI3K/AKT Pathway in Obesity and Type 2 Diabetes. *Int. J. Biol. Sci.* **2018**, *14* (11), 1483–1496. https://doi.org/10.7150/ijbs.27173.

(38) Zhang, S.; Zhang, Z. PTP1B as a Drug Target: Recent Developments in PTP1B Inhibitor Discovery. *Drug Discovery Today* **2007**, *12* (9–10), 373–381. https://doi.org/10.1016/j.drudis.2007.03.011.

(39) You-Ten, K. E.; Muise, E. S.; Itié, A.; Michaliszyn, E.; Wagner, J.; Jothy, S.; Lapp, W. S.; Tremblay, M. L. Impaired Bone Marrow Microenvironment and Immune Function in T Cell Protein Tyrosine Phosphatase–Deficient Mice. *Journal of Experimental Medicine* **1997**, *186* (5), 683–693. https://doi.org/10.1084/jem.186.5.683.

(40) Shinde, R. N.; Kumar, G. S.; Eqbal, S.; Sobhia, M. E. Screening and Identification of Potential PTP1B Allosteric Inhibitors Using in Silico and in Vitro Approaches. *PLoS ONE* **2018**, *13* (6), e0199020. https://doi.org/10.1371/journal.pone.0199020.

(41) SMartin12. PTP1B Mechanism, 2014. https://commons.wikimedia.org/wiki/user:SMartin12.

(42) Wiesmann, C.; Barr, K. J.; Kung, J.; Zhu, J.; Erlanson, D. A.; Shen, W.; Fahr, B. J.; Zhong, M.; Taylor, L.; Randal, M.; McDowell, R. S.; Hansen, S. K. Allosteric Inhibition of Protein Tyrosine Phosphatase 1B. *Nat Struct Mol Biol* **2004**, *11* (8), 730–737. https://doi.org/10.1038/nsmb803.

(43) Li, S.; Zhang, J.; Lu, S.; Huang, W.; Geng, L.; Shen, Q.; Zhang, J. The Mechanism of Allosteric Inhibition of Protein Tyrosine Phosphatase 1B. *PLoS ONE* **2014**, *9* (5), e97668. https://doi.org/10.1371/journal.pone.0097668.

(44) Raugei, G.; Ramponi, G.; Chiarugi, P. Low Molecular Weight Protein Tyrosine Phosphatases: Small, but Smart. *Cellular and Molecular Life Sciences (CMLS)* **2002**, *59* (6), 941–949. https://doi.org/10.1007/s00018-002-8481-z.

(45) Zhang, Z.-Y. Drugging the Undruggable: Therapeutic Potential of Targeting Protein Tyrosine Phosphatases. *Acc. Chem. Res.* **2017**, *50* (1), 122–129. https://doi.org/10.1021/acs.accounts.6b00537.

(46) Thomford, N.; Senthebane, D.; Rowe, A.; Munro, D.; Seele, P.; Maroyi, A.; Dzobo, K. Natural Products for Drug Discovery in the 21st Century: Innovations for Novel Drug Discovery. *IJMS* **2018**, *19* (6), 1578. https://doi.org/10.3390/ijms19061578.

(47) Weng, J.-K.; Philippe, R. N.; Noel, J. P. The Rise of Chemodiversity in Plants. *Science* **2012**, *336* (6089), 1667–1670. https://doi.org/10.1126/science.1217411.

(48) Patridge, E.; Gareiss, P.; Kinch, M. S.; Hoyer, D. An Analysis of FDA-Approved Drugs: Natural Products and Their Derivatives. *Drug Discovery Today* **2016**, *21* (2), 204–207. https://doi.org/10.1016/j.drudis.2015.01.009.

(49) Kiyohara, H.; Matsumoto, T.; Yamada, H. Combination Effects of Herbs in a Multi-Herbal Formula: Expression of Juzen-Taiho-to's Immuno-Modulatory Activity on the Intestinal Immune System. *Evidence-Based Complementary and Alternative Medicine* **2004**, *1* (1), 83–91. https://doi.org/10.1093/ecam/neh004.

(50) Genovese, M.; Luti, S.; Pardella, E.; Vivoli-Vega, M.; Pazzagli, L.; Parri, M.; Caselli, A.; Cirri, P.; Paoli, P. Differential Impact of Cold and Hot Tea Extracts on Tyrosine Phosphatases Regulating Insulin Receptor Activity: A Focus on PTP1B and LMW-PTP. *Eur J Nutr* **2022**, *61* (4), 1905–1918. https://doi.org/10.1007/s00394-021-02776-w.

(51) Ma, J.; Li, Z.; Xing, S.; Ho, W.-T. T.; Fu, X.; Zhao, Z. J. Tea Contains Potent Inhibitors of Tyrosine Phosphatase PTP1B. *Biochemical and Biophysical Research Communications* **2011**, *407* (1), 98–102. https://doi.org/10.1016/j.bbrc.2011.02.116.

(52) Proença, C.; Freitas, M.; Ribeiro, D.; Sousa, J. L. C.; Carvalho, F.; Silva, A. M. S.; Fernandes, P. A.; Fernandes, E. Inhibition of Protein Tyrosine Phosphatase 1B by Flavonoids: A Structure - Activity Relationship Study. *Food and Chemical Toxicology* **2018**, *111*, 474–481. https://doi.org/10.1016/j.fct.2017.11.039.

(53) Casertano, M.; Genovese, M.; Paoli, P.; Santi, A.; Aiello, A.; Menna, M.; Imperatore, C. Insights into Cytotoxic Behavior of Lepadins and Structure Elucidation of the New Alkaloid Lepadin L from the Mediterranean Ascidian Clavelina Lepadiformis. *Marine Drugs* **2022**, *20* (1), 65. https://doi.org/10.3390/md20010065.

(54) Yeung, B. K. Natural Product Drug Discovery: The Successful Optimization of ISP-1 and Halichondrin B. *Current Opinion in Chemical Biology* **2011**, *15* (4), 523–528. https://doi.org/10.1016/j.cbpa.2011.05.019.

(55) Ma, F.; He, C.; Wang, E.; Tong, R. Collective Asymmetric Total Syntheses of Marine Decahydroquinoline Alkaloid Lepadins A–E, H, and *Ent* -I. *Org. Lett.* **2021**, *23* (16), 6583–6588. https://doi.org/10.1021/acs.orglett.1c02435.

(56) Aktaş, N.; Gözcelioğlu, B.; Zang, Y.; Lin, W.-H.; Konuklugil, B. Avarone and Avarol from the Marine Sponge Dysidea Avara Schmidt from Aegean Coast of Turkey. **2010**, 7.

(57) Genovese, M.; Nesi, I.; Caselli, A.; Paoli, P. Natural α-Glucosidase and Protein Tyrosine Phosphatase 1B Inhibitors: A Source of Scaffold Molecules for Synthesis of New Multitarget Antidiabetic Drugs. *Molecules* **2021**, *26* (16), 4818. https://doi.org/10.3390/molecules26164818.

(58) Coskun, T.; Sloop, K. W.; Loghin, C.; Alsina-Fernandez, J.; Urva, S.; Bokvist, K. B.; Cui, X.; Briere, D. A.; Cabrera, O.;
Roell, W. C.; Kuchibhotla, U.; Moyers, J. S.; Benson, C. T.; Gimeno, R. E.; D'Alessio, D. A.; Haupt, A. LY3298176, a Novel Dual GIP and GLP-1 Receptor Agonist for the Treatment of Type 2 Diabetes Mellitus: From Discovery to Clinical Proof of Concept. *Molecular Metabolism* **2018**, *18*, 3–14. https://doi.org/10.1016/j.molmet.2018.09.009.

(59) Chepurny, O. G.; Bonaccorso, R. L.; Leech, C. A.; Wöllert, T.; Langford, G. M.; Schwede, F.; Roth, C. L.; Doyle, R. P.; Holz, G. G. Chimeric Peptide EP45 as a Dual Agonist at GLP-1 and NPY2R Receptors. *Sci Rep* **2018**, *8* (1), 3749. https://doi.org/10.1038/s41598-018-22106-1.

(60) Cheng, C.-F.; Ku, H.-C.; Lin, H. PGC-1α as a Pivotal Factor in Lipid and Metabolic Regulation. *IJMS* **2018**, *19* (11), 3447. https://doi.org/10.3390/ijms19113447.

(61) Wang, Y.-X.; Lee, C.-H.; Tiep, S.; Yu, R. T.; Ham, J.; Kang, H.; Evans, R. M. Peroxisome-Proliferator-Activated Receptor ? Activates Fat Metabolism to Prevent Obesity. 12.

(62) Matsushita, Y.; Ogawa, D.; Wada, J.; Yamamoto, N.; Shikata, K.; Sato, C.; Tachibana, H.; Toyota, N.; Makino, H. Activation of Peroxisome Proliferator–Activated Receptor δ Inhibits Streptozotocin-Induced Diabetic Nephropathy Through Anti-Inflammatory Mechanisms in Mice. *Diabetes* **2011**, *60* (3), 960–968. https://doi.org/10.2337/db10-1361.

(63) Laplante, M.; Sell, H.; MacNaul, K. L.; Richard, D.; Berger, J. P.; Deshaies, Y. PPAR-⁄ Activation Mediates Adipose Depot⁒…Specific Effects on Gene Expression and Lipoprotein Lipase Activity. **2003**, *52*, 9.

(64) Jain, N.; Bhansali, S.; Kurpad, A. V.; Hawkins, M.; Sharma, A.; Kaur, S.; Rastogi, A.; Bhansali, A. Effect of a Dual PPAR α/γ Agonist on Insulin Sensitivity in Patients of Type 2 Diabetes with Hypertriglyceridemia- Randomized Double-Blind Placebo-Controlled Trial. *Sci Rep* **2019**, *9* (1), 19017. https://doi.org/10.1038/s41598-019-55466-3.

(65) Zhou, Z.; Deng, L.; Hu, L.; Ren, Q.; Cai, Z.; Wang, B.; Li, Z.; Zhang, L. Hepatoprotective Effects of ZLY16, a Dual Peroxisome Proliferator-Activated Receptor α/δ Agonist, in Rodent Model of Nonalcoholic Steatohepatitis. *European Journal of Pharmacology* **2020**, *882*, 173300. https://doi.org/10.1016/j.ejphar.2020.173300.

(66) Chen, W.; Fan, S.; Xie, X.; Xue, N.; Jin, X.; Wang, L. Novel PPAR Pan Agonist, ZBH Ameliorates Hyperlipidemia and Insulin Resistance in High Fat Diet Induced Hyperlipidemic Hamster. *PLoS ONE* **2014**, *9* (4), e96056. https://doi.org/10.1371/journal.pone.0096056.

(67) Li, M. H.; Chen, W.; Wang, L. L.; Sun, J. L.; Zhou, L.; Shi, Y. C.; Wang, C. H.; Zhong, B. H.; Shi, W. G.; Guo, Z. W. RLA8—A New and Highly Effective Quadruple PPAR- *α* / *γ* / *δ* and GPR40 Agonist to Reverse Nonalcoholic Steatohepatitis and Fibrosis. *J Pharmacol Exp Ther* **2019**, *369* (1), 67–77. https://doi.org/10.1124/jpet.118.255216.

(68) Pan, Q.; Lin, S.; Li, Y.; Liu, L.; Li, X.; Gao, X.; Yan, J.; Gu, B.; Chen, X.; Li, W.; Tang, X.; Chen, C.; Guo, L. A Novel GLP-1 and FGF21 Dual Agonist Has Therapeutic Potential for Diabetes and Non-Alcoholic Steatohepatitis. *EBioMedicine* **2021**, *63*, 103202. https://doi.org/10.1016/j.ebiom.2020.103202.

(69) Yang, H. K.; Lee, S.-H.; Shin, J.; Choi, Y.-H.; Ahn, Y.-B.; Lee, B.-W.; Rhee, E. J.; Min, K. W.; Yoon, K.-H. Acarbose Addon Therapy in Patients with Type 2 Diabetes Mellitus with Metformin and Sitagliptin Failure: A Multicenter, Randomized, Double-Blind, Placebo-Controlled Study. *Diabetes Metab J* **2019**, *43* (3), 287. https://doi.org/10.4093/dmj.2018.0054.

(70) Lin, J.; Liang, Q.-M.; Ye, Y.-N.; Xiao, D.; Lu, L.; Li, M.-Y.; Li, J.-P.; Zhang, Y.-F.; Xiong, Z.; Feng, N.; Li, C. Synthesis and Biological Evaluation of 5-Fluoro-2-Oxindole Derivatives as Potential α-Glucosidase Inhibitors. *Front. Chem.* **2022**, *10*, 928295. https://doi.org/10.3389/fchem.2022.928295.

(71) Ferhati, X.; Matassini, C.; Fabbrini, M. G.; Goti, A.; Morrone, A.; Cardona, F.; Moreno-Vargas, A. J.; Paoli, P. Dual Targeting of PTP1B and Glucosidases with New Bifunctional Iminosugar Inhibitors to Address Type 2 Diabetes. *Bioorganic Chemistry* **2019**, *87*, 534–549. https://doi.org/10.1016/j.bioorg.2019.03.053.

(72) Mphahlele, M. J.; Choong, Y. S.; Maluleka, M. M.; Gildenhuys, S. Synthesis, In Vitro Evaluation and Molecular Docking of the 5-Acetyl-2-Aryl-6-Hydroxybenzo[b]Furans against Multiple Targets Linked to Type 2 Diabetes. *Biomolecules* **2020**, *10* (3), 418. https://doi.org/10.3390/biom10030418.

(73) Chung, S. S. M.; Ho, E. C. M.; Lam, K. S. L.; Chung, S. K. Contribution of Polyol Pathway to Diabetes-Induced Oxidative Stress. *JASN* **2003**, *14* (suppl 3), S233–S236. https://doi.org/10.1097/01.ASN.0000077408.15865.06.

(74) Ottanà, R.; Paoli, P.; Cappiello, M.; Nguyen, T. N.; Adornato, I.; Del Corso, A.; Genovese, M.; Nesi, I.; Moschini, R.; Naß, A.; Wolber, G.; Maccari, R. In Search for Multi-Target Ligands as Potential Agents for Diabetes Mellitus and Its Complications—A Structure-Activity Relationship Study on Inhibitors of Aldose Reductase and Protein Tyrosine Phosphatase 1B. *Molecules* **2021**, *26* (2), 330. https://doi.org/10.3390/molecules26020330.

(75) Gunathilaka, T. L.; Samarakoon, K.; Ranasinghe, P.; Peiris, L. D. C. Antidiabetic Potential of Marine Brown Algae—a Mini Review. *Journal of Diabetes Research* **2020**, *2020*, 1–13. https://doi.org/10.1155/2020/1230218.

(76) Ezzat, S.; Bishbishy, M.; Habtemariam, S.; Salehi, B.; Sharifi-Rad, M.; Martins, N.; Sharifi-Rad, J. Looking at MarineDerived Bioactive Molecules as Upcoming Anti-Diabetic Agents: A Special Emphasis on PTP1B Inhibitors. *Molecules* **2018**, *23* (12), 3334. https://doi.org/10.3390/molecules23123334.

(77) Imperatore, C.; Luciano, P.; Aiello, A.; Vitalone, R.; Irace, C.; Santamaria, R.; Li, J.; Guo, Y.-W.; Menna, M. Structure and Configuration of Phosphoeleganin, a Protein Tyrosine Phosphatase 1B Inhibitor from the Mediterranean Ascidian *Sidnyum Elegans*. *J. Nat. Prod.* **2016**, *79* (4), 1144–1148. https://doi.org/10.1021/acs.jnatprod.6b00063.

(78) Luciano, P.; Imperatore, C.; Senese, M.; Aiello, A.; Casertano, M.; Guo, Y.-W.; Menna, M. Assignment of the Absolute Configuration of Phosphoeleganin via Synthesis of Model Compounds. *J. Nat. Prod.* **2017**, *80* (7), 2118– 2123. https://doi.org/10.1021/acs.jnatprod.7b00397.

(79) Morphy, R.; Rankovic, Z. Designed Multiple Ligands. An Emerging Drug Discovery Paradigm. *J. Med. Chem.* **2005**, *48* (21), 6523–6543. https://doi.org/10.1021/jm058225d.

(80) Csermely, P.; Agoston, V.; Pongor, S. The Efficiency of Multi-Target Drugs: The Network Approach Might Help Drug Design. *Trends in Pharmacological Sciences* **2005**, *26* (4), 178–182. https://doi.org/10.1016/j.tips.2005.02.007.

(81) Hopkins, A. L. Network Pharmacology: The next Paradigm in Drug Discovery. *Nat Chem Biol* **2008**, *4* (11), 682–690. https://doi.org/10.1038/nchembio.118.

(82) Proschak, E.; Stark, H.; Merk, D. Polypharmacology by Design: A Medicinal Chemist's Perspective on Multitargeting Compounds. *J. Med. Chem.* **2019**, *62* (2), 420–444. https://doi.org/10.1021/acs.jmedchem.8b00760.

(83) Maccari, R.; Del Corso, A.; Paoli, P.; Adornato, I.; Lori, G.; Balestri, F.; Cappiello, M.; Naß, A.; Wolber, G.; Ottanà, R.
An Investigation on 4-Thiazolidinone Derivatives as Dual Inhibitors of Aldose Reductase and Protein Tyrosine Phosphatase 1B, in the Search for Potential Agents for the Treatment of Type 2 Diabetes Mellitus and Its Complications. *Bioorganic & Medicinal Chemistry Letters* **2018**, *28* (23–24), 3712–3720. https://doi.org/10.1016/j.bmcl.2018.10.024.
(84) Imperatore, C.; Gimmelli, R.; Persico, M.; Casertano, M.; Guidi, A.; Saccoccia, F.; Ruberti, G.; Luciano, P.; Aiello, A.;
Parapini, S.; Avunduk, S.; Basilico, N.; Fattorusso, C.; Menna, M. Investigating the Antiparasitic Potential of the Marine Sesquiterpene Avarone, Its Reduced Form Avarol, and the Novel Semisynthetic Thiazinoquinone Analogue Thiazoavarone. *Marine Drugs* **2020**, *18* (2), 112. https://doi.org/10.3390/md18020112.
(85) Minale, L.; Riccio, R.; Sodano, G. AVAROL, A NOVEL S~SQUIT~~rENOID HYDROQUINON~ WITH A R~A~~RANG~DDR~MAN~ SKELETON FROM THE SPONGE DISIDEA AVARA. No. 38, 4.
(86) Cozzolino, R.; De Giulio, A.; De Rosa, S.; Strazzullo, G.; Gašič, M. J.; Sladić, D.; Zlatović, M. Biological Activities of Avarol Derivatives, 1. Amino Derivatives. *J. Nat. Prod.* **1990**, *53* (3), 699–702. https://doi.org/10.1021/np50069a027.
(87) Perva-Uzunalić, A.; Škerget, M.; Knez, Ž.; Weinreich, B.; Otto, F.; Grüner, S. Extraction of Active Ingredients from Green Tea (Camellia Sinensis): Extraction Efficiency of Major Catechins and Caffeine. *Food Chemistry* **2006**, *96* (4), 597–605. https://doi.org/10.1016/j.foodchem.2005.03.015.
(88) Lori, G.; Cecchi, L.; Mulinacci, N.; Melani, F.; Caselli, A.; Cirri, P.; Pazzagli, L.; Luti, S.; Mazzoli, L.; Paoli, P. Honey Extracts Inhibit PTP1B, Upregulate Insulin Receptor Expression, and Enhance Glucose Uptake in Human HepG2 Cells. *Biomedicine & Pharmacotherapy* **2019**, *113*, 108752. https://doi.org/10.1016/j.biopha.2019.108752.
(89) Chou, T.-C. Theoretical Basis, Experimental Design, and Computerized Simulation of Synergism and Antagonism in Drug Combination Studies. *Pharmacol Rev* **2006**, *58* (3), 621–681. https://doi.org/10.1124/pr.58.3.10.
(90) Morris, G. M.; Huey, R.; Lindstrom, W.; Sanner, M. F.; Belew, R. K.; Goodsell, D. S.; Olson, A. J. AutoDock4 and AutoDockTools4: Automated Docking with Selective Receptor Flexibility. *J. Comput. Chem.* **2009**, *30* (16), 2785– 2791. https://doi.org/10.1002/jcc.21256.
(91) Andrej Šali and Tom L. Blundell. Comparative Protein Modelling by Satisfaction of Spatial Restrains. *Comparative Protein Modelling by Satisfaction of Spatial Restrains* **1993**, *J. Mol. Biol. 234, 779-815, 1993*.
(92) Pettersen, E. F.; Goddard, T. D.; Huang, C. C.; Couch, G. S.; Greenblatt, D. M.; Meng, E. C.; Ferrin, T. E. UCSF Chimera?A Visualization System for Exploratory Research and Analysis. *J. Comput. Chem.* **2004**, *25* (13), 1605–1612. https://doi.org/10.1002/jcc.20084.
(93) Zheng, X.; Zhang, L.; Chen, W.; Chen, Y.; Xie, W.; Hu, X. Partial Inhibition of Aldose Reductase by Nitazoxanide and Its Molecular Basis. *ChemMedChem* **2012**, *7* (11), 1921–1923. https://doi.org/10.1002/cmdc.201200333.
(94) Scapin, G.; Patel, S. B.; Becker, J. W.; Wang, Q.; Desponts, C.; Waddleton, D.; Skorey, K.; Cromlish, W.; Bayly, C.; Therien, M.; Gauthier, J. Y.; Li, C. S.; Lau, C. K.; Ramachandran, C.; Kennedy, B. P.; Asante-Appiah, E. The Structural Basis for the Selectivity of Benzotriazole Inhibitors of PTP1B. *Biochemistry* **2003**, *42* (39), 11451–11459. https://doi.org/10.1021/bi035098j.
(95) Jones, G. et al. Development and Validation of a Genetic Algorithm for Flexible Docking. 22.
(96) Wolber, G.; Langer, T. LigandScout: 3-D Pharmacophores Derived from Protein-Bound Ligands and Their Use as Virtual Screening Filters. *J. Chem. Inf. Model.* **2005**, *45* (1), 160–169. https://doi.org/10.1021/ci049885e.
(97) Wolber, G.; Dornhofer, A. A.; Langer, T. Efficient Overlay of Small Organic Molecules Using 3D Pharmacophores. *J Comput Aided Mol Des* **2007**, *20* (12), 773–788. https://doi.org/10.1007/s10822-006-9078-7.
(98) Halgren, T. A. Merck Molecular Force Field. II. MMFF94 van Der Waals and Electrostatic Parameters for Intermolecular Interactions. *J. Comput. Chem.* **1996**, *17* (5–6), 520–552. https://doi.org/10.1002/(SICI)1096987X(199604)17:5/6<520::AID-JCC2>3.0.CO;2-W.
(99) Chemical Computing Group ULC, Montreal, QC, Canada. Molecular Operating Environment (MOE), 2020.
(100) Laskowski, R. A.; Swindells, M. B. LigPlot+: Multiple Ligand–Protein Interaction Diagrams for Drug Discovery. *J. Chem. Inf. Model.* **2011**, *51* (10), 2778–2786. https://doi.org/10.1021/ci200227u.
(101) Dassault Systèmes. BIOVIA, Discovery Studio 2021.
(102) Sblano, S.; Cerchia, C.; Laghezza, A.; Piemontese, L.; Brunetti, L.; Leuci, R.; Gilardi, F.; Thomas, A.; Genovese, M.; Santi, A.; Tortorella, P.; Paoli, P.; Lavecchia, A.; Loiodice, F. A Chemoinformatics Search for Peroxisome

Proliferator-Activated Receptors Ligands Revealed a New Pan-Agonist Able to Reduce Lipid Accumulation and Improve Insulin Sensitivity. *European Journal of Medicinal Chemistry* **2022**, *235*, 114240. https://doi.org/10.1016/j.ejmech.2022.114240.

(103) Pranzini, E.; Pardella, E.; Muccillo, L.; Leo, A.; Nesi, I.; Santi, A.; Parri, M.; Zhang, T.; Uribe, A. H.; Lottini, T.; Sabatino, L.; Caselli, A.; Arcangeli, A.; Raugei, G.; Colantuoni, V.; Cirri, P.; Chiarugi, P.; Maddocks, O. D. K.; Paoli, P.; Taddei, M. L. SHMT2-Mediated Mitochondrial Serine Metabolism Drives 5-FU Resistance by Fueling Nucleotide Biosynthesis. *Cell Reports* **2022**, *40* (7), 111233. https://doi.org/10.1016/j.celrep.2022.111233.

(104) Na, B.; Nguyen, P.-H.; Zhao, B.-T.; Vo, Q.-H.; Sun, B.; Woo, M. H. Protein Tyrosine Phosphatase 1B (PTP1B) Inhibitory Activity and Glucosidase Inhibitory Activity of c. 8.

(105) Zhang, J.; Sasaki, T.; Li, W.; Nagata, K.; Higai, K.; Feng, F.; Wang, J.; Cheng, M.; Koike, K. Identification of Caffeoylquinic Acid Derivatives as Natural Protein Tyrosine Phosphatase 1B Inhibitors from Artemisia Princeps. *Bioorganic & Medicinal Chemistry Letters* **2018**, *28* (7), 1194–1197. https://doi.org/10.1016/j.bmcl.2018.02.052.

(106) Lipchock, J. M.; Hendrickson, H. P.; Douglas, B. B.; Bird, K. E.; Ginther, P. S.; Rivalta, I.; Ten, N. S.; Batista, V. S.; Loria, J. P. Characterization of Protein Tyrosine Phosphatase 1B Inhibition by Chlorogenic Acid and Cichoric Acid.

Biochemistry **2017**, *56* (1), 96–106. https://doi.org/10.1021/acs.biochem.6b01025.

(107) Dixit, M.; Tripathi, B. K.; Srivastava, A. K.; Goel, A. Synthesis of Functionalized Acetophenones as Protein Tyrosine Phosphatase 1B Inhibitors. *Bioorganic & Medicinal Chemistry Letters* **2005**, *15* (14), 3394–3397. https://doi.org/10.1016/j.bmcl.2005.05.024.

(108) Haftchenary, S.; Jouk, A. O.; Aubry, I.; Lewis, A. M.; Landry, M.; Ball, D. P.; Shouksmith, A. E.; Collins, C. V.; Tremblay, M. L.; Gunning, P. T. Identification of Bidentate Salicylic Acid Inhibitors of PTP1B. *ACS Med. Chem. Lett.* **2015**, *6* (9), 982–986. https://doi.org/10.1021/acsmedchemlett.5b00171.

(109) Shrestha, S.; Bhattarai, B. R.; Lee, K.-H.; Cho, H. Mono- and Disalicylic Acid Derivatives: PTP1B Inhibitors as Potential Anti-Obesity Drugs. *Bioorganic & Medicinal Chemistry* **2007**, *15* (20), 6535–6548. https://doi.org/10.1016/j.bmc.2007.07.010.

(110) Barik, S. K.; Russell, W. R.; Dehury, B.; Cruickshank, M.; Moar, K. M.; Thapa, D.; Hoggard, N. Dietary Phenolics Other than Anthocyanins Inhibit PTP1B; an in Vitro and in Silico Validation. 1.

(111) Wang, R.; Zhou, W.; Jiang, X. Reaction Kinetics of Degradation and Epimerization of Epigallocatechin Gallate (EGCG) in Aqueous System over a Wide Temperature Range. *J. Agric. Food Chem.* **2008**, *56* (8), 2694–2701. https://doi.org/10.1021/jf0730338.

(112) Kuzuhara, T.; Suganuma, M.; Fujiki, H. Green Tea Catechin as a Chemical Chaperone in Cancer Prevention. *Cancer Letters* **2008**, *261* (1), 12–20. https://doi.org/10.1016/j.canlet.2007.10.037.

(113) Kuban-Jankowska, A.; Kostrzewa, T.; Musial, C.; Barone, G.; Lo-Bosco, G.; Lo-Celso, F.; Gorska-Ponikowska, M. Green Tea Catechins Induce Inhibition of PTP1B Phosphatase in Breast Cancer Cells with Potent Anti-Cancer Properties: In Vitro Assay, Molecular Docking, and Dynamics Studies. **2020**, 12.

(114) Clifford, M. N.; van der Hooft, J. J.; Crozier, A. Human Studies on the Absorption, Distribution, Metabolism, and Excretion of Tea Polyphenols. *The American Journal of Clinical Nutrition* **2013**, *98* (6), 1619S-1630S. https://doi.org/10.3945/ajcn.113.058958.

(115) Chen, Y.-K.; Cheung, C.; Reuhl, K. R.; Liu, A.; Lee, M.-J.; Lu, Y.-P.; Yang, C. S. Effects of Green Tea Polyphenol (À)-Epigallocatechin-3-Gallate on Newly Developed High-Fat/Western-Style Diet-Induced Obesity and Metabolic Syndrome in Mice. *Journal of Agricultural and Food Chemistry* **2011**, 10.

(116) Bose, M.; Lambert, J. D.; Ju, J.; Reuhl, K. R.; Shapses, S. A.; Yang, C. S. The Major Green Tea Polyphenol, (-)Epigallocatechin-3-Gallate, Inhibits Obesity, Metabolic Syndrome, and Fatty Liver Disease in High-Fat–Fed Mice.

The Journal of Nutrition **2008**, *138* (9), 1677–1683. https://doi.org/10.1093/jn/138.9.1677.

(117) Molinaro, A. Insulin Signaling and Glucose Metabolism in Different Hepatoma Cell Lines Deviate from Hepatocyte Physiology toward a Convergent Aberrant Phenotype. *Scientific Reports* **2020**, 10.

(118) Wong, C. Y.; Al-Salami, H.; Dass, C. R. C2C12 Cell Model: Its Role in Understanding of Insulin Resistance at the Molecular Level and Pharmaceutical Development at the Preclinical Stage. *Journal of Pharmacy and Pharmacology* **2020**, *72* (12), 1667–1693. https://doi.org/10.1111/jphp.13359.

(119) Collins, Q. F.; Liu, H.-Y.; Pi, J.; Liu, Z.; Quon, M. J.; Cao, W. Epigallocatechin-3-Gallate (EGCG), A Green Tea Polyphenol, Suppresses Hepatic Gluconeogenesis through 5′-AMP-Activated Protein Kinase. *Journal of Biological Chemistry* **2007**, *282* (41), 30143–30149. https://doi.org/10.1074/jbc.M702390200.

(120) Wolfram, S.; Raederstorff, D.; Preller, M.; Wang, Y.; Teixeira, S. R.; Riegger, C.; Weber, P. Epigallocatechin Gallate Supplementation Alleviates Diabetes in Rodents. *The Journal of Nutrition* **2006**, *136* (10), 2512–2518. https://doi.org/10.1093/jn/136.10.2512.

(121) Crettaz, M.; Kahn, C. R. Insulin Receptor Regulation and Desensitization in Rat Hepatoma Cells. **1984**, *33*, 9.
(122) Won-Mo Yang, Hyo-Jin Jeong, Seung-Yoon Park, Wan Lee. Saturated Fatty Acid-Induced MiR-195 Impairs Insulin Signaling and Glycogen Metabolism in HepG2 Cells. **2014**. https://doi.org/10.1016/j.febslet.2014.09.006.
(123) Won-Mo Yang, Hyo-Jin Jeong, Se-Whan Park, Wan Lee. Obesity-Induced MiR-15b Is Linked Causally to the Development of Insulin Resistance through the Repression of the Insulin Receptor in Hepatocytes. **2015**. https://doi.org/10.1002/mnfr.201500107.
(124) Li, Y.; Zhong, Y.; Cheng, Q.; Wang, Y.; Fan, Y.; Yang, C.; Ma, Z.; Li, Y.; Li, L. MiR-378b Regulates Insulin Sensitivity by Targeting Insulin Receptor and P110α in Alcohol-Induced Hepatic Steatosis. *Frontiers in Pharmacology* **2020**, *11*, 15.
(125) Fan, F.-Y. Differential Behaviors of Tea Catechins under Thermal Processing: Formation of Non-Enzymatic Oligomers. *Food Chemistry* **2016**, 8.
(126) Jin, T.; Yu, H.; Huang, X.-F. Selective Binding Modes and Allosteric Inhibitory Effects of Lupane Triterpenes on Protein Tyrosine Phosphatase 1B. *Sci Rep* **2016**, *6* (1), 20766. https://doi.org/10.1038/srep20766.
(127) Paoli, P. The Insulin-Mimetic Effect of Morin: A Promising Molecule in Diabetes Treatment. *Biochimica et Biophysica Acta* **1830**, 10.
(128) Chou, T.-C. Drug Combination Studies and Their Synergy Quantification Using the Chou-Talalay Method. *Cancer Research* **2010**, *70* (2), 440–446. https://doi.org/10.1158/0008-5472.CAN-09-1947.
(129) Pannifer, A. D. B.; Flint, A. J.; Tonks, N. K.; Barford, D. Visualization of the Cysteinyl-Phosphate Intermediate of a Protein-Tyrosine Phosphatase by X-Ray Crystallography. *Journal of Biological Chemistry* **1998**, *273* (17), 10454– 10462. https://doi.org/10.1074/jbc.273.17.10454.
(130) Chou, T.-C.; Talalay, P. Generalized Equations for the Analysis of Inhibitions of Michaelis-Menten and HigherOrder Kinetic Systems with Two or More Mutually Exclusive and Nonexclusive Inhibitors. *European Journal of Biochemistry* **2005**, *115* (1), 207–216. https://doi.org/10.1111/j.1432-1033.1981.tb06218.x.
(131) Stanford, S. M.; Aleshin, A. E.; Zhang, V.; Ardecky, R. J.; Hedrick, M. P.; Zou, J.; Ganji, S. R.; Bliss, M. R.; Yamamoto, F.; Bobkov, A. A.; Kiselar, J.; Liu, Y.; Cadwell, G. W.; Khare, S.; Yu, J.; Barquilla, A.; Chung, T. D. Y.; Mustelin, T.; Schenk, S.; Bankston, L. A.; Liddington, R. C.; Pinkerton, A. B.; Bottini, N. Diabetes Reversal by Inhibition of the Low-Molecular-Weight Tyrosine Phosphatase. *Nat Chem Biol* **2017**, *13* (6), 624–632. https://doi.org/10.1038/nchembio.2344.
(132) Genovese, M.; Luti, S.; Pardella, E.; Vivoli-Vega, M.; Pazzagli, L.; Parri, M.; Caselli, A.; Cirri, P.; Paoli, P. Differential Impact of Cold and Hot Tea Extracts on Tyrosine Phosphatases Regulating Insulin Receptor Activity: A Focus on PTP1B and LMW-PTP. *Eur J Nutr* **2022**, *61* (4), 1905–1918. https://doi.org/10.1007/s00394-021-02776w.
(133) Benedetta Russo, Fabiana Picconi, Ilaria Malandrucco, Simona Frontoni. Flavonoids and Insulin-Resistance: From Molecular Evidences to Clinical Trials. **2019**. http://dx.doi.org/10.3390/ijms20092061.
(134) Genovese, M.; Imperatore, C.; Casertano, M.; Aiello, A.; Balestri, F.; Piazza, L.; Menna, M.; Del Corso, A.; Paoli, P. Dual Targeting of PTP1B and Aldose Reductase with Marine Drug Phosphoeleganin: A Promising Strategy for Treatment of Type 2 Diabetes. *Marine Drugs* **2021**, *19* (10), 535. https://doi.org/10.3390/md19100535.
(135) Chiarugi, P.; Cirri, P.; Marra, F.; Raugei, G.; Camici, G.; Manao, G.; Ramponi, G. LMW-PTP Is a Negative Regulator of Insulin-Mediated Mitotic and Metabolic Signalling. *Biochemical and Biophysical Research Communications* **1997**, *238* (2), 676–682. https://doi.org/10.1006/bbrc.1997.7355.
(136) Wier, B. V. D. The Potential of Flavonoids in the Treatment of Non-Alcoholic Fatty Liver Disease. *CRITICAL REVIEWS IN FOOD SCIENCE AND NUTRITION* 23.
(137) Brewer, P. D.; Habtemichael, E. N.; Romenskaia, I.; Mastick, C. C.; Coster, A. C. F. Insulin-Regulated Glut4 Translocation. *Journal of Biological Chemistry* **2014**, *289* (25), 17280–17298. https://doi.org/10.1074/jbc.M114.555714.
(138) Ryder, J. W.; Kawano, Y.; Chibalin, A. V.; Rinco, J.; Tsao, T.-S.; Stenbit, A. E.; Combatsiaris, T.; Yang, J.; Holman, G. D.; Charron, M. J.; Zierath, J. R. In Vitro Analysis of the Glucose-Transport System in GLUT4-Null Skeletal Muscle. **1999**, 8.
(139) Divakaruni, A. S.; Wiley, S. E.; Rogers, G. W.; Andreyev, A. Y.; Petrosyan, S.; Loviscach, M.; Wall, E. A.; Yadava, N.; Heuck, A. P.; Ferrick, D. A.; Henry, R. R.; McDonald, W. G.; Colca, J. R.; Simon, M. I.; Ciaraldi, T. P.; Murphy, A.
N. Thiazolidinediones Are Acute, Specific Inhibitors of the Mitochondrial Pyruvate Carrier. *Proc. Natl. Acad. Sci. U.S.A.* **2013**, *110* (14), 5422–5427. https://doi.org/10.1073/pnas.1303360110.

(140) Sisir Nandi. Potential Inhibitors of Protein Tyrosine Phosphatase (PTP1B) Enzyme: Promising Target for Type-II Diabetes Mellitus. http://dx.doi.org/10.2174/1568026620999200904121432.
(141) Posner, B. I. Insulin Signalling: The Inside Story. *Canadian Journal of Diabetes* **2017**, *41* (1), 108–113. https://doi.org/10.1016/j.jcjd.2016.07.002.
(142) Teimouri, M.; Hosseini, H.; ArabSadeghabadi, Z.; Babaei-Khorzoughi, R.; Gorgani-Firuzjaee, S.; Meshkani, R. The Role of Protein Tyrosine Phosphatase 1B (PTP1B) in the Pathogenesis of Type 2 Diabetes Mellitus and Its Complications. *J Physiol Biochem* **2022**, *78* (2), 307–322. https://doi.org/10.1007/s13105-021-00860-7.
(143) Koren, S.; Fantus, I. G. Inhibition of the Protein Tyrosine Phosphatase PTP1B: Potential Therapy for Obesity, Insulin Resistance and Type-2 Diabetes Mellitus. *Best Practice & Research Clinical Endocrinology & Metabolism* **2007**, *21* (4), 621–640. https://doi.org/10.1016/j.beem.2007.08.004.
(144) Somwar, R.; Kim, D. Y.; Sweeney, G.; Huang, C.; Niu, W.; Lador, C.; Ramlal, T.; Klip, A. GLUT4 Translocation Precedes the Stimulation of Glucose Uptake by Insulin in Muscle Cells : Potential Activation of GLUT4 via P38 Mitogen-Activated Protein Kinase. **2001**, 11.
(145) Nicholls, D. G. Spare Respiratory Capacity, Oxidative Stress and Excitotoxicity. *Biochemical Society Transactions* **2009**, *37* (6), 1385–1388. https://doi.org/10.1042/BST0371385.
(146) Marchetti, P.; Fovez, Q.; Germain, N.; Khamari, R.; Kluza, J. Mitochondrial Spare Respiratory Capacity: Mechanisms, Regulation, and Significance in Non-transformed and Cancer Cells. *FASEB j.* **2020**, *34* (10), 13106– 13124. https://doi.org/10.1096/fj.202000767R.
(147) Kelley, D. E.; He, J.; Menshikova, E. V.; Ritov, V. B. Dysfunction of Mitochondria in Human Skeletal Muscle in Type 2 Diabetes. *Diabetes* **2002**, *51* (10), 2944–2950. https://doi.org/10.2337/diabetes.51.10.2944.
(148) Kador, P. F.; Wyman, M.; Oates, P. J. Aldose Reductase, Ocular Diabetic Complications and the Development of Topical Kinostat®. *Progress in Retinal and Eye Research* **2016**, *54*, 1–29. https://doi.org/10.1016/j.preteyeres.2016.04.006.
(149) Kang, Q.; Yang, C. Oxidative Stress and Diabetic Retinopathy: Molecular Mechanisms, Pathogenetic Role and Therapeutic Implications. *Redox Biology* **2020**, *37*, 101799. https://doi.org/10.1016/j.redox.2020.101799.
(150) Imperatore, C.; Luciano, P.; Aiello, A.; Vitalone, R.; Irace, C.; Santamaria, R.; Li, J.; Guo, Y.-W.; Menna, M. Structure and Configuration of Phosphoeleganin, a Protein Tyrosine Phosphatase 1B Inhibitor from the Mediterranean Ascidian *Sidnyum Elegans*. *J. Nat. Prod.* **2016**, *79* (4), 1144–1148. https://doi.org/10.1021/acs.jnatprod.6b00063.
(151) Imperatore, C.; Luciano, P.; Aiello, A.; Vitalone, R.; Irace, C.; Santamaria, R.; Li, J.; Guo, Y.-W.; Menna, M. Structure and Configuration of Phosphoeleganin, a Protein Tyrosine Phosphatase 1B Inhibitor from the Mediterranean Ascidian *Sidnyum Elegans*. *J. Nat. Prod.* **2016**, *79* (4), 1144–1148. https://doi.org/10.1021/acs.jnatprod.6b00063.
(152) Asante-Appiah, E.; Patel, S.; Dufresne, C.; Roy, P.; Wang, Q.; Patel, V.; Friesen, R. W.; Ramachandran, C.; Becker, J. W.; Leblanc, Y.; Kennedy, B. P.; Scapin, G. The Structure of PTP-1B in Complex with a Peptide Inhibitor Reveals an Alternative Binding Mode for Bisphosphonates. *Biochemistry* **2002**, *41* (29), 9043–9051. https://doi.org/10.1021/bi0259554.
(153) Sun, J.-P.; Fedorov, A. A.; Lee, S.-Y.; Guo, X.-L.; Shen, K.; Lawrence, D. S.; Almo, S. C.; Zhang, Z.-Y. Crystal Structure of PTP1B Complexed with a Potent and Selective Bidentate Inhibitor. *Journal of Biological Chemistry* **2003**, *278* (14), 12406–12414. https://doi.org/10.1074/jbc.M212491200.
(154) Xie, L.; Lee, S.-Y.; Andersen, J. N.; Waters, S.; Shen, K.; Guo, X.-L.; Moller, N. P. H.; Olefsky, J. M.; Lawrence, D. S.; Zhang, Z.-Y. Cellular Effects of Small Molecule PTP1B Inhibitors on Insulin Signaling. *Biochemistry* **2003**, *42* (44), 12792–12804. https://doi.org/10.1021/bi035238p.
(155) Ottanà, R.; Maccari, R.; Mortier, J.; Caselli, A.; Amuso, S.; Camici, G.; Rotondo, A.; Wolber, G.; Paoli, P. Synthesis, Biological Activity and Structure–Activity Relationships of New Benzoic Acid-Based Protein Tyrosine Phosphatase Inhibitors Endowed with Insulinomimetic Effects in Mouse C2C12 Skeletal Muscle Cells. *European Journal of Medicinal Chemistry* **2014**, *71*, 112–127. https://doi.org/10.1016/j.ejmech.2013.11.001.
(156) Qin, Z.; Pandey, N. R.; Zhou, X.; Stewart, C. A.; Hari, A.; Huang, H.; Stewart, A. F. R.; Brunel, J. M.; Chen, H.-H. Functional Properties of Claramine: A Novel PTP1B Inhibitor and Insulin-Mimetic Compound. *Biochemical and Biophysical Research Communications* **2015**, *458* (1), 21–27. https://doi.org/10.1016/j.bbrc.2015.01.040.
(157) Hooft van Huijsduijnen, R.; Sauer, W. H. B.; Bombrun, A.; Swinnen, D. Prospects for Inhibitors of Protein Tyrosine Phosphatase 1B as Antidiabetic Drugs. *J. Med. Chem.* **2004**, *47* (17), 4142–4146. https://doi.org/10.1021/jm030629n.
(158) Balestri, F.; Cappiello, M.; Moschini, R.; Rotondo, R.; Buggiani, I.; Pelosi, P.; Mura, U.; Del-Corso, A. L-Idose: An Attractive Substrate Alternative to d-Glucose for Measuring Aldose Reductase Activity. *Biochemical and Biophysical Research Communications* **2015**, *456* (4), 891–895. https://doi.org/10.1016/j.bbrc.2014.12.054.

(159) Tang, W. H.; Martin, K. A.; Hwa, J. Aldose Reductase, Oxidative Stress, and Diabetic Mellitus. *Front. Pharmacol.* **2012**, *3*. https://doi.org/10.3389/fphar.2012.00087.

(160) Freidenberg, G. R.; Klein, H. H.; Cordera, R.; Olefsky, J. M. Insulin Receptor Kinase Activity in Rat Liver. Regulation by Fasting and High Carbohydrate Feeding. *Journal of Biological Chemistry* **1985**, *260* (23), 12444–12453. https://doi.org/10.1016/S0021-9258(17)38893-2.

(161) Venable, C. L.; Frevert, E. U.; Kim, Y.-B.; Fischer, B. M.; Kamatkar, S.; Neel, B. G.; Kahn, B. B. Overexpression of Protein-Tyrosine Phosphatase-1B in Adipocytes Inhibits Insulin-Stimulated Phosphoinositide 3-Kinase Activity without Altering Glucose Transport or Akt/Protein Kinase B Activation. *Journal of Biological Chemistry* **2000**, *275* (24), 18318–18326. https://doi.org/10.1074/jbc.M908392199.

(162) Bleasdale, J. E.; Ogg, D.; Palazuk, B. J.; Jacob, C. S.; Swanson, M. L.; Wang, X.-Y.; Thompson, D. P.; Conradi, R. A.; Mathews, W. R.; Laborde, A. L.; Stuchly, C. W.; Heijbel, A.; Bergdahl, K.; Bannow, C. A.; Smith, C. W.; Svensson, C.; Liljebris, C.; Schostarez, H. J.; May, P. D.; Stevens, F. C.; Larsen, S. D. Small Molecule Peptidomimetics Containing a Novel Phosphotyrosine Bioisostere Inhibit Protein Tyrosine Phosphatase 1B and Augment Insulin Action. *Biochemistry* **2001**, *40* (19), 5642–5654. https://doi.org/10.1021/bi002865v.